Report No. 5

RF 2411

Laboratory for Isotope Geology and Geochemistry

Institute of Polar Studies
and
Department of Geology
THE OHIO STATE UNIVERSITY

STUDIES IN THE GEOCHRONOLOGY AND GEOCHEMISTRY OF THE TRANSANTARCTIC MOUNTAINS

September, 1970

Submitted to:
The National Science Foundation
Grant GA-898X

STUDIES IN THE GEOCHRONOLOGY AND GEOCHEMISTRY OF THE TRANSANTARCTIC MOUNTAINS

by

G. Faure, R. Eastin, J. Gunner, R. L. Hill
L. M. Jones and D. H. Elliot

Institute of Polar Studies
and
Department of Geology
The Ohio State University
Columbus, Ohio 43210

Third Annual Progress Report
Grant GA-898X

The National Science Foundation
Washington, D.C.

The Ohio State University
Research Foundation

PREFACE

This report was prepared for the National Science Foundation which has supported our research program in Antarctica through Grant 898-X. It contains data and preliminary interpretations, most of which have not yet been published or are in press. Copies of this report are available free of charge by request to G. Faure, Department of Geology, The Ohio State University, Columbus, Ohio 43210.

Because of the preliminary nature of many of the conclusions contained in this report, scientists wishing to use information contained herein should first consult the author.

It is a pleasure to acknowledge the help of John F. Splettstoesser of the Institute of Polar Studies in the administration of this grant. This report was prepared by the Research Foundation of The Ohio State University.

Gunter Faure
September 1, 1970

TABLE OF CONTENTS

ISOTOPE COMPOSITION OF STRONTIUM AND SILICA CONTENT OF MESOZOIC BASALT AND DOLERITE FROM ANTARCTICA

G. Faure, R. L. Hill, L. M. Jones and D. H. Elliot
Institute of Polar Studies and Department of Geology
The Ohio State University, Columbus, Ohio 43210, U.S.A.
(Presented to SCAR Symposium, Oslo, Norway, August 6-15, 1970)

ABSTRACT

Tholeiites of the Kirkpatrick Basalt and the Ferrar Dolerite in the Transantarctic Mountains have anomalously high initial Sr^{87}/Sr^{86} ratios. They differ in this respect from basaltic rocks of probable Jurassic age from Vestfjella, Mannefallknausane, and Heimefrontfjella of Queen Maud Land, which have normal initial Sr^{87}/Sr^{86} ratios. Eighteen specimens of tholeiite of the Ferrar Group have an average initial Sr^{87}/Sr^{86} ratio of 0.71206±0.00036 ($\bar{\sigma}$). Two specimens from the Dufek Massif have an initial ratio of 0.7093±0.0006. Twelve specimens of basalt and dolerite from Queen Maud Land have a bi-modal distribution with mean values of 0.7037±0.0004 ($\bar{\sigma}$) and 0.7072±0.0003 ($\bar{\sigma}$)

The silica content of tholeiites from the Ferrar Group correlates positively with initial Sr^{87}/Sr^{86} ratios. This correlation is especially convincing for flows of the Kirkpatrick Basalt at Storm Peak in the Marshall Mountains of the Queen Alexandra Range. Collectively, the basaltic rocks of the Ferrar Group and from Queen Maud Land form a colinear array in a plot of SiO_2 versus initial Sr^{87}/Sr^{86} ratios. Positive correlations are suggested also for K_2O and Rb, while CaO, MgO, Sr and Ni appear to correlate negatively with initial Sr^{87}/Sr^{86} ratios.

The relationship between initial Sr^{87}/Sr^{86} ratios and chemical composition of the basalts and dolerites indicates that these rocks have been contaminated by incorporation of sialic material enriched in SiO_2, K_2O, and Rb and depleted in CaO, MgO, Sr, and Ni and having a high Sr^{87}/Sr^{86} ratio. Therefore the petrogenetic history of these rocks includes not only magmatic differentiation, but also mixing in varying proportions with sialic material.

INTRODUCTION

Following the work of McDougall (1962) on the differentiation of the Jurassic dolerites of Tasmania, Heier, Compston and McDougall (1965) subsequently showed that these rocks have high Th/K, U/K, and initial Sr^{87}/Sr^{86}, but low K/Rb ratios compared to basaltic rocks elsewhere. In a later paper Compston, McDougall and Heier (1968) extended this study to the Jurassic dolerites of the Ferrar Group in the Transantarctic Mountains and found that these rocks exhibit the same geochemical and isotopic anomalies as the Tasmanian dolerites. A summary of their results is given in Table I.

Table I. Anomalous Geochemical Parameters of Jurassic Dolerites of Tasmania and Antarctica

	Tasmanian Dolerites Heier et al. (1965)	Ferrar Dolerites Compston et al. (1968)
$(Th/K) \times 10^4$	$5.0 \pm 8\%$	5.6
$(U/K) \times 10^4$	$1.25 \pm 14\%$	1.8
Th/U	$4.0 \pm 12\%$	3.3
K/Rb	209	240
Initial Sr^{87}/Sr^{86}	0.7115 ± 0.0007	0.7116
Age	165 m.y.	155 m.y.

The values of these ratios in the Tasmanian and Antarctic dolerites are anomalous because they are similar to those commonly found in granitic rocks (Heier and Rogers, 1963) and thereby suggest a crustal origin for these rocks. The previous authors considered several possible explanations for this anomaly, including

(1) generation of magma within the sialic crust;

(2) generation of magma in the upper mantle which was locally enriched in Rb, U, and Th;

(3) large-scale contamination of basaltic magma derived from the upper mantle by assimilation of granitic rocks in the crust;

(4) selective diffusion of certain elements from granitic rocks into the magma; and

(5) partial melting of granitic rocks by the basaltic magma and subsequent mixing of the two silicate liquids.

The previous authors suggested that assimilation of granitic rocks by an oceanic tholeiite magma could explain the anomalies, but pointed out that the apparent chemical and isotopic homogeneity and the very large volume and areal extent of the dolerites in Tasmania and Antarctica required that this process occurred on a gigantic scale prior to intrusion of the dolerite magma.

The anomalous geochemical and isotopic properties of the Tasmanian and Antarctic dolerites appear to be unique. Compston et al. (1968) also examined Karroo dolerites from South Africa and Serra Geral dolerites from Brazil and found them to be normal, although some assimilation of granitic material may have occurred there too. In fact, Manton (1968) found evidence that Karroo basalt in the Lebombo-Nuanetsi igneous province of South Africa was contaminated with radiogenic Sr^{87} derived from the underlying granitic basement. Nevertheless, the initial Sr^{87}/Sr^{86} ratios of the Karroo basalts are significantly lower than those of the Tasmanian or Antarctic dolerites.

Philpotts and Schnetzler (1968) measured rare earth (RE) and barium concentrations of chilled contact samples of Karroo dolerite, Ferrar dolerite, Red Hill dolerite (Tasmania), the Palisade Sill (U.S.A.), and the U.S.G.S. diabase standard W-1. Surprisingly, they found that these rocks have very similar relative and absolute abundances of the rare earths and barium. The chondrite-normalized RE and Ba abundance patterns of these rocks are very similar to those of continental tholeiites, but differ significantly from those of oceanic tholeiites. Philpotts and Schnetzler (1968, p. 941) concluded that: "The compositional similarity of diabases suggests that the same type and extent of genetic process was operative and that the source materials all had essentially the same abundances of the RE and Ba."

The latest contributions to the study of the anomalous abundance of radiogenic Sr^{87} in the tholeiites of the Ferrar Group was made by Hill (1969) who analyzed suites of Kirkpatrick Basalt and Ferrar Dolerite from Northern Victoria Land and from the Queen Alexandra Range (Beardmore Glacier). He found high initial Sr^{87}/Sr^{86} ratios, very similar to those reported earlier by Compston et al. (1968). This result firmly established the genetic equivalence of the Kirkpatrick Basalt and the Ferrar Dolerite and appeared to confirm the prediction of Compston et al. (1968) that all tholeiites of the Ferrar Group possess anomalous initial Sr^{87}/Sr^{86} rations.

However, Faure and Elliot (1970) found that basalts and dolerites believed to be of Jurassic age from Maud Land (Vestfjella, Mannefallknausane, and Heimefrontfjella) have normal initial Sr^{87}/Sr^{86} ratios ranging from 0.7018 to 0.7076, with a bi-modal distribution having averages of 0.7037 ± 0.0004 ($\bar{\sigma}$) and 0.7072 ± 0.0003 ($\bar{\sigma}$). In addition,

they found that the basaltic rocks from Queen Maud Land have consistently higher strontium and lower rubidium concentrations compared to the tholeiites of the Ferrar Group in the Transantarctic Mountains. Juckes (1968) showed earlier that dolerites from Queen Maud Land also have lower silica and K_2O contents than the rocks of the Ferrar Group in Victoria Land.

It is clear from the foregoing that Antarctica contains two suites of tholeiites of Jurassic age which differ not only in terms of initial Sr^{87}/Sr^{86} ratios, but apparently also in terms of their bulk chemical composition. Composton et al. (1968) also noted small differences in initial Sr^{87}/Sr^{86} ratios of Ferrar dolerite samples representing the different magma types established by Gunn (1962, 1965, 1966) and suggested that a correlation of this ratio with bulk chemistry is possible.

In this report we present new measurements of initial Sr^{87}/Sr^{86} ratios of samples of Ferrar Dolerite, including two from the Dufek Massif. In addition we report concentrations of SiO_2 and K_2O and test the correlation of the initial Sr^{87}/Sr^{86} ratios with these and other chemical parameters.

ANALYTICAL PROCEDURES

We are reporting concentrations of Rb, Sr, K, Fe, SiO_2, and Ni, as well as Sr^{87}/Sr^{86} ratios of Mesozoic tholeiites from Antarctica. Rubidium and strontium were measured both by isotope dilution and X-ray fluorescence techniques. Potassium and sodium were determined by flame photometry. Total Fe and Ni were done by X-ray fluorescence using W-1 and BCR-1 (for Fe) and W-1, DTS-1, and PCC-1 (for Ni) as comparison standards. Silica was determined by McCreath and Sons, Inc., using standard wet chemical methods. The accuracy of their analyses was checked by analysis of W-1 (disguised as an unknown) for which they reported SiO_2=52.34%, in excellent agreement with the preferred value of Fleischer (1969). The isotopic composition of strontium was determined on a 60° sector, 6-inch radius of curvature, single-filament, solid-source mass spectrometer (Nuclide Corp., Model 6-60-S). The Eimer and Amend $SrCO_3$ standard was analyzed repeatedly and was found to have a Sr^{87}/Sr^{86} ratio of 0.7082±0.0005 (σ). On this basis we believe that a single determination of this ratio in a rock is reproducible to within ±0.0010 at the 95% confidence limit. All measured Sr^{87}/Sr^{86} ratios were corrected for isotope fractionation, assuming that Sr^{86}/Sr^{88}=0.1194. The analytical results are compiled in Appendix 1. Details of sample locations are given in Appendix 2.

THE INITIAL Sr^{87}/Sr^{86} RATIOS

Initial Sr^{87}/Sr^{86} ratios have been calculated for all samples using the measured Rb/Sr ratios and a value of 1.39×10^{-11} yr^{-1}

for the decay constant of Rb^{87}. For samples from Victoria Land we have assumed a common age of 155 million years, based on age determinations reviewed by Compston, McDougall and Heier (1968). However, the Kirkpatrick Basalt from the Queen Alexandra Range appears to be somewhat older (Elliot, 1970). For these rocks, as well as those from the Nilsen Plateau and the Dufek Massif, we have assumed an age of 170 million years.

The ages of the basalts and dolerites from Queen Maud Land are much less certain. At least one of the specimens (#400, Z.372.1 of Juckes, 1968) has a K-Ar date of 174±7 million years (Adie, private communication). This specimen is from western Bjornnutane at latitude 74°36'S long. 10°04'W in Heimefrontfjella. Its initial Sr^{87}/Sr^{86} ratio is 0.7039, placing it in the lower of the two groups described by Faure and Elliot (1970). In addition, Rex (1967) reported dates of 168±6 and 172±6 for two basalt specimens from Vestfjella. One of our specimens (#403, Z.395.1 of Juckes, 1968) is from Vestfjella. It too has a low initial Sr^{87}/Sr^{86} ratio of 0.7037. The available evidence therefore seems to indicate that Jurassic basalt flows and dolerite dikes and sills exist in Heimefrontfjella and Vestfjella and that they have low initial Sr^{87}/Sr^{86} ratios.

Recently Allsopp and Neethling (1970) reported an age of 1700±130 million years for the Borg Metamafics at Ahlmann Ridge in Queen Maud Land east of Heimefrontfjella. Some of these metamafics had been analyzed earlier by Erlank and Hofmeyer (1968) who believed them to be of Jurassic age. However, the present-day Sr^{87}/Sr^{86} ratios of the Borg Metamafics analyzed by Allsopp and Neethling range from 0.7219 to 0.7405 and are thus far greater than any values measured by us. For these reasons it seems unlikely to us that any of the basalts and dolerites from Queen Maud Land analyzed by Faure and Elliot (1970) and by us belong to the Borg Metamafics. We have therefore assumed a common age of 170 million years for all of the basalts and dolerites from Queen Maud Land included in this study.

The range of initial Sr^{87}/Sr^{86} ratios of Mesozoic tholeiites from different locations in Antarctica is shown in Figure 1. In addition, we have plotted the values reported by Heier et al. (1965) and by Compston et al. (1968) as well as previously unpublished analyses of Sr^{87}/Sr^{86} ratios of a suite of alkali-rich olivine basalts of the McMurdo Volcanics and of basaltic rocks from Deception Island, including specimens extruded in the 1969 eruption.

It is evident by inspection of Figure 1 that the basalts and dolerites of the Ferrar Group in the Transantarctic Mountains all have anomalously high initial Sr^{87}/Sr^{86} ratios, similar to the Tasmanian dolerites. On the other hand, the basalts and dolerites of Queen Maud Land have significantly lower, and more normal, initial Sr^{87}/Sr^{86} ratios. The difference in the initial Sr^{87}/Sr^{86} ratios indicates that the two basalt and dolerite suites were either derived from different source

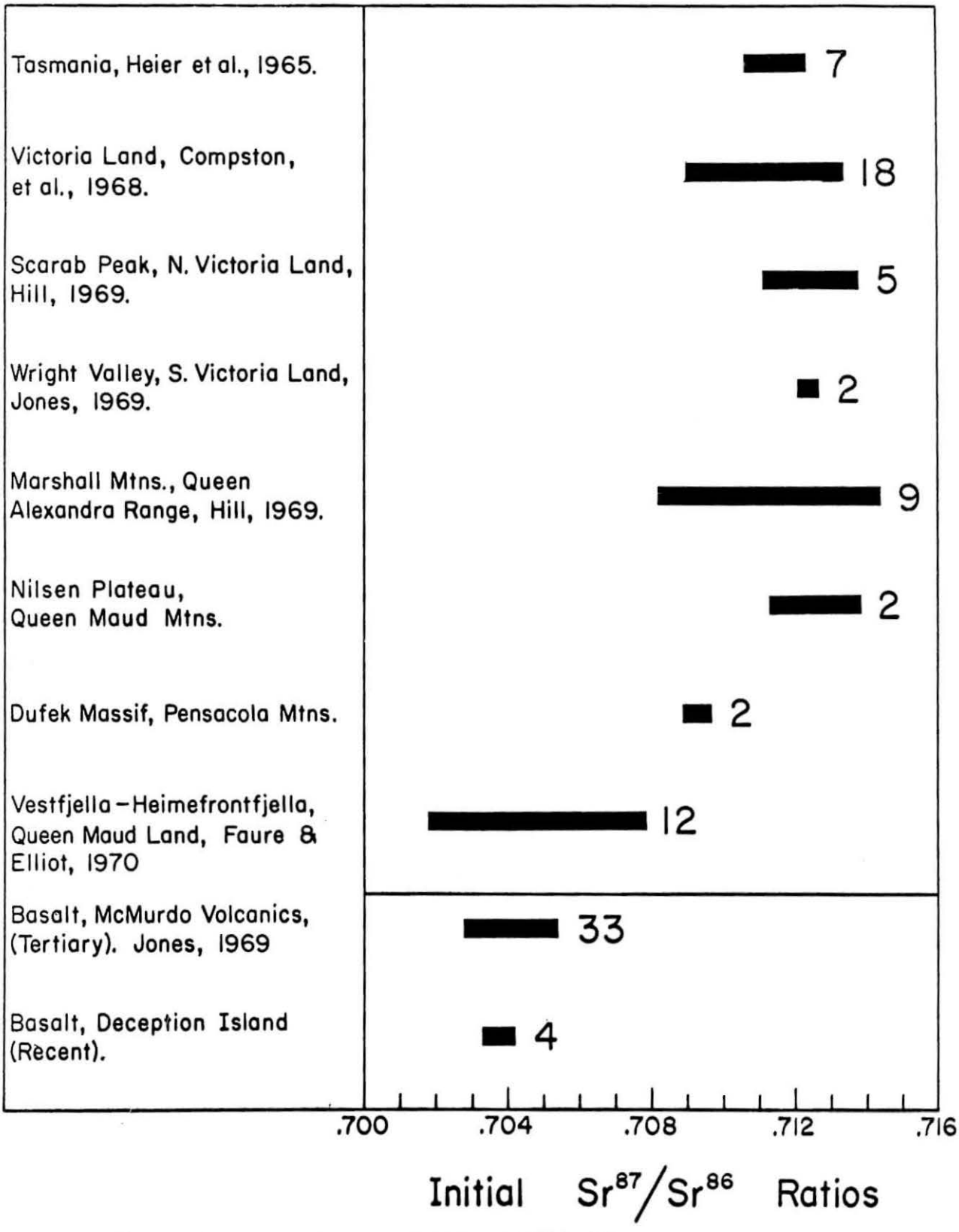

Figure 1. Comparison of initial Sr^{87}/Sr^{86} ratios of basalt and dolerite from Antarctica and Tasmania.

regions in the upper mantle, or were subsequently contaminated in varying degrees with radiogenic Sr^{87}, derived presumably from rocks of the sialic crust.

The two specimens of pyroxenite from the Dufek Massif have an initial Sr^{87}/Sr^{86} ratio of 0.7093±0.0006. This value is somewhat lower than the initial ratios of basaltic rocks of the Ferrar Group elsewhere in the Transantarctic Mountains. Nevertheless, its initial ratio is unusually high compared to normal continental basalts and gabbros which suggests that the Dufek Massif should be included in the Ferrar Group.

The Tertiary basalts of the McMurdo Volcanics as well as the Recent basalts of Deception Island have normal Sr^{87}/Sr^{86} ratios of about 0.704, in marked contrast to the Mesozoic basalts and dolerites of the Ferrar Group. Evidently the source regions in the upper mantle, from which these rocks were presumably derived, have a normal Rb/Sr ratio. This is all the more significant because the samples of McMurdo Volcanics analyzed by Jones (1969) originated from Victoria Land, between Cape Hallet and Taylor Valley, where the Mesozoic basalts and dolerites have anomalously high initial Sr^{87}/Sr^{86} ratios.

CORRELATIONS OF INITIAL Sr^{87}/Sr^{86} RATIOS WITH BULK CHEMICAL COMPOSITION

The most significant new information derivable from our data is the apparent positive correlation of the SiO_2 content and initial Sr^{87}/Sr^{86} ratios of the Mesozoic tholeiites of Antarctica, shown in Figure 2. The tholeiites from Queen Maud Land have consistently lower initial Sr^{87}/Sr^{86} ratios and SiO_2 concentrations than the tholeiites of the Transantarctic Mountains. Within each group, SiO_2 and initial Sr^{87}/Sr^{86} ratios are positively correlated and the two suites together form a reasonably colinear array, approximately indicated by the straight line drawn in Figure 2.

The correlation of SiO_2 and Sr^{87}/Sr^{86} ratios is particularly well shown by the suite of samples of Kirkpatrick Basalt from a sequence of flows exposed on Storm Peak of the Marshall Mountains in the Queen Alexandra Range. The petrology and bulk chemical composition of these flows are described by Elliot (1970). Six specimens of basalt from this locality, each representing a different flow, are plotted separately in Figure 2 and clearly define a straight line. The silica concentration decreases from the bottom of the succession toward the top, as does the initial Sr^{87}/Sr^{86} ratio. This relationship cannot be produced by magmatic differentiation, but rather indicates that the silica content and the Sr^{87}/Sr^{86} ratio of individual flows result from the addition of silica and radiogenic Sr^{87} to the magma prior to or during extrusion.

A positive correlation of the Sr^{87}/Sr^{86} ratio and SiO_2 content was

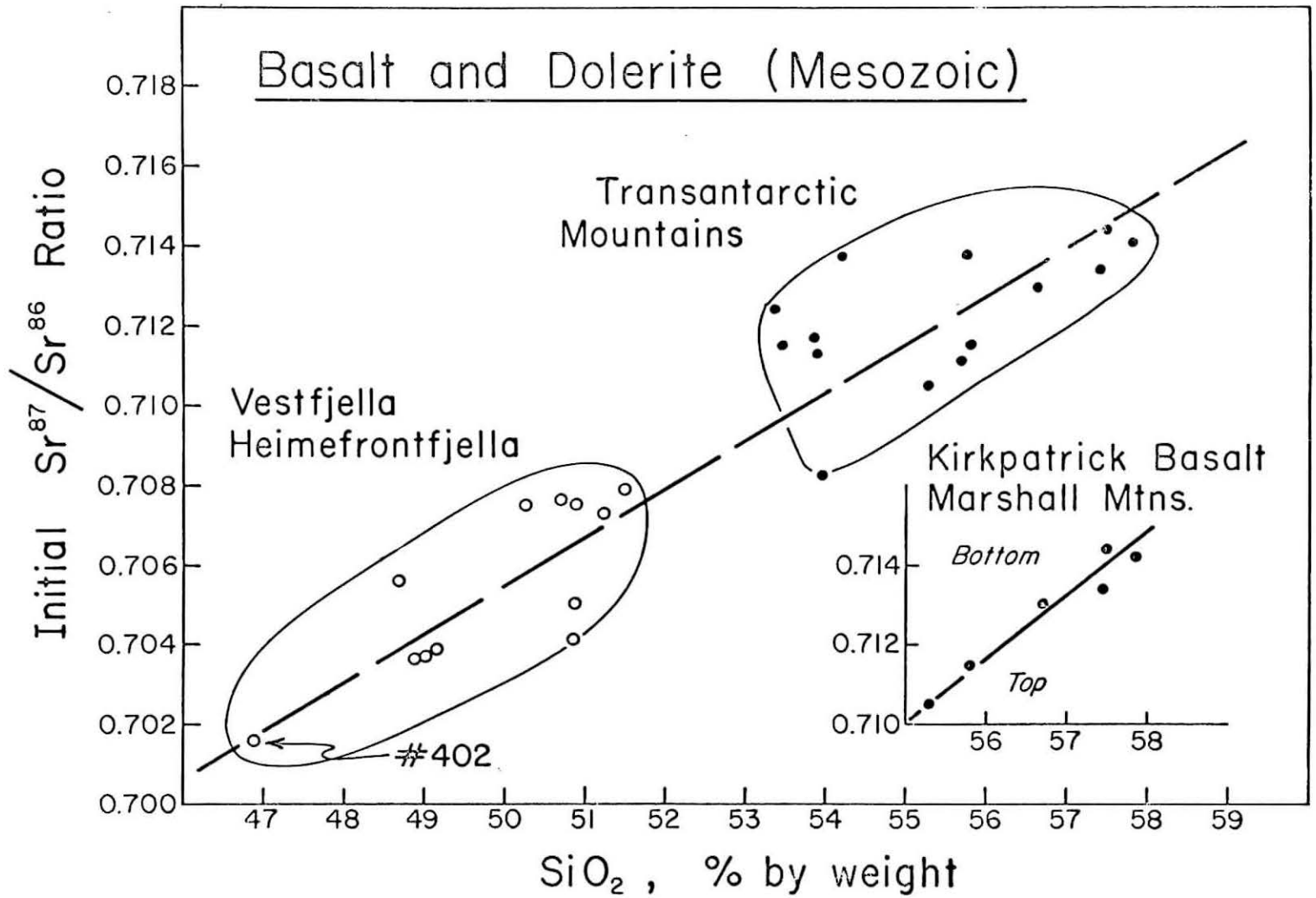

Figure 2. Correlation of initial Sr^{87}/Sr^{86} ratios with concentrations of SiO_2 for Mesozoic basalt and dolerite from Antarctica.

reported also by Bell and Powell (1969) for potassium-rich lavas of the Birunga and Toro-Ankole regions of east and central equatorial Africa. On the basis of this and similar correlations of Sr^{87}/Sr^{86} and Rb/Sr ratios, they suggested that the highly differentiated volcanic rocks in this petrographic province were produced by mixing of basalt magma with old, alkali-rich granodiorite, rather than by magmatic differentiation.

Among the samples from Queen Maud Land specimen #402 (2.391.5 of Juckes, 1968) is of special interest. It is a chilled olivine dolerite from the upper margin of a differentiated sill (5 m thick) at Wildskorvene, Mannefallknausane. The petrology and chemistry of this sill was discussed in considerable detail by Juckes (1968). This specimen has the lowest initial Sr^{87}/Sr^{86} ratio (0.7018), lowest K_2O and SiO_2 content, and the highest concentration of Ni of any of the basalts and dolerites included in this study. The Sr^{87}/Sr^{86} ratio of this rock was measured in triplicate with excellent results (Appendix 1). Its initial Sr^{87}/Sr^{86} ratio is identical to those of oceanic olivine basalts reported by Tatsumoto, Hedge and Engel (1965) and is, in fact, among the lowest values ever recorded in terrestrial rocks. The position of this rock in Figure 2 relative to the others suggests that it could be regarded as representing a possible parent magma from which the other basaltic rocks were derived by progressive additions of radiogenic Sr^{87} and silica.

The extent to which the initial Sr^{87}/Sr^{86} ratios correlate with other chemical components can be examined in Figure 3. Concentrations of CaO and MgO for rocks from the Queen Alexandra Range and CaO, MgO, and Na_2O for rocks from Queen Maud Land are from Elliot (1970), and Juckes (1968), respectively. The diagrams show not only the degree of correlation of initial Sr^{87}/Sr^{86} ratios with various oxides and elements, but also allow comparisons of their concentrations in the two suites.

Examination of Figure 3 suggests to us that K_2O and Rb correlate positively, while CaO, MgO, Sr, and Ni correlate negatively with initial Sr^{87}/Sr^{86} ratios. No correlation is indicated for Na_2O and total iron.

These apparent relationships between initial Sr^{87}/Sr^{86} ratios and chemical parameters suggest that mixing has played a significant role in determining the bulk chemical composition of these rocks. If specimen #402 is taken as one end member, the other component must have had significantly higher concentrations of SiO_2, K_2O, and Rb, and lower concentrations of CaO, MgO, Sr, and Ni, in addition to having a higher Sr^{87}/Sr^{86} ratio. However, we emphasize the tentative nature of these deductions because they are based on a limited number of specimens drawn from two different petrologic suites whose genetic and age relationship is still uncertain. Moreover, Elliot (1970) has pointed out that the unusually low MgO and CaO concentrations of the Kirkpatrick Basalts may be due to early crystallization of orthopyroxene. The

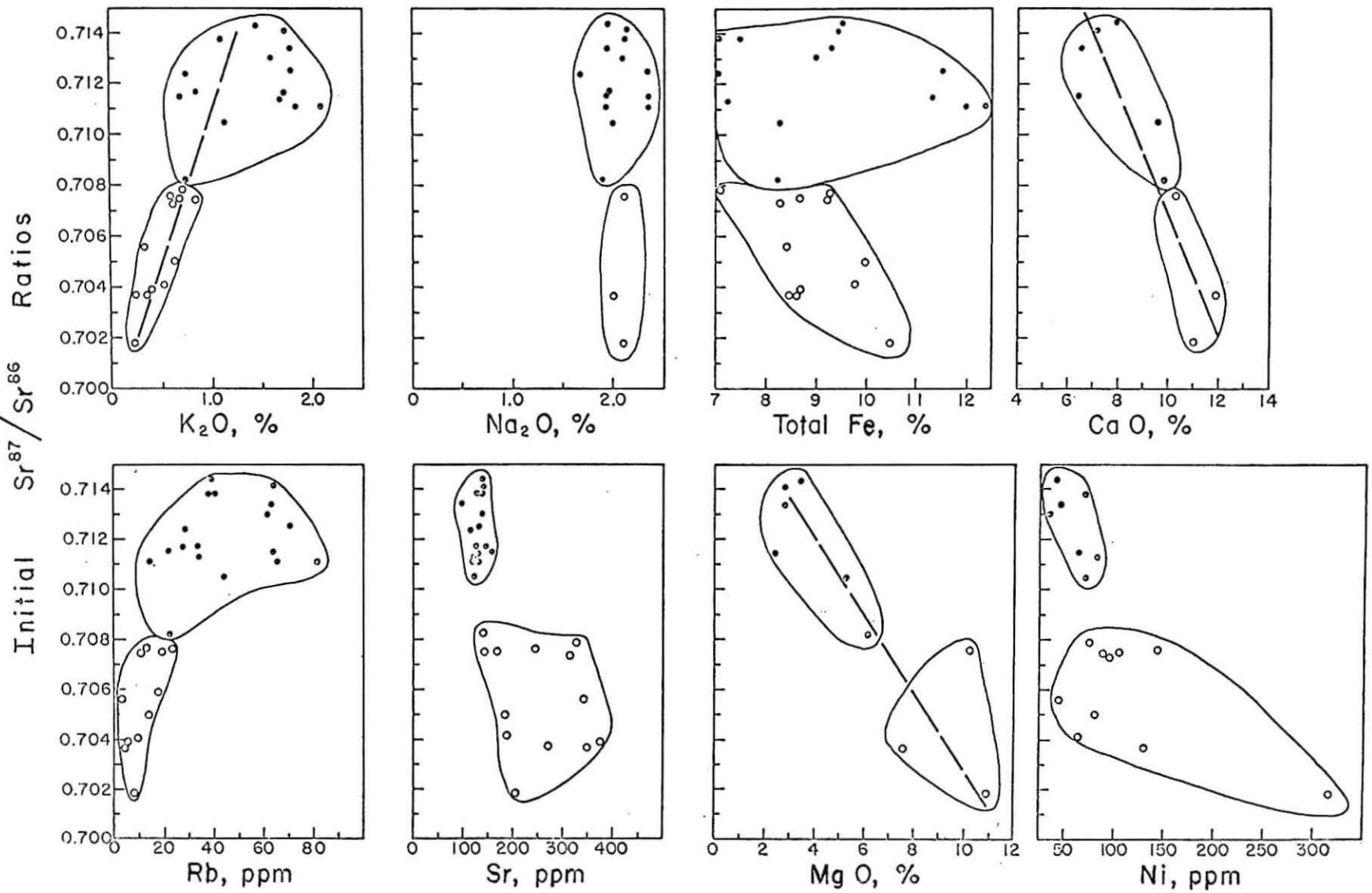

Figure 3. Relationship of initial Sr^{87}/Sr^{86} ratios of Mesozoic basalt and dolerite from Antarctica with concentrations of K_2O, Na_2O, CaO, MgO, Rb, Sr, and Ni.

chemical compositions of these basaltic rocks is, therefore, due not only to mixing of two contrasting end members, but also to subsequent magmatic differentiation. This may account for the apparent variability of K_2O, total Fe, and Rb in the tholeiites of the Ferrar Group.

Table II summarizes the apparent differences and similarities of the chemical composition of the two suites. The tholeiites of the Ferrar Group of the Transantarctic Mountains are enriched in SiO_2, K_2O, and Rb, but are depleted in MgO, CaO, Sr, and Ni compared to the basalts and dolerites from Queen Maud Land. Concentrations of Al_2O_3, total Fe, and Na_2O are similar.

The K/Rb ratio is of special interest because different rock types tend to have different values of this ratio. Our data indicate an average K/Rb ratio of 238±8 ($\bar{\sigma}$) for basaltic rocks of the Ferrar Group, in excellent agreement with values reported by Compston et al. (1968). The rocks from Queen Maud Land, on the other hand, have more variable ratios ranging from 206 to 812 with an average of 443±110 ($\bar{\sigma}$). The higher value of the K/Rb ratio of the basaltic rocks from Queen Maud Land is consistent with average K/Rb ratios of basic rocks, compiled by Erlank (1968, p. 880). Juckes (1970) has recently published trace element concentrations of dolerites from Queen Maud Land and found K/Rb ratios ranging from 83 to 771.

CONCLUDING REMARKS

The information presented here suggests strongly that the chemical compositions of the Mesozoic basalts and dolerites of Antarctica have been affected by mixing of basalt magma with sialic material, presumably derived from the underlying Precambrian basement. The process by which this mixing occurred is not clear, but could include assimilation or partial melting of the granitic basement or selective diffusion of ions from the country rock into the magma (Pankhurst, 1969).

These tentative conclusions emphasize the need for additional studies of the relationship of initial Sr^{87}/Sr^{86} ratios and chemical compositions of lava flows and sills in specific localities. Such data can be used to calculate the chemical composition of the contaminant by models developed by Powell (1969) and used by Bell and Powell (1969) to explain the petrogenesis of alkali basalts in the African rift valleys.

The important conclusion emerging from these studies is that the variety of rock types within a petrographic province can result not only by magmatic differentiation, but also by progressive contamination of a basaltic parent magma with granitic material derived from the continental crust.

Table II. Comparison of Some Major and Trace Element Concentrations in Tholeiites from the Transantarctic Mountains and Queen Maud Land.

	Transantarctic Mountains	Queen Maud Land
SiO_2	55.33 (14)	49.93 (12)
Al_2O_3	12.67* (6)	13.22* (3)
MgO	3.74* (6)	8.65* (3)
CaO	7.87* (6)	11.04* (3)
Total Fe	9.26 (14)	8.92 (12)
Na_2O	2.05 (14)	2.07* (3)
K_2O	1.37 (14)	0.517 (12)
Rb	47.1 (19)	11.2 (12)
Sr	131.0 (18)	258.8 (12)
Ni	59 (7)	114 (10)
K/Rb	238±8 ($\bar{\sigma}$) (14)	443±110 ($\bar{\sigma}$) (12)

*Data from Elliot (1970) and Juckes (1968), respectively, for samples whose Sr^{87}/Sr^{86} ratios were analyzed by us.

ACKNOWLEDGMENTS

We are grateful to many individuals who shared their rock collections with us: R. J. Adie, H. S. Gair, D. McLelland, J. M. Murtaugh, and others. The specimens from Deception Island were collected by C. H. Schultz. René Eastin, R. P. Rao, and R. H. Carwile assisted with the analyses. Mrs. K. E. Freudenreich drafted the figures and the manuscript was typed by Mrs. Helen Jones. This research was supported by the National Science Foundation through Grants No. 898-X (G. Faure), GA-1159 (D. H. Elliot) and GA-4146 (C. H. Shultz).

Appendix I. Analytical Data for Basalts and Dolerites of the Ferrar Group and from Queen Maud Land.

Sample	Description	SiO_2, %	Na_2O, %	K_2O, %	Total Fe, %	Ni (ppm)	Rb (ppm)	Sr (ppm)	$\frac{Sr^{87}}{Sr^{86}}$	Initial $\frac{Sr^{87}}{Sr^{86}}$
Scarab Peak and Illusion Hills, Northern Victoria Land										
296	Basalt	--	2.34	1.79	11.5	--	70.4	131.5	0.7158	0.7125
297	Basalt	55.69	2.35	1.83	12.0	--	64.7	130.4	0.7141	0.7111
298	Basalt	--	1.95	2.09	12.4	--	80.8	130.0	0.7150	0.7111
299	Basalt	53.34	1.67	0.755	7.0	--	28.0	114.5*	0.714	0.7124
300	Dolerite	55.78	2.11	1.09	7.51	--	39.5	141.2	0.7155	0.7138
Wright and Taylor Valleys, Southern Victoria Land										
310	Dolerite	--	--	--	--	--	86.0	--	0.7121	--
368	Dolerite	--	--	--	--	--	33.0	123.8	0.7134	0.7117
Dv-66-160	Dolerite	--	--	--	--	--	14.4	120.0	0.7118	0.7111
Marshall Mtns., Queen Alexandra Range										
332B	Basalt	57.84	2.12	1.74	9.45	--	64.1	141.0	0.7172	0.7141
333	Basalt	57.43	1.96	1.78	9.29	45	63.1	96.6	0.7179	0.7134
334	Basalt	57.52	1.94	1.47	9.47	40	38.9	140.3	0.7163	0.7144
335	Basalt	56.67	2.10	1.56	9.00	36	61.6	138.8	0.7160	0.7130
336	Basalt	55.27	2.02	1.15	8.29	71	44.1	123.9	0.7129	0.7105
365	Basalt	55.82	2.38	1.73	11.3	64	63.6	128.1	0.7149	0.7115
338	Dolerite	53.45	1.92	0.680	--	--	21.6	156.2	0.7124	0.7115
339	Dolerite	53.82	1.96	0.832	--	--	27.1	148.9	0.7127	0.7117
340	Dolerite	53.96	1.93	0.721	8.25	--	21.7	139.4	0.7093	0.7082
Nilsen Plateau, Queen Maud Mountains*										
175	Dolerite	53.91	--	--	7.24	82	33.6	124.5	0.7131	0.7113
185	Dolerite	54.16	--	--	6.90	73	38.4	129.1	0.7158	0.7138
Dufek Massif, Pensacola Mountains*										
410	Pyroxenite	46.46	0.049	0.022	--	50	2.1	395.7	0.7097	0.7097
411	Pyroxenite	51.94	0.306	0.100	--	--	8.9	19.8	0.7120	0.7089
Vestfjella, Mannefallknausane and Heimefrontfjella, Queen Maud Land*										
392	Basalt	51.26	--	0.614	8.32	97	13.4	310.0	0.7076	0.7073
393	Basalt	48.69	--	0.322	8.47	45	3.3	337.0	0.7057	0.7056
394	Basalt	50.92	--	0.523	9.78	63	10.0	187.5	0.7045	0.7041
395	Basalt	50.87	--	0.851	8.67	89	19.2	169.7	0.7083	0.7075
396	Basalt	50.26	--	0.687	9.25	103	10.8	144.7	0.7080	0.7075
398	Basalt	49.06	--	0.366	8.49	--	4.5	350.3	0.7038	0.7037
399	Basalt	51.33	--	0.738	7.08	74	18.2	325.1	0.7083	0.7079
400	Basalt	49.12	--	0.404	8.70	--	5.0	378.0	0.7040	0.7039
401	Dolerite	50.74	2.11**	0.573	9.25	144	23.0	247.0	0.7082	0.7076
402	Dolerite	46.94	2.11**	0.238	10.5	316	8.9	201.5	0.7018 0.7023 0.7023	0.7018
403	Dolerite	48.90	2.00**	0.242	8.59	130	4.3	269.4	0.7038	0.7037
397	Dolerite	5092	--	0.657	9.98	80	14.5	184.9	0.7055	0.7050

*Rb and Sr concentrations determined by XRF analysis
**Juckes, 1968, Table II

APPENDIX II

A. Basalt and Dolerite, Ferrar Group, from Scarab Peak and Illusion Hills, Northern Victoria Land, described by Gair (1967)

296 (Gair #1)
Basalt, collected from the top of a 67 m flow forming the top of Scarab Peak

297 (Gair #5)
Basalt, collected 2.7 m below #296 on Scarab Peak

298 (Gair #9)
Basalt, collected 67 m below #296 on Scarab Peak

299 (Gair #17)
Basalt, collected about 700 m below the top of Scarab Peak

300 (Gair #25)
Dolerite, collected within a few feet of the base of the lavas at Illusion Hills, described by Gair (1967, p. 337)

B. Dolerite, Ferrar Group, from Wright and Taylor Valleys, Southern Victoria Land

310 Dolerite, Taylor Valley, collected as float by J. M. Murtaugh in 1964/1965

368 Dolerite, Wright Valley, collected by R. E. Behling near Meserve Glacier, Wright Valley

DV-66-160
Dolerite, Wright Valley, collected by R. J. E. Montigny in 1966/1967

C. Basalt and Dolerite, Ferrar Group, Queen Alexandra Range, Beardmore Glacier

All specimens were collected by D. H. Elliot. The petrology of these rocks has been described by Elliot (1970).

332B (Elliot #27.1)
Basalt, north spur of Storm Peak, Marshall Mtns., Queen Alexandra Range, 40 m above the base of the Kirkpatrick Basalt flows

333 (Elliot #27.13)
Basalt, same locality, 278 m above the base of the flows

334 (Elliot #27.17)
Basalt, same locality, 308 m above the base of the flows

335 (Elliot #27.24)
Basalt, same locality, 363 m above the base of the flows

336 (Elliot #27.28)
Basalt, same locality, 428 m above the base of the flows

365 (Elliot #27.41)
Basalt, same locality, 543 m above the base of the flows

338 (Elliot #14-17)
Dolerite, from the top of a 164 m sill on the western side of Tillite Glacier, Queen Alexandra Range. Intrudes shale of the McKellar Fm and sandstone of the Fairchild Fm of Permian age

339 (Elliot #14-6)
Dolerite, same sill, same locality 97 m above the base

340 (Elliot #14-1)
Dolerite, same sill, same locality, collected near the base

D. Dolerite, Ferrar Group, Nilsen Plateau, Queen Maud Mountains

All specimens were collected by D. McLelland
175 Dolerite, Cougar Canyon, Nilsen Plateau
185 Dolerite, Cougar Canyon, Nilsen Plateau

E. Gabbro and Ultramafics, Dufek Massif, Pensacola Mtns.

These specimens were collected in December of 1957 by P. T. Walker and were described by Walker (1958, p. 209)

410 (Walker #W-36E)
Coarse-grained pyroxenite

411 (Walker #W-0-37)
Pyroxenite, with rusty-brown weathering crust

F. Basalt and Dolerite, Vestfjella, Mannefallknausane and Heimefrontfjella, Queen Maud Land

All specimens were collected by members of the British Antarctic Survey and were made available for study by R. J. Adie

Basalt

OSU No.	Field No.	Description
392	Z.308.4.	Lat. 74°37'S, long. 10°00'W. From the centre of a 16 m. thick flow near the base of the succession; eastern Bjørnnutane.
393	Z.310.2.	Lat. 74°37'S, long. 10°00'W. From the centre of a 6 m. thick flow near the base of the succession; eastern Bjørnnutane.
394	Z.349.1.	Lat. 74°29'S, long. 8°13'W. Specimen showing flow banding, from the base of the exposed succession at "BR Nunatak".
395	Z.350.1.	Lat. 74°29'S, long. 8°13'W. Coarse basalt from a thick flow (at least 16 m.) near the middle of the section at "BR Nunatak".
396	Z.350.2.	Lat. 74°29'S, long. 8°13'W. Lighter-colored basalt with trachytic texture from near the middle of the section at "BR Nunatak".
398	Z.370.1.	Lat. 74°36'S, long. 10°04'W. Coarse basalt from western Bjørnnutane.
399	Z.371.7.	Lat. 74°36'S, long. 10°06'W. Uppermost exposed part of the basal flow (at least 10 m. thick); collected from a small nunatak about 2 km. west of Bjørnnutane.
400	Z.372.1.	Lat. 74°36'S, long. 10°04'W. Coarse basalt from western Bjørnnutane; dated by the K-Ar whole rock method as 174 ± 7 m. yr.

Dolerite

397	Z.353.7.	Lat. 74°19'S, long. 9°49'W. Fine-grained dolerite from 2 m. below the upper contact of a 10 m. thick sill intruding? Lower Permian sediments; northeast Heimefrontfjella.
401	Z.388.1.	Lat. 74°36'S, long. 14°21'W. Basaltic dyke 0.6. m. wide, intruding Basement Complex gneisses, Mannefallknausane.
402	Z.391.5.	Lat. 74°35'S, long. 14°18'W. Chilled margin of a differentiated 5 m. thick sill of olivine-dolerite intruding Basement Complex gneisses; Mannefallknausane.

OSU No.	Field No.	Description
403	Z.395.1.	Approximate position: lat. 73°48'S, long. 14°30'W. Dolerite, presumably from a sill; Vestfjella.

REFERENCES

Allsopp, H. L. and Neethling, D. C., 1970, Rb-Sr isotopic ages of Precambrian intrusives from Queen Maud Land, Antarctica. Earth Planet. Sci. Letters, 8, 66-70.

Bell, K. and Powell, J. L., 1969, Strontium isotopic studies of alkalic rocks: The potassium-rich lavas of the Birunga and Toro-Ankole regions, east and central equatorial Africa. J. Petrology, 10, 536-572.

Compston, W., McDougall, I., and Heier, K. S., 1968, Geochemical comparison of the Mesozoic basaltic rocks of Antarctica, South Africa, South America and Tasmania. Geochim. Cosmochim. Acta, 32, 129-149.

Elliot, D. H., 1970, Major oxide chemistry of the Kirkpatrick Basalt, Central Transantarctic Mountains, Antarctica. SCAR Symposium, Oslo, Norway, August 6-15, 1970.

Erlank, A. J., 1968, The terrestrial abundance relationship between potassium and rubidium. In "Origin and Distribution of Elements", L. A. Ahrens, ed., Pergamon Press, Oxford and New York, 871-888.

Erlank, A. J. and Hofmeyer, P. K., 1968, K/Rb ratios in Mesozoic tholeiites from Antarctica, Brazil and India. Earth Planet. Sci. Letters, 4, 33-38.

Faure, G. and Elliot, D. H., 1970, Isotope composition of strontium in Mesozoic basalt and dolerite from Dronning Maud Land, Antarctica. Br. Antarct. Surv. Bull., in press.

Fleischer, M., 1969, U. S. Geological Survey standards - I. Additional data on rocks G-1 and W-1, 1965-1967. Geochim. Cosmochim. Acta, 33, 65-80.

Gair, H. S., 1967, The geology from the Upper Rennick Glacier to the coast, northern Victoria Land, Antarctica. New Zealand J. Geol. Geophys., 10, 309-344.

Gunn, B. M., 1966 Modal and element variation in Antarctic tholeiites. Geochim. Cosmochim. Acta, 30, 881-920.

Gunn, B. M., 1965, K/Rb and K/Ba ratios in Antarctica and New Zealand tholeiites and alkali basalts. J. Geophys. Res., 70, 6241-6247.

Gunn, B. M., 1962, Differentiation in Ferrar Dolerites, Antarctica. New Zealand J. Geol. Geophys., 5, 820-863.

Heier, K. S., Compston, W. and McDougall, I., 1965, Thorium and uranium concentrations, and the isotopic composition of strontium in the differentiated Tasmanian dolerites. Geochim. Cosmochim. Acta, 29, 643-659.

Heier, K. S. and Rogers, J. J. W., 1963, Radiometric determinations of thorium, uranium and potassium in basalts and in two magmatic differentiation series. Geochim. Cosmochim. Acta, 27, 137-154.

Hill, R. L., 1969, Strontium isotope composition of basaltic rocks of the Transantarctic Mountains, Antarctica. Unpublished M.S. Thesis, Dep . of Geology, The Ohio State University, Columbus, Ohio, U.S.A., 87 p.

Jones, L. M., 1969, The application of strontium isotopes as natural tracers: The origin of the salts in the lakes and soils of Southern Victoria Land, Antarctica. Unpublished Ph.D. dissertation, Geol. Dept., The Ohio State University, 336 p.

Juckes, L. M., 1970, Trace-element values for dolerites from Western Dronning Maud Land. Br. Antarct. Surv. Bull., No. 22, 95-98.

Juckes, L. M., 1968, The geology of Mannefallknausane and part of Vestfjella, Dronning Maud Land. Br. Antarct. Surv. Bull., No. 18, 65-78.

Manton, W. I., 1968, The origin of associated basic and acid rocks in the Lebombo-Nuanetsi igneous province, Southern Africa, as implied by strontium isotopes. J. Petrology, 9, 23-39.

McDougall, I., 1962, Differentiation of the Tasmanian dolerites: Red Hill dolerite-granophyre associated. Geol. Soc. Amer, Bull., 73, 279-316.

Pankhurst, R. J., 1969, Strontium isotope studies applied to petrogenesis in the basic igneous province of North-East Scotland. J. Petrology, 10, 116-145.

Philpotts, J. A. and Schnetzler, C. C., 1968, Genesis of continental diabases and oceanic tholeiites considered in light of rare-earth and barium abundances and partition coefficients. In "Origin and Distribution of the Elements," L. H. Ahrens, ed., Pergamon Press, Oxford and New York, 939-947.

Powell, J. H., 1969, Recognition of contamination in igneous rocks using strontium isotopes. Abstract. Geol. Soc. Amer., North-Central Section, Abstracts with Programs, Part 6, 37.

Rex, D. C., 1967, Age of a dolerite from Dronning Maud Land. Brit. Antarct. Surv. Bull., No. 11, 101.

Tatsumoto, M., Hedge, C. E., and Engel A. E. J., 1965, Potassium, Rubidium, strontium, thorium, uranium, and the ratio of strontium - 87 to strontium - 86 in oceanic tholeiitic basalt. Science, 150, 886-888.

Walker, P. T., 1958, Study of some rocks and minerals from the Dufek Massif, Antarctica. Inst. Polar Stud., The Ohio State Univ., Rept. #1, 209.

RUBIDIUM-STRONTIUM GEOCHRONOLOGY OF THE NIMROD GROUP, CENTRAL TRANSANTARCTIC MOUNTAINS

by
John D. Gunner and Gunter Faure
(Presented to SCAR Symposium, Oslo, Norway, August 6-15, 1970)

Institute of Polar Studies and Department of Geology,
The Ohio State University, Columbus, Ohio 43210, U.S.A.

ABSTRACT

Rudidium-strontium age determinations on high-grade metasedimentary rocks of the Nimrod Group in the central Transantarctic Mountains indicate that these rocks are at least 1.98×10^9 years old. An isochron on whole-rock samples suggests that the Nimrod Group underwent isotopic equilibration at this time to an initial Sr^{87}/Sr^{86} ratio of about 0.711. This may have occurred either during sedimentation and diagenesis or during metamorphism. A second whole-rock isochron indicates that parts of the Nimrod Group may have been isotopically re-equilibrated about 600 million years (m.y.) ago. It is postulated that this event was due to the Beardmore Orogeny. An internal isochron on a metasedimentary sample suggests that minerals in the Nimrod Group were isotopically re-equilibrated 456 ± 14 m.y. ago, at the time of the Ross Orogeny.

INTRODUCTION

In this paper we present the results of an attempt to date the time of sedimentation and regional metamorphism of the Nimrod Group by the rubidium-strontium (Rb-Sr) method. The Nimrod Group, defined by Grindley, McGregor and Walcott (1964, p. 209), crops out in the Miller and Geologists Ranges, located in the Nimrod Glacier region of the Transantarctic Mountains (Fig. 1). The Group includes a highly varied assemblage of rock types, principally of quartzo-feldspathic, pelitic, calcareous, and basic composition, as described by Grindley and others (1964, p. 209-210), Gunner (1969, p. 7-35), and Grindley and Laird (1969). All the rocks have been regionally metamorphosed to the almandine-amphibolite facies (Gunner, 1969, p. 35), and subjected to intense structural deformation. Several granitic stocks, of undoubted magmatic origin, intruded the Nimrod Group subsequent to its deformation. These have been included in the Hope Granite (see legend, Fig. 1), which was originally described by Mawson (1916) from the lower Beardmore Glacier, 100 km east of the Miller Range, and which is included in the Granite Harbour Intrusives (Gunn and Warren, 1962, p. 85).

The pre-Devonian stratigraphy of the region is tabulated in the legend of Fig. 1. The geology of the region has been described by Grindley and others (1964), Grindley and Laird (1969), Gunner (1969), and Barrett, Lindsay and Gunner (1970). East of the Marsh Glacier (Fig. 1) the oldest known geologic unit in the region is the Beardmore Group (Gunn and Walcott, 1962). This is a thick succession of predominantly detrital sedimentary rocks of geosynclinal aspect, which have been tightly folded and subjected to low-grade metamorphism. The Byrd Group (Laird, 1963), a sequence of shallow-water sediments dominated by carbonate rocks, overlies the Beardmore Group with angular unconformity (Grindley and Laird, 1969). The Byrd Group contains Lower Cambrian archeocyathids (Laird and Waterhouse, 1962) and is the oldest paleontologically-dated unit in the region. The Nimrod Group crops out only west of the Marsh Glacier and its relations to the Beardmore and Byrd Groups are hidden by glaciers. According to Grindley and Laird (1969), most of the folding of the Beardmore and Byrd Groups occurred in the Cambro-Ordovician Ross Orogeny (Gunn and Warren, 1962, p. 56), of which the emplacement of the Granite Harbour Intrusives was the intrusive phase. However, Grindley and others (1964, p. 211) have argued on structural and metamorphic grounds that the Nimrod Group was folded twice; i.e., in the Pre-cambrian during the Nimrod Orogeny of Grindley and Laird (1969), and again during the Ross Orogeny.

In the absence of fossils, the only available direct method of dating the Nimrod and Beardmore Groups is radiometric. Potassium-argon (K-Ar) age determinations on minerals from the Granite Harbour Intrusives and the Nimrod Group have been reported by McDougall and Grindley (1965) and by Grindley and McDougall (1969). Micas from an intrusion of Hope Granite and an associated pegmatite have K-Ar ages of 463 and

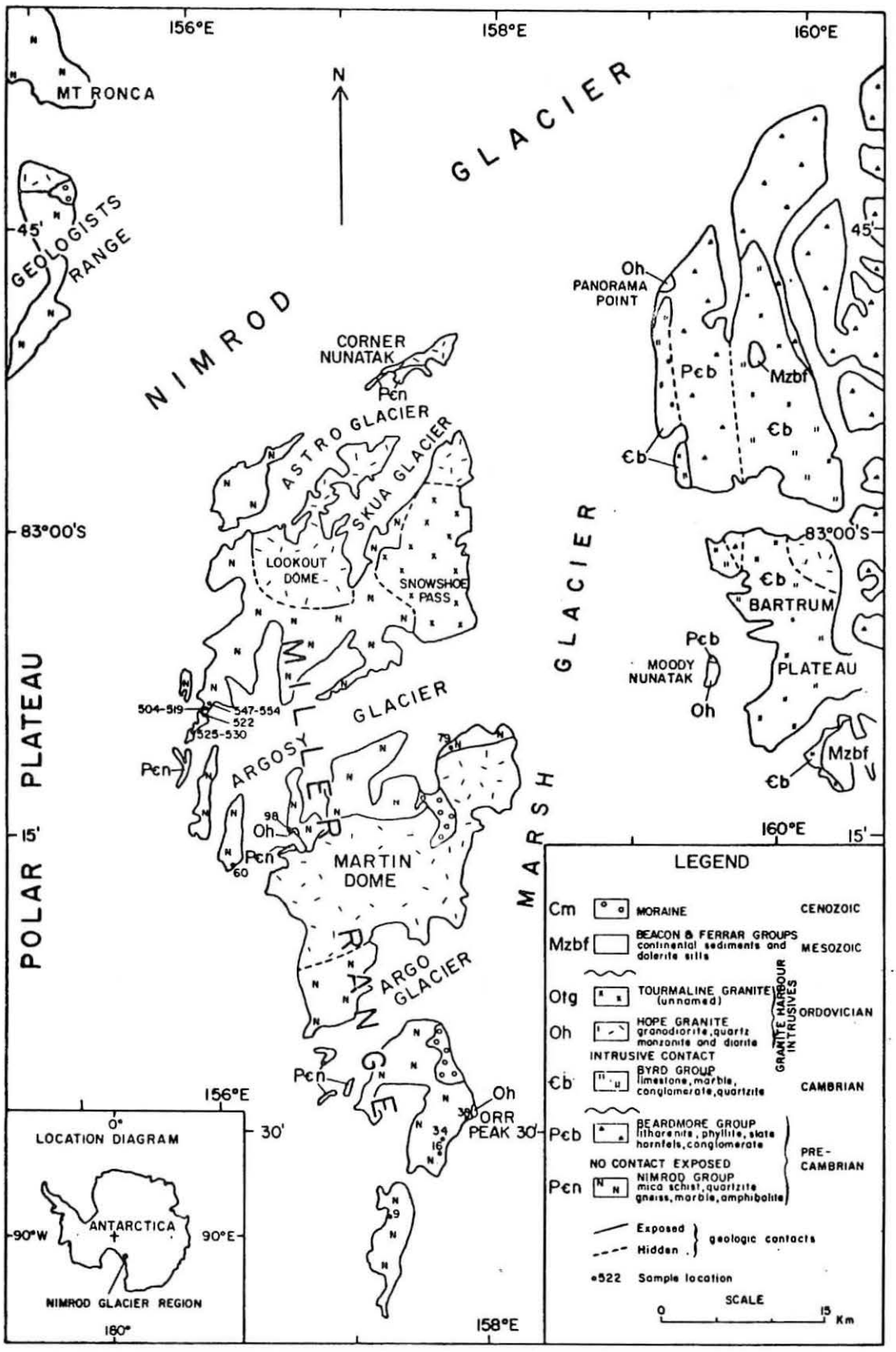

Figure 1. Geologic map of the Miller Range based on Grindley and Laird (1969), Gunner (1969), and Barrett and others (1970).

478 m.y., respectively. These results are consistent with the Cambro-Ordovician age now generally accepted for the Granite Harbour Intrusives and the Ross Orogeny. Less firm conclusions can be drawn from the K-Ar mineral ages of Nimrod Group metasediments reported by McDougall and Grindley (1965). Of seven muscovite and biotite ages, five fall in the range of 450 to 490 m.y., consistent with K-Ar ages of Hope Granite micas (McDougall and Grindley, 1965, p. 309). Only two biotites have significantly older apparent dates, 520 and 630 m.y. McDougall and Grindley interpreted this scatter of apparent ages as a "typical pattern of argon loss" imposed on the micas by the thermal event which affected the region during the emplacement of the Hope Granite plutons. They inferred a Precambrian regional metamorphism of the Nimrod Group, for which 630 m.y. was a minimum age.

A study of K-Ar dates of hornblendes from amphibolites within the Nimrod Group led Grindley and McDougall (1969) to draw broader conclusions regarding the Precambrian history of East Antarctica. Dates on five hornblende samples were reported. These were, in order of increasing age, 528 ± 5, 618 ± 6, 1006 ± 9, 1011 ± 9, 1043 ± 16 m.y. (Grindley and McDougall, 1969, p. 396). The authors reached the tentative conclusion that the cluster of the three oldest dates around an average of 1020 m.y. gave an estimate of the age of high-grade metamorphism during the Nimrod Orogeny.

The major long-term objectives of our current study of the Nimrod Group are four-fold: (1) to obtain detailed documentation of the Nimrod Orogeny, which appears to be the earliest known geologic event in the Transantarctic Mountains; (2) to search for evidence bearing on the early history of the closely adjacent East Antarctic Shield; (3) to evaluate the hypothesis that the Nimrod Group is a cratonic sedimentary deposit of the ancestral East Antarctic Shield; and (4) to determine the time-stratigraphic relationship between the Nimrod and Beardmore Groups.

Age determinations on sediments of the Rb-Sr method were first described by Compston and Pidgeon (1962). It is now well established that, under favorable conditions, unmetamorphosed sedimentary rocks can be dated by the isochron technique (Moorbath, 1969). A summary of this method and of its recent applications to sedimentary rocks is given by Moorbath (1969, p. 157). In principle the method should be applicable to metasedimentary rocks as well. Provided that the rocks have remained closed to Rb and Sr, an isochron on whole-rock metasedimentary samples should date the time when they last had the same or similar Sr^{87}/Sr^{86} ratios, which, in this case, is likely to be the time of initial recrystallization of the sediments. An internal isochron on mineral separates from a single rock, on the other hand, should date the last time these minerals were isotopically equilibrated. It is possible that, in the case of a polymetamorphic rock, the whole-rock Rb-Sr isochron may record the first recrystallization, while mineral isochrons may record the last metamorphic event.

Samples studied were collected from the Nimrod Group in the Miller Range by one of us (J.G.) during the 1967-1968 and 1969-1970 field seasons (samples numbered 9-98 and 504-554, respectively). Sample descriptions are given in the Appendix.

ANALYTICAL METHODS

Representative whole-rock samples of about 75 g were sawn or chipped from fist-sized hand specimens, ground to less than 200 mesh (U.S. standard), and homogenized in a Spex Industries mixer mill. Mineral fractions were prepared using standard magnetic and heavy liquid separation techniques. Procedures for sample dissolution and separation of Rb and Sr followed those described by Chaudhuri and Faure (1967).

Rb and Sr were determined for ten whole-rock samples and mineral separates by isotope dilution, using spikes enriched in Rb^{87} and Sr^{86}, respectively. All isotopic determinations were made on a Nuclide Corp. mass spectrometer with a 6-inch radius analyzer tube (Model 6-60-S). Sr^{87}/Sr^{86} ratios were normalized to $Sr^{86}/Sr^{88} = 0.1194$. Six analyses of the Eimer and Amend Sr-isotope standard in this laboratory during 1969 and 1970 have a mean normalized value of 0.7076.

Rb/Sr ratios were determined for 22 samples by X-ray fluorescence, using an air-path G.E. X-ray spectrometer (Model XRD-6), with LiF (220) analyzing crystal, scintillation counter, and molybdenum target tube operated at 70 kV (peak) and 50 ma. Analysis with this instrument of five U.S. Geological Survey rock standards and of 44 laboratory standards has demonstrated that a linear relationship exists between the RbKα/SrKα peak intensity ratio and the Rb/Sr weight ratio, as determined by isotope dilution (Eastin, 1970). The peak intensity ratio is independent of the mass absorption coefficient, and the Rb/Sr weight ratios can therefore be determined from it by applying a constant factor. For purposes of dating by the Rb-Sr method, only Rb/Sr ratios are needed, and it is therefore not necessary to determine Rb and Sr concentrations separately. For the nine samples in this study which were analyzed by both isotope dilution and X-ray fluorescence techniques, the Rb^{87}/Sr^{86} ratios agree within the statistically determined errors. It has been found that, for most samples which have Rb and Sr concentrations greater than about 25 ppm, the reproducibilities of the Rb^{87}/Sr^{86} ratios determined by the two methods are of the same order of magnitude.

Straight-line isochrons were fitted to points on isochron diagrams by the "least squares cubic" method of York (1966). Rb^{87}/Sr^{86} and Sr^{87}/Sr^{86} ratios were weighted in proportion to their standard deviations for these computations. A value of 1.39×10^{-11} yr $^{-1}$ was used for the decay constant of Rb^{87}. Errors are given as one standard deviation, unless otherwise stated.

DISCUSSION OF RESULTS

Analytical results are given in Table I. Isochron diagrams are plotted in Figs. 2, 3, and 4. Figure 2 presents data on three mineral fractions separated from a single rock (sample 522). Data for the whole-rock are plotted as a fourth point. The four points closely approximate colinearity, and a straight-line isochron has been fitted to them by the least squares method described above. From the slope of this line and its zero intercept, an apparent age of 456 ± 14 m.y., and an initial Sr^{87}/Sr^{86} ratio of 0.7511 ± 0.0007 have been calculated. If the biotite analysis is neglected, a second isochron can be drawn through the three remaining points. This line has a slightly steeper slope than the first and yields an age of 561 ± 23 m.y. and an initial Sr^{87}/Sr^{86} ratio of 0.7478 ± 0.0003.

An internal mineral isochron dates the time when the minerals were last isotopically re-equilibrated, and indicates that the minerals have remained closed to Rb and Sr since that time. The apparent age of 456 m.y. calculated from the four-point isochron is in excellent agreement with the K-Ar ages of micas from Hope Granite intrusions and Nimrod Group metasediments (McDougall and Grindley, 1965, p. 308-309). The inclusion of the biotite point gives the isochron a much greater spread of Rb/Sr ratios and improves the precision of the date. For these reasons we consider 456 ± 14 m.y. to be the better estimate of the Rb-Sr internal isochron age of sample 522. It represents the time when the rocks in the region cooled sufficiently for quantitative retention of radiogenic Sr^{87} in minerals to begin and corresponds to the time of cooling of the Hope Granite and associated intrusions, as determined by K-Ar studies.

The initial Sr^{87}/Sr^{86} ratio (0.7511) of the minerals in sample 522 is high compared with average values for mantle-derived igneous rocks (Faure and Hurley, 1963), but is consistent with the interpretation that sample 522 had an extensive pre-Ordovician geologic history, prior to isotopic equilibration during the Ross Orogeny.

The analytical results for 19 whole-rock samples of the Nimrod Group are plotted in Fig. 3. The points scatter widely on the diagram. This indicates that the samples either (1) had different initial Sr^{87}/Sr^{86} ratios, and/or (2) have different ages, and/or (3) have gained or lost variable amounts of Rb and Sr. Although no single isochron fits the data, all the points lie between two limiting isochrons of ages 3720 m.y. and 602 ± 38 m.y. (Fig. 3). Isochron I (upper limit was drawn through sample 530 and is based on an assumed initial Sr^{87}/Sr^{86} ratio of 0.704. Sample 518 has been omitted, since it gives a date of about 20×10^9 years based on this model, which is a geologically meaningless result. We interpret the date of 3720 m.y. (isochron I) as a maximum estimate of the age of the Nimrod Group. The lower isochron (isochron II, Fig. 3) is a "best-fit" straight line for samples 9, 16, 34, 60, 79, and 98. We interpret the date of 602 ± 38 m.y. given by this isochron as a lower limit for the age of the Nimrod Group.

Table I. Rb-Sr Analytical data - Nimrod Group (Whole-rock samples)

Sample	Description	Isotope Dilution			X-ray fluorescence
		Sr^{87}/Sr^{86}	Rb(ppm)	Sr(ppm)	Rb^{87}/Sr^{86}	Rb^{87}/Sr^{86}
9	Andesine-hornblende amphibolite	0.7117	13.86	224.9	0.1785	0.1942
16	Plagioclase-quartz-diopside -orthoclase-biotite schist	0.7232				1.194
34	Augite-biotite-hornblende -plagioclase schist	0.7169				1.357
38	Hornblende-biotite gneiss	0.7799				1.978
60	Microcline augen gneiss	0.7447				4.348
79	Chloritoid-garnet-biotite schist	0.8668	301.4	53.74	16.49	15.23
98	Biotite-hornblende schist	0.8505	250.8	40.74	18.07	17.22
504	Granitic dike	1.0115	188.7	49.26	11.42	11.60
512	Microcline pegmatite	0.7642				3.869
517	Epidote-hornblende schist	0.7257				0.8166
518	Epidote-hornblende-diopside gneiss	0.7308				0.0809
519	Muscovite-kyanite-biotite metaquartzite	0.7775	59.09	70.06	2.458	2.440
522	Biotite-microcline-oligoclase augen gneiss	0.7666				2.393
525	Granitic gneiss	1.0631 1.0561	199.6	75.55	7.910	7.287
530	Leucocratic granite-gneiss	0.7939				1.694
547	Biotite-quartz-hornblende schist	0.7358	91.05	287.9	0.9180	0.8825
549	Fuchsite metaquartzite	1.6043 1.6287	125.0	12.60	31.24	30.86
552	Andesine-biotite-hornblende schist	0.7587				2.026
554	Biotite-plagioclase-microcline gneissic metaquartzite	0.7535				1.082
Sample 522- mineral separates and whole-rock						
	Biotite	0.9761 0.9918	787.1	63.50	36.85	
	K-feldspar	0.7723	321.8	293.1	3.199	3.343
	Quartz-plagioclase	0.7578				1.294
	Whole-rock	0.7666				2.393

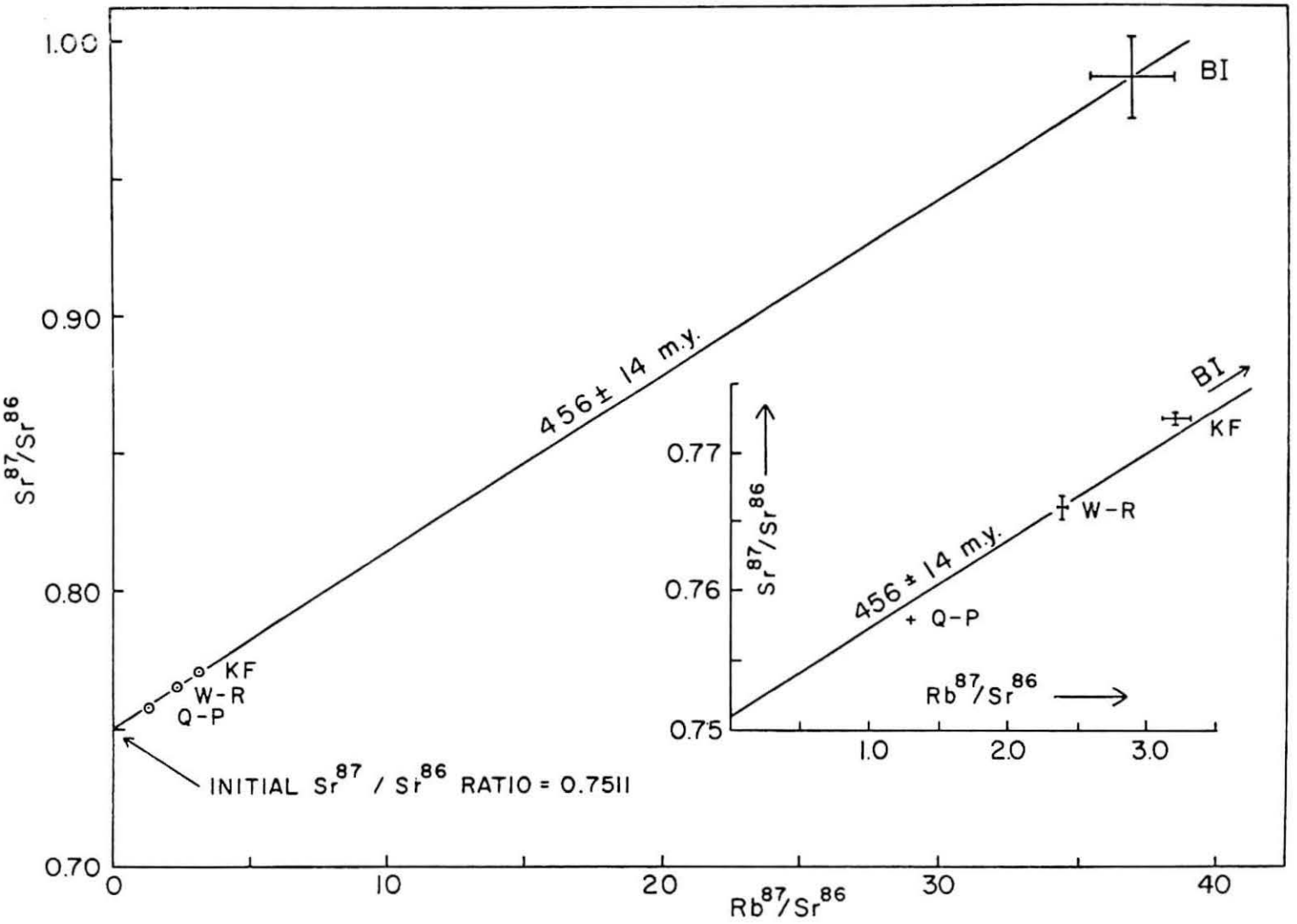

Figure 2. Internal Rb-Sr isochron for mineral fractions and whole-rock sample of specimen 522.

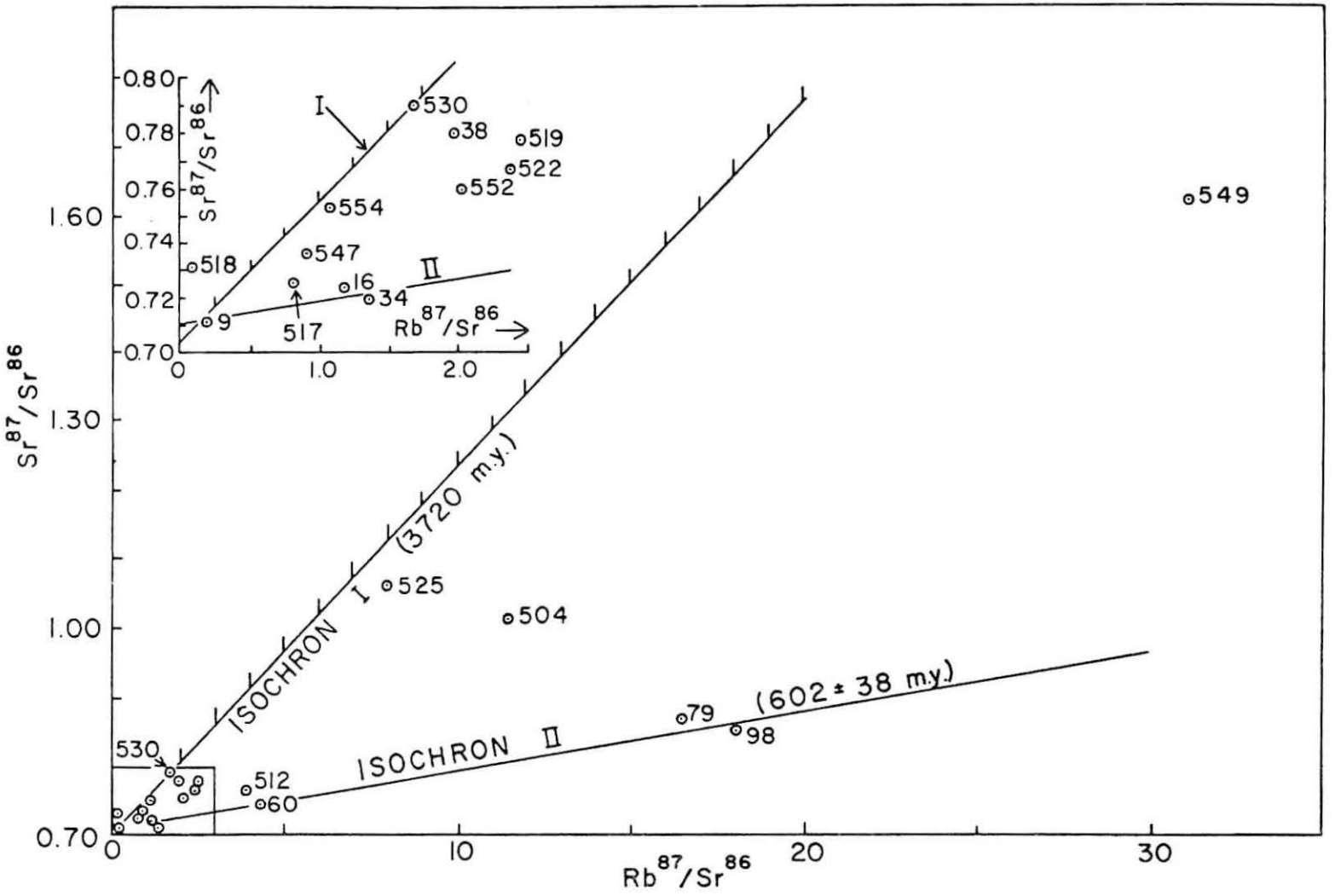

Figure 3. Limiting Rb-Sr isochrons for 19 whole-rock samples from the Nimrod Group.

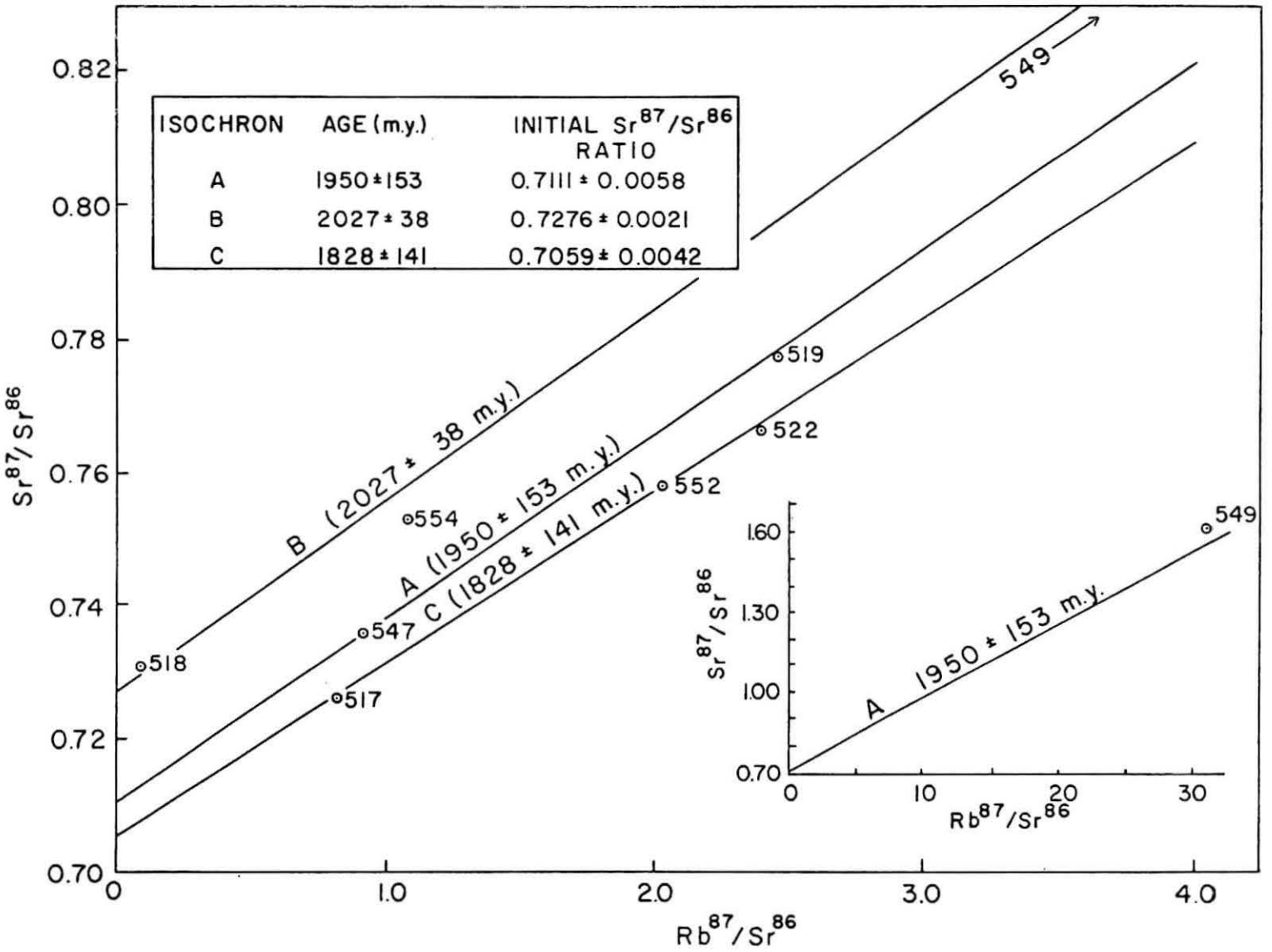

Figure 4. Rb-Sr isochron diagram for whole-rock metasedimentary samples which satisfy criteria (1), (2) and (3).

This isochron has wider geological implications, which are discussed later in this paper. If an isochron is fitted to all the points in Fig. 3, assigning equal weight to each point, an apparent age of 1615 ± 221 m.y. and an initial Sr^{87}/Sr^{86} ratio of 0.706 ± 0.031 are obtained.

A geologically more meaningful approach is to attempt to group the samples on the basis of some common property. It became clear to us at an early stage of this study that a relationship existed between the location and rock type of the samples, on the one hand, and their positions on an isochron diagram, on the other. Consequently the samples plotted in Fig. 4 were selected on the basis of three criteria; i.e., (1) they were collected from a small area (Fig. 1), (2) they were distant (at least 12 km) from outcrops of Hope Granite, and (3) their field relations and petrographic characters indicate that they have not had molten histories. Samples which fail to satisfy criteria (1) and (2) (9-98) and (3) (504, 512, 525, 530) have been omitted from the following discussion.

The points in Fig. 4 which satisfy our criteria are not colinear, but they are grouped in a definite band, to which certain limiting slopes can be assigned. This indicates to us that these samples were isotopically re-equilibrated at the same time and have remained closed to Rb and Sr since, although they may have had different initial Sr^{87}/Sr^{86} ratios. Isochron A includes all the eight points in Fig. 4. For it we have calculated a date of 1950 ± 153 m.y. and an initial Sr^{87}/Sr^{86} ratio of 0.7111 ± 0.0058. In addition, we have plotted two isochrons (B and C in Fig. 4) which fit points near the upper and lower margins of the band (isochron B: samples 518, 549 and 554; and isochron C: samples 517, 522 and 552). Results for all three isochrons are tabulated in Fig. 4. Isochrons B and C give dates of 2027 ± 38 m.y. and 1828 ± 141 m.y., and initial Sr^{87}/Sr^{86} ratios of 0.7276 ± 0.0021 and 0.7059 ± 0.0042, respectively.

There is a significant difference between the initial Sr^{87}/Sr^{86} ratios calculated for isochrons B and C, which leads to corresponding high errors in the initial ratio (σ = 0.0058) and in the date (σ = 153 m.y.) indicated by isochron A. We interpret the difference in the initial ratios as being due to incomplete isotopic homogenization of these samples at the time of equilibration. If isotopic equilibration is complete, a group of samples should have identical Sr^{87}/Sr^{86} ratios, and they should lie on a single isochron at any later time. However, if the initial ratios of the samples were variable, the points will scatter about the isochron. We believe that the scatter of points in Fig. 4 results from differences in the initial ratios of the samples.

The close agreement of the dates computed for isochrons A, B, and C confirms our assumption that these samples have the same age. In order to minimize the effects of the differing initial Sr^{87}/Sr^{86} ratios, we have calculated a weighted mean of the slopes of isochrons B and C, weighting the slopes in proportion to their standard errors. The pooled

slope gives an isochron date of 1984 ± 77 m.y. This includes six of the points in Fig. 4, and the date does not differ significantly from the date of 1950 ± 153 m.y., calculated for all eight points (isochron A). However, the precision of the date is much improved by the pooling procedure, which eliminates the interference of differing initial ratios.

We consider that 1984 ± 77 m.y. is the best estimate of the age of the samples in Fig. 4. The Nimrod Group therefore appears to be 1.98×10^9 years old, or older, and thus may be one of the oldest rock units in the crystalline basement complex of the Transantarctic Mountains.

Although samples 9-98 do not satisfy criteria (1) and (2), they do satisfy the "non-molten" criterion (3). Five of these samples (34-98) do not fit either isochrons A, B, or C (Fig. 4). Sample 38 will be omitted from further consideration because it was collected 200 m from a granite stock, and its field relations and petrography suggest to us that it has been metasomatically contaminated, possibly by hydrothermal alteration during intrusion of the Hope Granite. Contamination by material rich in radiogenic Sr^{87} could explain the anomalously high Sr^{87}/Sr^{86} ratio of this sample. The remaining samples (9, 16, 34, 60, 79, and 98) fit an isochron reasonably well (isochron II, Fig. 3), giving an age of 602 ± 38 m.y. and an initial Sr^{87}/Sr^{86} ratio of 0.7099 ± 0.0033. We tentatively interpret this isochron as an indication that these samples underwent isotopic re-equilibration about 600 m.y. ago. Samples 9 and 16 can be fitted to both the 600 m.y. and the 1950 m.y. isochrons (Figs. 2 and 4) without significantly affecting their slopes. It cannot be determined from available data whether samples 9 and 16 were subjected to the 600 m.y. isotopic equilibration.

It may be significant that samples 34, 60, 79, and 98 are located closer to the granite outcrops of Martin Dome and Orr Peak than any of the other samples, except sample 38. It is possible that the emplacement of these granites may have been related to the postulated 600 m.y. isotopic equilibration. Radiometric dates have not been reported on the Martin Dome and Orr Peak granites. These rocks are grey, medium-grained, variably porphyritic, biotite-bearing mesocratic granitic types, probably granodiorite to quartz monzonite, and are macroscopically indistinguishable from the type Hope Granite. We cannot entirely exclude the possibility that the 600 m.y. date is a fictitious event caused by chemical alteration of these rocks during the Ross Orogeny. However, the date does coincide with the Beardmore Orogeny, which Grindley and McDougall (1969, p. 405) defined on the basis of deformational, metamorphic, and intrusive events which affected the Beardmore and related geosynclinal groups of the central Transantarctic Mountains in the late Precambrian. This orogeny corresponds to the Mawson Orogeny, a term proposed by Angino and Turner (1964, p. 553) on the basis of a grouping of radiometric dates from East Antarctica in the interval 600 to 800 m.y. ago.

Dates in the 600 to 700 m.y. interval for granitic rocks in the Transantarctic Mountains have been reported from the Thiel Mountains (Ford et al., 1963; Ford, 1964; Eastin, 1970), from the Wisconsin Range (Faure et al., 1968) and from the upper Amundsen Glacier (Eastin, 1970). There is, therefore, good evidence for orogenic activity in the central Transantarctic Mountains during the 600 to 700 m.y. interval. We conclude that the Beardmore Orogeny probably affected the Nimrod Group, causing isotopic re-equilibration of Sr in some of the samples studied. Further work is needed to determine the relation of this event to the granite plutons of the Miller Range.

SUMMARY

We can now attempt a synthesis of the geochronological data available on the Nimrod Group. The rocks were deposited in a shallow-water environment during the early Precambrian and were isotopically equilibrated about 1.98×10^9 years ago. The available data do not indicate whether this event occurred during transportation, deposition, and diagenesis of the original sediments, or during a later metamorphism. The 1000 m.y. dates on hornblendes reported by Grindley and McDougall (1969) may have been hybridized by partial loss of radiogenic argon during either the Beardmore or the Ross Orogenies, as suggested by Grindley and McDougall (1969, p. 393). Alternatively, these dates may record the time of crystallization of these hornblendes during a separate geologic event, not recorded by our Rb-Sr data. Thus, the Nimrod Orogeny may have occurred about 1.0×10^9 m.y. or about 1.98×10^9 m.y. ago. Presently available data do not allow us to distinguish between these alternatives. A U-Pb study of zircons from the Nimrod Group, currently in progress, may solve this problem.

About 600 m.y. ago at least part of the Nimrod Group may have experienced isotopic re-equilibration of Sr. Our data give the first suggestion of a geologic event at this date in the Nimrod Glacier region, although there is good evidence for orogenic activity at this time in other parts of the central Transantarctic Mountains. McDougall and Grindley (1965, p. 309) reported K-Ar ages of 520 m.y. and 633 m.y. of Nimrod Group biotites, but interpreted these as minimum ages because of partial loss of radiogenic argon. Grindley and McDougall (1969, p. 405) have suggested that the unconformity which separates the Beardmore and Byrd Groups (Fig. 1) in the Nimrod Glacier region is the expression of the Beardmore Orogeny. Our data can be interpreted to suggest that the Beardmore Orogeny affected the Nimrod Group also. The relation of this event to the granite plutons in the Miller Range is uncertain.

During the Ross Orogeny, the Nimrod Group was re-folded and intruded by stocks of Hope Granite and associated intrusives. Contact metamorphism and minor retrograde metamorphism affected rocks near the pluton margins. By about 450 m.y. ago all of the rocks in the Miller

Range had cooled sufficiently for quantitative retention of radiogenic Ar and Sr in minerals of both the Hope Granite and the Nimrod Group to begin.

The 1.98×10^9 m.y. minimum age of the Nimrod Group which we report affects our knowledge of the whole of East Antarctica. The extreme antiquity of the Nimrod Group suggests that it is part of the East Antarctic Shield, which is consistent with the supposition that the East Antarctic ice cap covers shield material. The Nimrod Group sediments may have accreted onto the ancestral nucleus of the East Antarctic Shield 1.98×10^9 years ago, or earlier. The wider implications of these results will be discussed in a later paper.

ACKNOWLEDGMENTS

We are indebted to the members of the 1967-1968 and 1969-1970 Ohio State University Institute of Polar Studies expeditions to the central Transantarctic Mountains, and especially to D. Johnston and Dr. I. C. Rust for able assistance and stimulating discussions in the field. Logistic support was provided by Squadron VXE-6 of the U. S. Naval Support Force, Antarctica, without whose help this study would not have been possible. We thank R. Eastin for advice and assistance in computer programming and for use of unpublished information, and our colleagues at the Institute of Polar Studies, The Ohio State University, who critically reviewed the manuscript. This research was financed by U. S. National Science Foundation Grants Nos. GA-898X, GA-1159 and GA-12315.

APPENDIX

DESCRIPTIONS OF SAMPLES STUDIED

Petrographic terminology follows that of Winkler (1967).

Sample locations are given in Fig. 1.

Modal analyses of samples 9, 16, 34, 38, and 79 are given by Gunner (1969, p. 4).

Minerals are fresh or very slightly altered unless otherwise stated.

Sample 9

Amphibolite; 2 m thick band in sequence of marble, quartzite, amphibolite, and garnet-biotite schist.

An unfoliated rock composed of hornblende and andesine, with abundant accessory biotite and sphene, and minor apatite.

Sample 16

Plagioclase-quartz-diopside-orthoclase-biotite schist; interbanded with quartzo-feldspathic gneiss and graphitic metaquartzite.

Occasional porphyroblasts of diopside set in a matrix of biotite, orthoclase, quartz, albite-oligoclase, and accessory sphene, apatite and epidote. The rock has a strong foliation and lineation due to preferred orientation of elongate biotite flakes.

Sample 34

Augite-biotite-hornblende-plagioclase schist; interfolded with banded gneiss, augen gneiss, mica schist, and metaquartzite.

Oligoclase-andesine, hornblende, biotite, augite, quartz, and accessory sphene and apatite, in a schistose, nematoblastic fabric. Augite crystals contain exsolution lamellae of hypersthene or pigeonite, parallel to (100).

Sample 38

Hornblende-biotite gneiss; interlayered with banded gneisses and schists, 200 m from margin of Hope Granite stock, Orr Peak.

Scattered porphyroblasts of microcline are set in a compositionally-banded matrix of quartz, albite, microcline, biotite, and hornblende. Biotite and hornblende tend to occur as discontinuous patches and laminae. Felsic minerals tend to be segregated into microcline-rich and quartz-albite-rich laminae. Sphene and apatite are accessory.

Sample 60

Microcline augen gneiss; interfolded with biotite-rich banded gneiss and schist, and grading into massive porphyroblastic gneiss.

Rounded augen of microcline-microperthite containing inclusions of sericitized albite-oligoclase are set in a granoblastic matrix of quartz, microcline-microperthite, albite-oligoclase, and myrmekite. Discontinuous patches and streaks of biotite-rich material, with monor zircon and clinozoisite, are scattered through the rock, defining a weak gneissic foliation. Cataclastic textures surround some feldspar augen.

Sample 79

Chloritoid-garnet-biotite schist; in sequence of metaquartzite, schist and metaconglomerate, containing bands of marble 30 and 40 m thick.

Abundant idioblastic garnet porphyroblasts are concentrated in laminae in a strongly foliated (S_1) matrix of biotite, quartz, and muscovite. Idioblastic porphyroblasts of chloritoid grow across the foliation in a random fashion, and contain inclusions of biotite and muscovite parallel to S_1. An incipient later foliation (S_2) is developed by crenulation of S_1.

Sample 98

Biotite-hornblende schist; interfolded with leucocratic to mesocratic granitic gneiss; criss-cut by a network of pegmatite and granite dikes, which are probably associated with the adjacent stock of Hope Granite.

A strongly foliated rock composed principally of biotite and hornblende, with minor quartz as interstitial grains and inclusions within hornblende crystals. Parallelism of biotite and hornblende crystal long axes gives the rock a strong lineation.

Sample 504

Granitic dike; cutting augen gneiss discordantly. The dike has a

sinuous outcrop pattern, it has a secondary foliation parallel to and continuous with the augen gneiss foliation, and granite and augen gneiss are interleaved on a small scale at the dike margin, which indicate that the dike was folded after its intrusion.

A non-porphyritic rock composed of microcline, quartz, orthoclase, albite, and biotite, with accessory zircon, garnet, and iron ore. The texture is xeno-morphic-granular, modified by parallelism of apparently recrystallized biotite flakes.

Sample 512

Pegmatite dike; cutting augen gneiss discordantly; unfolded.

Interlocking very coarse crystals of coarsely perthitic microcline, with minor interstitial quartz and muscovite.

Samples 517-519 were collected from a 5 m thick sequence of interlayered diopside-hornblende gneiss, biotite gneiss, micaceous metaquartzite, and mica schist. These rocks grade upwards successively into augen-free hornblende-biotite gneiss, dark green biotite-feldspar augen gneiss, and pink and green, pinkish-brown-weathering biotite-feldspar augen gneiss. A few concordant bands of diopside-bearing marble, with associated epidote-diopside-hornblende granofels pods are scattered through the sequence, indicating that the gneisses are metasedimentary. The augen gneiss succession is at least 100 m thick. All the rocks are strongly lineated, and scattered small-scale folds occur throughout the sequence.

Sample 517

Epidote-hornblende-biotite schist.

Green biotite, epidote, and hornblende with quartz, oligoclase-andesine, and minor microcline. Hornblende tends to be porphyroblastic and probably post-dates biotite and epidote. Sphene, apatite, zircon, and iron ore are accessory.

Sample 518

Epidote-hornblende-diopside gneiss.

Weakly developed segregation of diopside-epidote-rich and quartz-oligoclase-rich bands gives the rock a gneissic foliation. Hornblende occurs as patches and discontinuous laminae. Sphene and apatite are accessory.

Sample 519

Muscovite-kyanite-biotite metaquartzite.

Well-oriented biotite, kyanite, and muscovite set in a matrix of quartz. Many quartz crystals are elongate and oriented parallel to the long axes of the other minerals, giving the rock a nematoblastic fabric.

Sample 522

Biotite-microcline-oligoclase augen gneiss; near middle of augen gneiss sequence.

Augen of slightly sericitized oligoclase and some microcline, set in a finergrained, compositionally-banded matrix of quartz, green biotite, microcline, and oligoclase, with accessory sphene, zircon, apatite, carbonate, and magnetite. Preferred orientation of biotite and sphene crystals and of elongate augen gives the rock a strong lineation.

Samples 525 and 530 were collected from a sequence of strongly folded and extensively migmatized hornblende- and biotite-bearing gneisses, at least 100 m thick.

Sample 525

Porphyroblastic granitic gneiss; strongly folded on a small scale; associated with migmatized granite-gneiss.

Scattered xeno orphic-granular matrix of quartz, microcline biotite, and slightly sericitized oligoclase. Muscovite and iron ore are accessory. Interstitial patches of myrmekite are present. Sub-parallel orientation of biotite flakes gives the rock a weak foliation.

Sample 530

Porphyroblastic leucocratic granite-gneiss; 50 × 10 cm lens enclosed in hornblende-biotite melanocratic gneiss.

Xenomorphic porphyroblasts of microcline and some slightly sericitized oligoclase in a xenomorphic-granular matrix of microcline, quartz, oligoclase, and biotite. Porphyroblasts are frequently rounded, and the matrix at their margins may have cataclastic texture. Foliation is due to discontinuous compositional banding of quartz and feldspar, and to parallelism of mica flakes. Interstitial myrmekite is abundant.

Samples 547-554 were collected from a petrologically varied succession of banded biotite gneiss, foliated micaceous metaquartzite, marble, hornblende schist, and lenticular feldspathic gneiss. The sequence appears to pass up, without discordance, into the gneisses and schists which contained samples 517-519. Folding and lineation of the rocks in the two sections are similar.

Sample 547

Biotite-quartz-hornblende schist.

A nematoblastic barfic of hornblende and biotite enclosing quartz, with oligoclase and accessory sphene and epidote.

Sample 549

A nematoblastic fabric of extremely well-oriented green muscovite (fuchsite), set in granoblastic quartz with minor feldspar. Zircon and hematite are rare accessories, usually associated with muscovite.

Sample 552

Andesine-biotite-hornblende schist.

A nematoblastic fabric of hornblende with biotite and interstitial andesine and quartz. Sphene and epidote are abundant accessories.

Sample 554

Biotite-plagioclase-microcline gneissic metaquartzite.

Scattered flakes of well-oriented brown biotite are set in granoblastic quartz, albite-oligoclase, and microcline, with minor zircon and apatite. Compositional banding of biotite-rich and biotite-poor laminae gives the rock a gneissic foliation.

REFERENCES

Angino, E. E., and Turner, M. D., Antarctic orogenic belts as delineated by absolute age dates, in Adie, R. J., ed. Antarctic Geology. Amsterdam, North-Holland Publishing Company, (1964), 551-62.

Barrett, P. J.; Lindsay, J. F.; Gunner, J., Reconnaissance geologic map of the Mount Rabot Quadrangle, Transantarctic Mountains, U. S. Geol. Surv. Special Maps, Antarctic Map No. 1, (1970).

Chaudhuri, S., and Faure, G., Geochronology of the Keweenawan rocks, White Pine, Michigan, Econ. Geol. 62, (1967), 1011-33.

Compston, W., and Pidgeon, R. T., Rubidium-strontium dating of shales by the total-rock method. J. Geophys. Res., 67 (9) (1962), 3493-3502.

Eastin, R., Geochronology of the basement rocks of the central Transantarctic Mountains, Unpublished Ph.D. dissertation; Dept. of Geology, The Ohio State University (1970).

Faure, G., and Hurley, P. M., The isotopic composition of strontium in oceanic and continental basalt: Application to the origin of igneous rocks. J. Petrol., 4 (1963), 31-50.

Faure, G.; Murtaugh, J. G.; and Montigny, R. J. E., The geology and geochronology of the basement complex of the central Transantarctic Mountains. Canad. J. Earth Sci., 5, 1968, 555-60.

Ford, A. B., Cordierite-bearing hypersthene-quartz-monozonite-porphyry in the Thiel Mountains and its regional importance, in, Adie, R. J., ed. Antarctic Geology. Amsterdam, North-Holland Publishing Company, (1964), 429-41.

Ford, A. B.; Hubbard, H. A.; and Stern, T. W., Lead-alpha ages of zircon in quartz monzonite porphyry, Thiel Mountains, Antarctica - a preliminary report, Prof. Pap. U. S. Geol. Surv. 450E, (1963), 105-7.

Grindley, G. W., and Laird, M. G., Geology of the Shackleton Coast. Am. Geogr. Soc. Geologic Map of Antarctica, Folio 12, Plate XIV, Sheet 15 (1969).

Grindley, G. W., and McDougall, I., Age and correlation of the Nimrod Group and other Precambrian rock units in the central Transantarctic Mountains, Antarctica, N. Z. J. Geol. Geophys., 12 (2 & 3), (1969), 391-411.

Grindley, G. W.; McGregor, V. R.; and Walcott, R. I., Outline of the geology of the Nimrod-Beardmore-Axel Heiberg Glaciers Region, Ross Dependency. In Adie, R. J. ed. Antarctic Geology. Amsterdam, North-Holland Publishing Company, (1964) 206-19.

Gunn, B. M., and Walcott, R. I., The geology of the Mount Markham region, Ross Dependency, Antarctica, N. Z. J. Geol. Geophys., 5(3), (1962) 407-26.

Gunner, J. D., Petrography of metamorphic rocks from the Miller Range, Antarctica, Institute of Polar Studies Report (32), 44, Columbus, Ohio. The Ohio State University Research Foundation (1969).

Laird, M. G., Geomorphology and stratigraphy of the Nimrod Glacier-Beaumont Bay region, southern Victoria Land, Antarctica, N. Z. J. Geol. Geophys., 6(3), (1963), 465-84.

Laird, M. G., and Waterhouse, J. B., Archaeocyathine limestones of Antarctica. Nature, Lond., 194, (4831), (1962) 861.

McDougall, I., and Grindley, G. W., Potassium-argon dates on micas from the Nimrod-Beardmore-Axel Heiberg Region, Ross Dependency, Antarctica. N. Z. J. Geol. Geophys., 8(2), 1965, 304-13.

Mawson, D., Petrology of rock collections from the mainland of South Victoria Land. Brit. Antarct. Exped. 1907-09, Rep. Sci. Investig., Geol., 2(13), (1916), 201-34.

Moorbath, S., Evidence for the age of deposition of the Torridonian sediments of northwest Scotland, Scott. J. Geol., 5(2), (1969), 154-70.

Winkler, H. G. F., Petrogenesis of metamorphic rocks. Revised second edition, (New York, Springer-Verlag New York Inc.) (1967).

York, D., Least-squares fitting of a straight line. Canad. J. Phys., 44, 1079-86.

THE AGE OF THE TROLLKJELLRYGG VOLCANICS OF WESTERN QUEEN MAUD LAND

Eastin, R., Faure, G., and Neethling, D. C.*
Institute of Polar Studies and Department of Geology,
The Ohio State University, Columbus, Ohio
(Submitted for publication to the Antarctic Journal of the U.S.A.)

The Trollkjellrygg Group consists of mafic to intermediate lava flows with minor agglomerate and tuff. These rocks are exposed on Trollkjell Ridge located west of Jutulstraumen Glacier in Western Queen Maud Land. The geology of this area has been described by Neethling (1970) and Roots (1970), both of whom make reference to the earlier literature.

We are reporting an age determination by the whole-rock Rb-Sr method of volcanic rocks belonging to the Trollkjellrygg Group. Rb/Sr ratios were determined by x-ray fluorescence (Eastin, 1970), while the isotope composition of strontium was measured by standard methods (Chaudhuri and Faure, 1967) using a solid-source mass spectrometer. The reproducibility of the Rb^{87}/Sr^{86} ratio is ± 1.0%, or better, and that of the Sr^{87}/Sr^{86} ratio is ± 0.001, or better. The data are presented in Table I and Fig. 1.

Eight of the nine rock specimens fit a straight line within experimental errors. The slope and intercept of this line were calculated by the least-squares cubic regression of York (1966). The best estimate of the age of these rocks is 856 ± 30 million years and their initial Sr^{87}/Sr^{86} ratio is 0.7097 ± 0.0009. (λRb^{87}-1.39 × 10^{-11}yr.$^{-1}$)

All measured Sr^{87}/Sr^{86} ratios have been normalized to Sr^{86}/Sr^{88} = 0.1194. Average Sr^{87}/Sr^{86} ratio of Eimer and Amend Isotope Standard: 0.7082 ± 0.0005 (σ). Rb/Sr ratios were determined by XRF analysis.

Specimen #484 (from the lower member of the Trollkjellrygg Volcanics) does not fit the isochron and was therefore excluded from the statistical treatment of the data. Assuming an initial ratio of 0.710, a model age of 1.72 billion years can be calculated for this rock. This date is similar to that of the Borg Metamafics which intrude the Ahlmannrygg Group and for which Allsopp and Neethling (1970) have reported an age of 1700 ± 130 million years.

We conclude that the Trollkjellrygg Volcanics are Late Precambrian in age and appear to be significantly younger than the Ahlmannrygg Group which is intruded by the Borg Metamafics.

*Geological Survey, Pretoria, South Africa

Table I. Analytical Data for the Trollkjellrygg Volcanic Formation of Western Queen Maud Land

OSU Number	Field Number	Locality	$\frac{Rb^{87}}{Sr^{86}}$ Atomic	$\frac{Sr^{87}}{Sr^{86}}$ N
Upper Member (860 m)				
489	B8	Bolten	2.496	0.7374
491	SN39	Snokallen [1]	0.756	0.7210
486	SN20	Snokallen (main nunatak)	2.756	0.7446
492	SN6	"	0.852	0.7205
490	SN5	"	1.623	0.7285
488	SJ22	Snøkjerringa	1.502	0.7281
487	SJ11	"	5.241	0.7725
Transitional or Middle Member (460 m)				
485	SL1	Nunatak 820 [2]	1.560	0.7284
Lower Member (260 m)				
484	U3	Utkikken	0.761	0.7282

[1]Small satellite nunatak farthest to SE

[2]Exact location of this outcrop in the sequence is uncertain; i.e., either transitional or middle member.

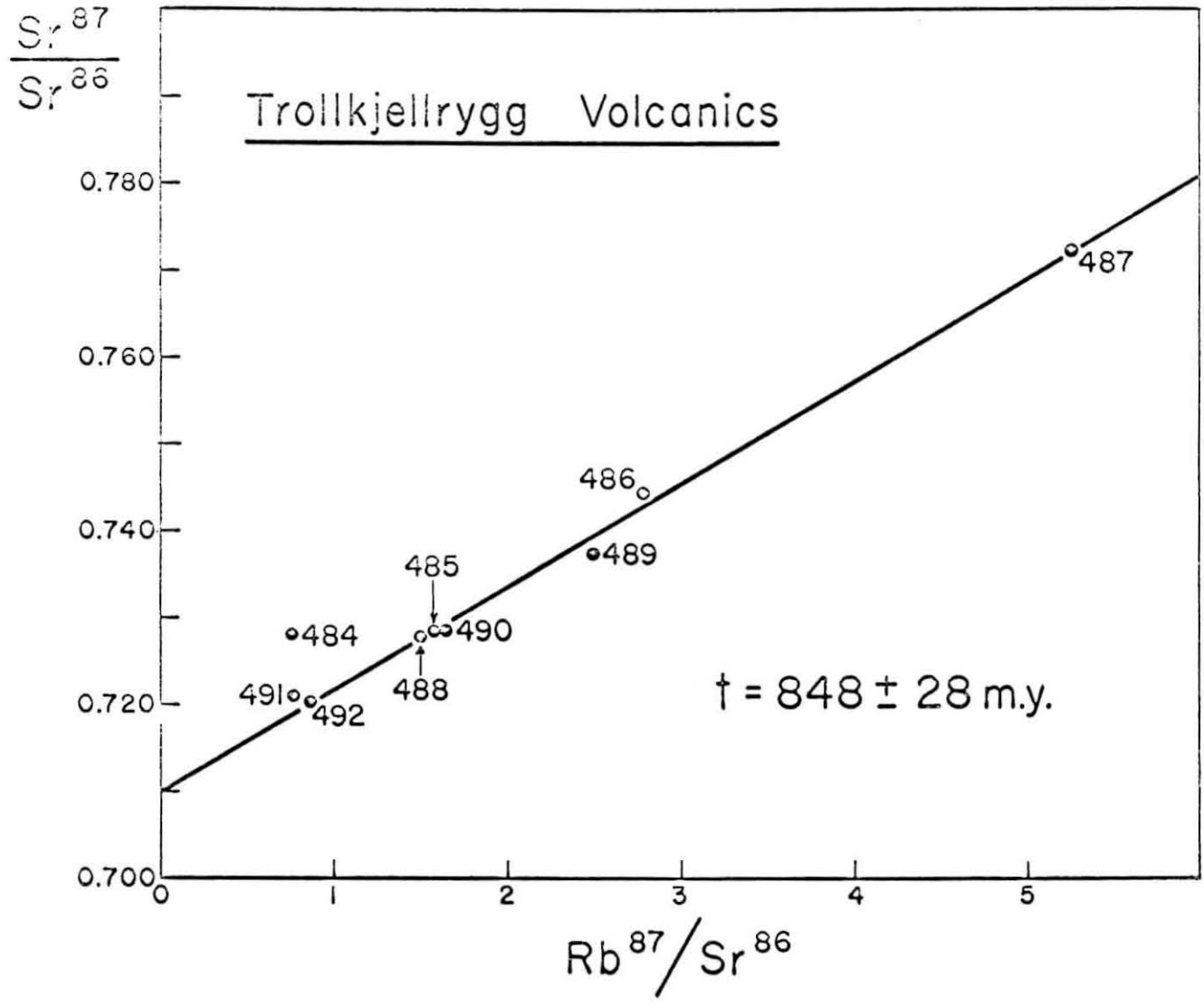

Figure 1. Whole-rock Rb-Sr isochron for mafic to intermediate lava flows of the Trollkjellrygg Group

REFERENCES

Allsopp, H. L., and Neethling, D. C., Rb-Sr isotopic ages of Precambrian intrusives from Queen Maud Land, Antarctica, Earth Planet. Sci. Lett., 8 (1970), 66-70.

Chaudhuri, S., and Faure, G., Geochronology of the Keweenawan rocks, White Pine, Michigan Econ. Geol., 62 (1967), 1011-1033.

Eastin, R., Geochronology of the basement rocks of the Central Transantarctic Mountains, Unpublished Ph.D. dissertation, Department of Geology, The Ohio State University, (1970).

Neethling, D. C., Geology of the Ahlmann Ridge, Western Queen Maud Land (sheet 7) American Geographical Society, (1970), in press.

Roots, E. F., Geology of Western Queen Maud Land (Sheet 6), American Geographical Society, (1970), in press.

York, D., Least-squares fitting of a straight line, Canadian J. Phys., 44 (1966), 1079-1086.

ACKNOWLEDGMENTS

This work was supported by the National Science Foundation through Grant No. 898-X. The rock samples were collected by B. R. Watten of the Antarctic Division, Geological Survey of South Africa.

THE AGE OF THE LITTLEWOOD VOLCANICS OF COATS LAND, ANTARCTICA

Réne Eastin and Gunter Faure,
Department of Geology and Institute of Polar Studies,
The Ohio State University, Columbus, Ohio 43210.

ABSTRACT

Acid volcanic or hypabyssal rocks from the Bertrab and the Littlewood Nunataks in Coats Land have been dated by the whole-rock Rb-Sr method. Five specimens from the Bertrab Nunatak define an isochron indicating an age of 999 ± 19 million years (m.y.), based on a value of 1.39×10^{-11} yr^{-1} for the decay constant of Rb^{8} . Two specimens from the Littlewood Nunataks have possible ages ranging from 985 to 1033 m.y. and fit the Bertrab isochron within experimental error. A pooled isochron of all the data leads to a best estimate of 1001 ± 16 m.y. for the age of these rocks. The initial Sr^{87}/Sr^{86} ratio is 0.7042 ± 0.0011. A whole-rock K-Ar date of 840 ± 30 m.y. reported in the literature shows no evidence of the expected argon loss caused by the Ross Orogeny.

INTRODUCTION

The Littlewood and Bertrab Nunataks are located approximately 20 km inland from Duke Ernst Bay at the eastern edge of the Filchner Iceshelf in Coats Land. The exact location of these and the nearby Moltke Nunataks is shown in Figure 1.

The geology of the Littlewood Nunataks has been described by Aughenbaugh, Lounsbury and Behrendt (1965). The rocks exposed in the Bertrab Nunatak, were described by Capurro (1955); while the Moltke Nunataks may have been visited by Cordini (1959). According to Aughenbaugh et al. (1965), the bedrock in all three localities consists of similar brick-red acid volcanic rocks which they named the Littlewood Volcanics. On the basis of petrographic descriptions and a partial chemical analysis of specimens from one of the Littlewood Nunataks they classified the rocks as rhyolite or rhyodacite.

The stratigraphic relationship of the Littlewood Volcanics to the rocks of the Transantarctic Mountains is not known because no contacts with other rocks are exposed. Aughenbaugh et al. (1965) reported a whole-rock K-Ar date of 840 ± 30 m.y. for a specimen of rhyolite from one of the Littlewood Nunataks. They regarded this date as a minimum estimate of the age of these rocks because of the probability of argon loss from the feldspar. Aughenbaugh et al. (1965) concluded that the Littlewood Volcanics are of Precambrian age and suggested their tentative correlation with the older units of the crystalline basement complex of the Transantarctic Mountains.

We are reporting whole-rock Rb-Sr isochron ages of rocks from the Bertrab and the Littlewood Nunataks. The specimens from the Bertrab Nunatak were made available to us by the Instituto Antartico Argentino. The rocks from the Littlewood Nunataks were provided by N. B. Aughenbaugh and J. C. Behrendt. Preliminary reports of the results of this investigation have been published by Eastin et al. (1969) and Eastin (1970).

ANALYTICAL METHODS

Concentrations of rubidium and strontium were determined by isotope dilution using calibrated spikes enriched in Rb^{87} and Sr^{86}, respectively. The Sr^{87}/Sr^{86} ratios were measured as separate, unspiked aliquots using a Nuclide Corp. Model 6-60-S mass spectrometer. All measured Sr^{87}/Sr^{86} ratios were corrected for isotope fractionation, assuming that $Sr^{86}/Sr^{88} = 0.1194$. The Eimer and Amend $SrCo_3$ (lot 492327) isotope standard has been analyzed repeatedly in this laboratory. The average of 24 analyses since 1965 is $Sr^{87}/Sr^{86} = 0.7082 \pm 0.0005$ (σ).

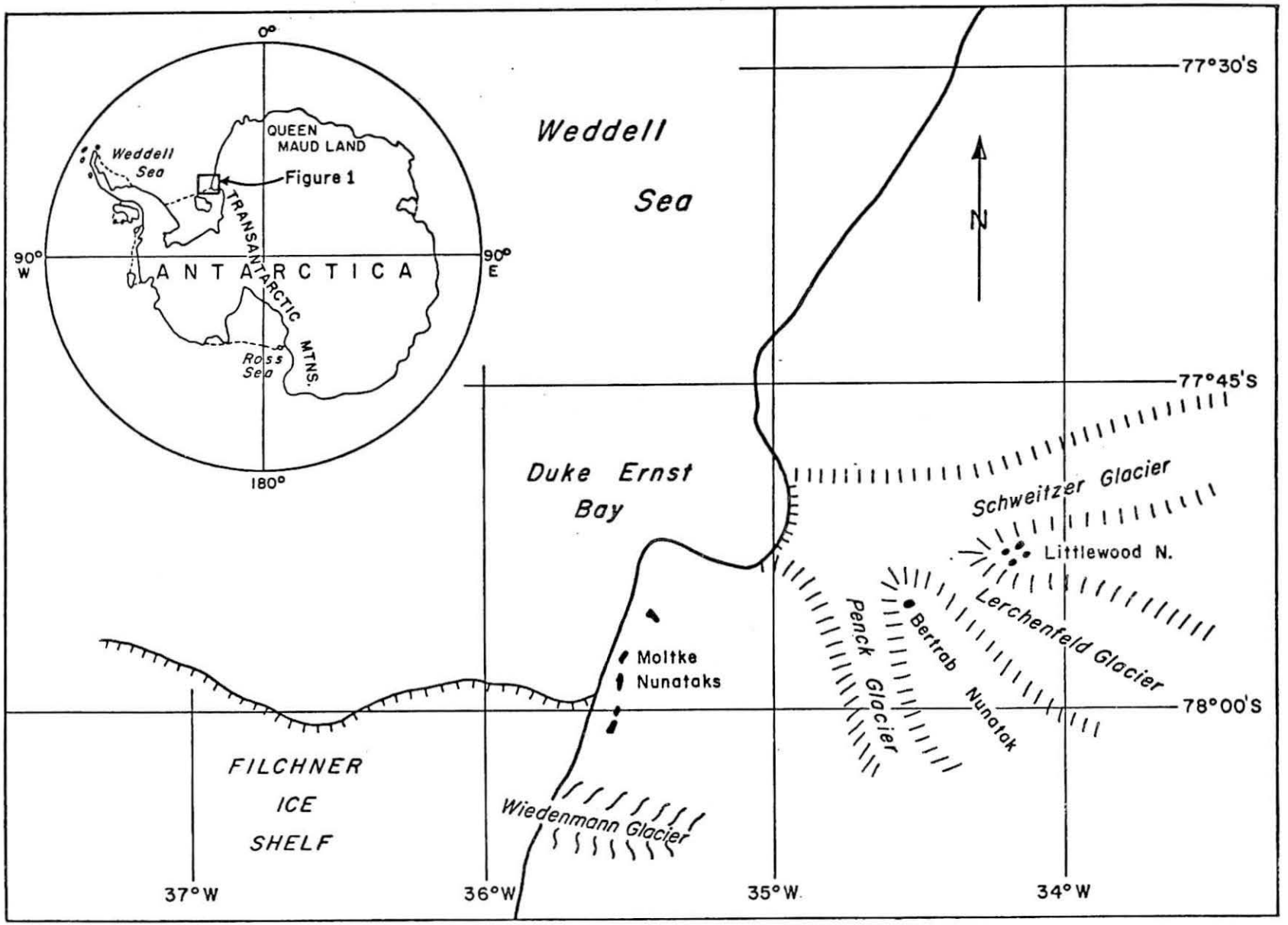

Figure 1. Index Map of Antarctica and Location of the Bertrab and Littlewood Nunataks.

The reproducibility of the Rb^{87}/Sr^{86} ratio for rocks having rubidium and strontium concentrations in excess of about 50 ppm is ± 1.12%. This estimate is based on about 20 duplicate analyses of rocks and minerals. The reproducibility of the Sr^{87}/Sr^{86} ratio is commonly better than ± 0.0010, based on experience with replicate analyses.

The analytical results are listed in Table I and have been plotted in coordinates of Sr^{87}/Sr^{86} and Rb^{87}/Sr^{86} in Figure 2. The slope and intercept of the isochron were calculated by least-squares cubic regression of York (1966).

DISCUSSION OF THE RESULTS

The five rock specimens from the Bertrab Nunatak form a satisfactory isochron which indicates a date of 999 ± 19 m.y. based on a value of 1.39×10^{-11} $yr.^{-1}$ for the decay constant of Rb^{87}. The initial Sr^{87}/Sr^{86} ratio is 0.7042 ± 0.0014. The data for the two rock specimens from the Littlewood Nunataks are compatible with dates ranging from 985 to 1033 m.y., relative to an assumed initial Sr^{87}/Sr^{86} ratio of 0.7042. A pooled isochron (shown in Figure 2) of all the specimens from the Bertrab and Littlewood Nunataks gives a combined age of 1001 ± 16 m.y. for these rocks. The initial Sr^{87}/Sr^{86} ratio for the pooled samples is 0.7042 ± 0.0011.

These results are consistent with the interpretation that the rocks of the Bertrab and the Littlewood Nunataks crystallized within a short interval of time, 1001 ± 16 m.y. ago and that they had similar initial Sr^{87}/Sr^{86} ratios. This confirms that the K-Ar date (840 ± 30 m.y.) reported by Aughenbaugh et al. (1965) is indeed an underestimate of the time elapsed since these rocks crystallized.

A remarkable feature of these volcanic rocks is that they appear not to have lost radiogenic Ar^{40} during the Ross Orogeny, which occurred in Cambro-Ordovician time about 460-500 m.y. ago. Most of the potassium in these rocks is probably located in K-feldspar which has a notoriously low retentivity for argon. The unexpectedly high value of the K-Ar date suggests that the rocks of the Bertrab and Littlewood Nunataks may not have been subjected to the Ross Orogeny which caused widespread metamorphism of the pre-Beacon rocks in the nearby Transantarctic Mountains.

ACKNOWLEDGMENTS

The rock specimens from the Bertrab Nunatak were made available to us through the courtesy of G. W. B. Mackinlay, Director, and of Dr. N. H. Fourcade of the Instituto Antartico Argentino. Dr. N. B. Aughenbaugh, University of Missouri at Rolla, and Dr. J. C. Behrendt, U. S. Geological Survey, each contributed one rock specimen from the Littlewood Nunataks. This work was supported by the National Science Foundation through Grant No. 898X.

Table I. Analytical Data for Rhyolites from the Littlewood and Bertrab Nunataks, Coats Land, Antarctica

Sample		Rb (ppm)	Total Sr (ppm)	$\left(\frac{Rb^{87}}{Sr^{86}}\right)_{atomic}$	$\left(\frac{Sr^{87}}{Sr^{86}}\right)^{*}$
Littlewood	235	95.9	48.8	5.69	0.7871
Littlewood	367	82.2	62.4	3.83	0.7570
Bertrab	405	98.4	95.8	2.98	0.7429 0.7442
Bertrab	406	82.9	99.9	2.41	0.7397
Bertrab	407	240.5	45.1	15.74	0.9274
Bertrab	408	46.8	357.8	0.38	0.7083 0.7098
Bertrab	409	94.4	11.2	25.16	1.044 1.050

*Corrected for fractionation, assuming $\frac{Sr^{86}}{Sr^{87}} = 0.1194$

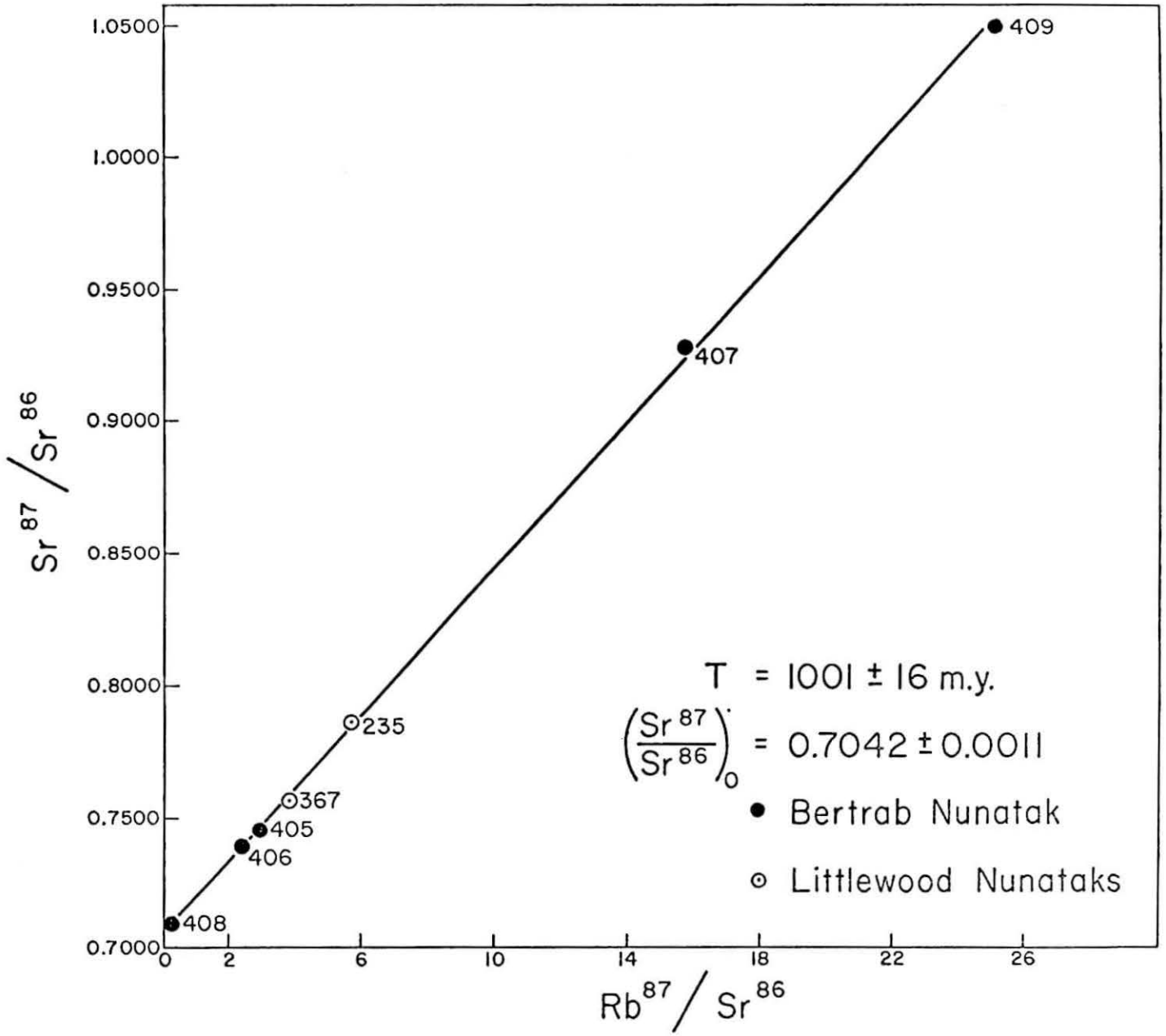

Figure 2. Rb-Sr whole-rock isochron for the Littlewood Volcanics.

APPENDIX

Sample 235. Littlewood Nunataks, Antarctica. 77°53.5' S., 34° 10' W.

Collected by N. B. Aughenbaugh and described in Aughenbaugh et al. (1965). Rhyolite or rhyodacite.

Sample 367. Littlewood Nunataks, Antarctica.

Collected by J. C. Behrendt, U. S. Geological Survey, Denver.

Sample 405. Bertrab Nunatak, Coats Land, Antarctica. Instituto Antarctico Argentino, No. CE75.533.

Described as: "Graphic granite: shows graphic texture, quartz in feldspar. Potassic feldspar (microcline) and some individual plagioclase grains are idiomorphic, somewhat altered to kaolin, calcite, and iron oxide. Biotite has altered to chlorite. Magnetite exists as grains and masses."

Sample 406. Bertrab Nunatak. Instituto Antartico Argentino, No. CE.75.534.

Described as: "Graphic granite; description similar to CE.75.533."

Sample 407. Bertrab Nunatak. Instituto Antartico Argentino, No. CE.75.535.

Described as: "Micro trodjemite: rock consists of quartz with undulating extinction, plagioclase with indices less or equal to balsom (olig.-andes.); turbid because of the advanced state of alteration of the rock. Abundant biotite altered to chlorite. K-feldspar is absent because biotite has absorbed all the potassium. Alotriomorphic crystals or hornblende."

Sample 408. Bertrab Nunatak. Instituto Antartico Argentino, No. CE.75.536.

Described as: "Microdiorite, subject to confirmation."

Sample 409. Bertrab Nunatak. Instituto Antartico Argentino, No. CE.75.537.

Described as: "Graphic granite: Similar to samples CE.75.533 and

CE.75.534. Because of the fine groundmass the mineral composition cannot be determined."

REFERENCES

Aughenbaugh, N. B.; Lounsbury, R. W.; and Behrendt, J. C., The Littlewood Nunataks, Antarctica., J. Geol., 73 (1965), 889-894.

Capurro, L. R. A., Expedicion Argentina al Mar de Weddell: Ministerio de Marina, Direccion General de Navegacion e Hidrografia, (1955), 129-131.

Cordini, I. R., El conocimiento geologico de la Antartica, Instituto Antartico Argentino, Pub. No. 6, (1959), 141-145.

Eastin, René, The age of the Littlewood Volcanics of Coats Land, Antarctica, Abstract, Program, North-central Section, Geol. Soc. Amer., 2 (1970), No. 6, p. 386.

Eastin, R.; Faure, G.; Shultz, C. H.; and Schmidt, D. L., Rb-Sr ages of the Littlewood Volcanics and of the acid volcanic rocks of the Neptune Range, Pensacola Mountains, Antarctica, Abstract, Program, North-central Section, Geol. Soc. Amer., Part 6, (1969), p. 13.

York, D., Least-squares fitting of a straight line, Canad. J. Phip., 44 (1966), 1079-1086.

AGE DETERMINATIONS OF ROCKS FROM NORTHERN VICTORIA LAND, ANTARCTICA
(Submitted to the N.Z.J. of Geol. and Geophys.)

Sir:

The purpose of this note is to report new age determinations by the Rb-Sr method of whole-rock samples from Northern Victoria Land in Antarctica. The rocks which have been dated include a specimen of quartz-biotite schist of the Rennick Group and a specimen of muscovite-biotite granite of the Campbell Plutonics from the mountains along the western edge of the upper Rennick Glacier. These specimens were collected by S. J. Carryer in the Gallipoli Heights of the Southern Freyberg Mountains.

Powdered whole-rock samples of these specimens were analyzed by conventional methods. The concentrations of rubidium and strontium were determined by isotope dilution using spikes enriched in Rb^{87} and Sr^{86}, respectively. The isotope composition of strontium was measured on unspiked aliquots using a Nuclide Corp. Model 6-60-S mass spectrometer. Past experience has shown that the average difference between duplicate determinations of the Rb^{87}/Sr^{86} ratio is about 3 per cent. We therefore assign an experimental uncertainty of ± 1.5 per cent to single determinations of this ratio. The reproducibility of the Sr^{87}/Sr^{86} is ± 0.0010 at the 95% confidence limit, based on replicate analyses of standards. The analytical results are summarized in Table I. The error limits of the calculated dates are based on the uncertainties of the analytical data.

The rocks of the Rennick Group are metamorphosed sedimentary rocks believed to be of Precambrian age, according to Gair (1967). The date obtained here for the specimen of quartz-biotite schist from the Rennick Group is 770 ± 20 million years (m.y.). It is possible, and perhaps likely, that this rock specimen was altered chemically during metamorphism. Gair (1967, p. 319) states that appreciable amounts of microcline may have been introduced into the specimen (#47) which we have dated. It is therefore possible that the date we are reporting is an underestimate of the time elapsed since deposition of the original sediment. Nevertheless, a Precambrian age for the Rennick Group appears to be confirmed.

The granite, granitic gneisses, and pegmatites of the Campbell Plutonics intrude the rocks of the Rennick Group. Gair (1967) thought it probable that the gneissic granites are Precambrian in age and were emplaced toward the end of the metamorphism. He suggested that the younger post-tectonic granites of the Campbell Intrusives may be Early Paleozoic in age and may be correlative with the Granite Harbour Intrusives of Gunn and Warren (1962). The specimen dated by us is a coarse-grained, non-foliated, presumably post-tectonic granite. Its age is 530 ± 13 m.y. which confirms an Early Paleozoic (Cambrian) age for the non-foliated granites of the Campbell Plutonics.

Table I. Analytical Data and Age Determinations of Whole-Rock Samples from Northern Victoria Land

Sample Number	Description and Location	Rb (ppm)	Total Sr (ppm)	$\left(\frac{Rb^{87}}{Sr^{86}}\right)_{atomic}$	$\left(\frac{Sr^{87}}{Sr^{86}}\right)_N^*$	Age, m.y.
289 (#47 of Gair, 1967)	Qtz-biotite schist Rennick Group Sequence Hills Rennick Glacier	214.9	104.4	5.99	0.7683	770 ± 20
					(Sr^{87}/Sr^{86})	= 0.7040
234 (#78 of Gair, 1967)	Musc.-biot. granite Campbell Plutonics West of Upper Rennick Glacier	219.7	38.4	16.7	0.8274	530 ± 13
					(Sr^{87}/Sr^{86})	= 0.7040
315 (#C/76 of Carryer)	Qtz-feldspar porphyry Gallipoli Heights S. Freyberg Mountains	173.3	47.8	10.5	0.7606	375 ± 40
316 (#C/78 of Carryer)	Banded felsite, containing feldspar phenocrysts Gallipoli Heights S. Freyberg Mountains	100.7	46.4	6.29	0.7385	

*Corrected for isotope fractionation assuming $Sr^{86}/Sr^{88} = 0.1194$. Decay constant of Rb^{87}, $\lambda = 1.39 \times 10^{-11}$ yr.$^{-1}$. Sr^{87}/Sr^{86} ratio of the Eimer and Amend Isotope Standard = 0.7083 ± 0.0003($\bar{\sigma}$).

Samples 315 and 316 originated from the Gallipoli Porphyries which rest unconformably on the granitic rocks of the Granite Harbour intrusives at Gallipoli Heights east of the Rennick Glacier. Gair et al. (in press) have suggested that the Gallipoli Porphyries are an extrusive phase of the Admiralty Intrusives whose age may range from Devonian to Early Carboniferous. These interpretations are supported by the date of 375 ± 40 m.y. which is based on the assumption that the two samples are comagmatic and had the same initial Sr^{87}/Sr^{86} ratios The calculated value of this ratio is 0.7057.

This research was supported by the National Science Foundation through Grant 898-X. We are pleased to acknowledge the laboratory assistance of Rene Eastin. This report is contribution No. 10 of the Laboratory for Isotope Geology and Geochemistry of the Department of Geology and the Institute of Polar Studies of The Ohio State University, Columbus, Ohio, 43210.

December 5, 1969

Gunter Faure
H. S. Gair

REFERENCES

Gair, H. S., The geology from the Upper Rennick Glacier to the coast, Northern Victoria Land, Antarctica, New Zealand J. Geol. and Geophys., 10 (1967), 309-344.

Gair, H. S.; Sturm, A.; Carryer, S. J.; and Grindley, G. W., The geology of Northern Victoria Land, Antarctica Map Folio Series, Amer. Geogr. Soc., New York, N.Y., U.S.A. (in press).

Gunn, B. M., and Warren, G., Geology of Victoria Land between the Mawson and Mulock Glaciers, Antarctica, New Zealand Geol. Surv. Bull., 71 (1962).

AGE OF THE FALLA FORMATION, QUEEN ALEXANDRA RANGE

R. L. Hill

Five samples of tuff from the Falla Formation were analyzed for an age determination by the whole-rock Rb-Sr isochron method. Sample locations with respect to Falla Formation stratigraphy are shown in Figure 1. This age determination is significant in that it provides firm radiometric evidence of the time of deposition of the Falla tuffs. This is the first radiometric date obtained for any unit of the Beacon Group. It also provides an age for the fossil plant Dicroidium odontopteroides, leaves of which have been found in the non-volcanic sediments of the lower part of the Falla Formation. In addition, the age of the Falla tuffs is a lower limit for the age of the previously mentioned labyrinthodont amphibian discovered in the underlying Fremouw Formation (Barrett et al., 1968a). This discovery of a Triassic tetrapod on the Antarctic continent is of great importance because it is the first direct evidence that terrestrial vertebrates inhabited the now physically isolated Antarctic continent during the Triassic period. The Antarctic amphibian bears strong affinities to Triassic amphibians found in Gondwana sequences of other southern continents. This strengthens the evidence for the existence of a land connection permitting Triassic tetrapods to migrate between South America, South Africa, and Antarctica.

The tuff samples to be analyzed were selected to achieve the greatest possible range of Rb^{87}/Sr^{86} ratios. The relative Rb and Sr abundances were initially determined by X-ray fluorescence of powder samples. Each of the selected samples was analyzed for its strontium isotope composition and for its rubidium and strontium concentrations. The Rb and Sr concentrations were determined by isotope dilution analysis. Duplicate isotope ratio analyses were made for two of the samples, No. 321 and 322. The results were found to be consistent within 0.1% of their mean. The analytical data are compiled in Table I. The whole-rock Rb-Sr isochron diagram is given in Figure 2.

Inspection of the isochron reveals that one point - No. 324 - falls significantly farther from the isochron than any of the rest. It does not fit the isochron within the limits of experimental error. Duplicate analyses were performed on this sample to make certain that no errors had been made in measuring its rubidium and strontium concentrations, and that it had not been contaminated in preparation. In both duplicate isotope dilution analyses, the new values were well within 1% of the mean. It seems certain therefore, that this sample is anomalous, and may not have been a closed system with respect to Rb and Sr since its deposition. For this reason, this sample was rejected, and it was not used in calculating the slope of the isochron.

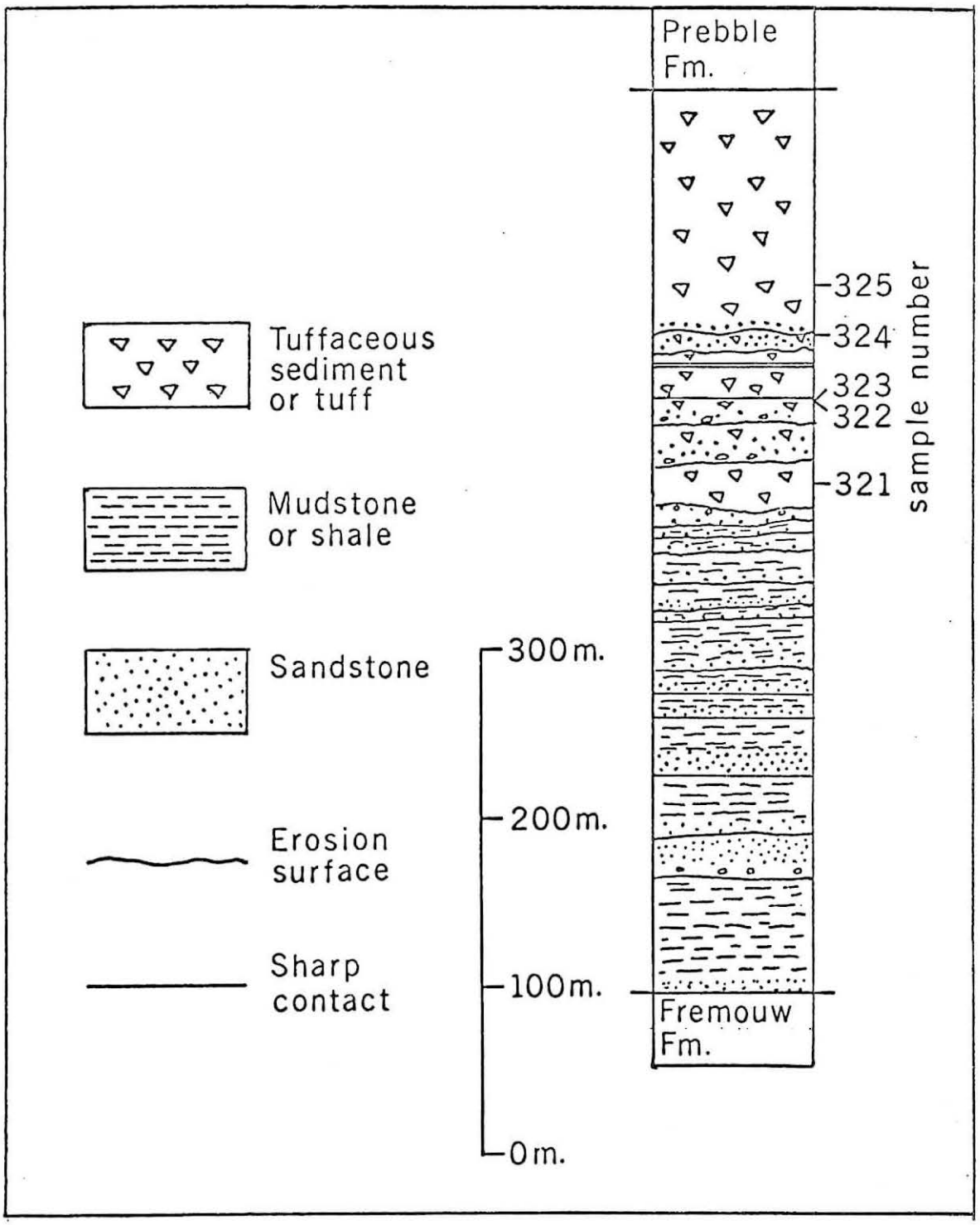

Figure 1. Falla Formation Stratigraphic Section on Mount Falla, Queen Alexandra Range

Table I. Rb-Sr Analytical Data for the Falla Tuffs, Queen Alexandra Range, Antarctica

Sample	Rb(ppm)	Sr(ppm)	Rb^{87}/Sr^{86}	Sr^{87}/Sr^{86}*
321	147.6	124.0	3.46	0.7215 0.7339
322	241.2	46.21	15.1	0.7554 0.7561
323	215.1	58.85	10.6	0.7394
324	391.4 394.1	57.79 57.26	19.7 20.0	0.7574
325	147.8	307.3	1.38	0.7161

*Normalized to Sr^{86}/Sr^{88} - 0.1194

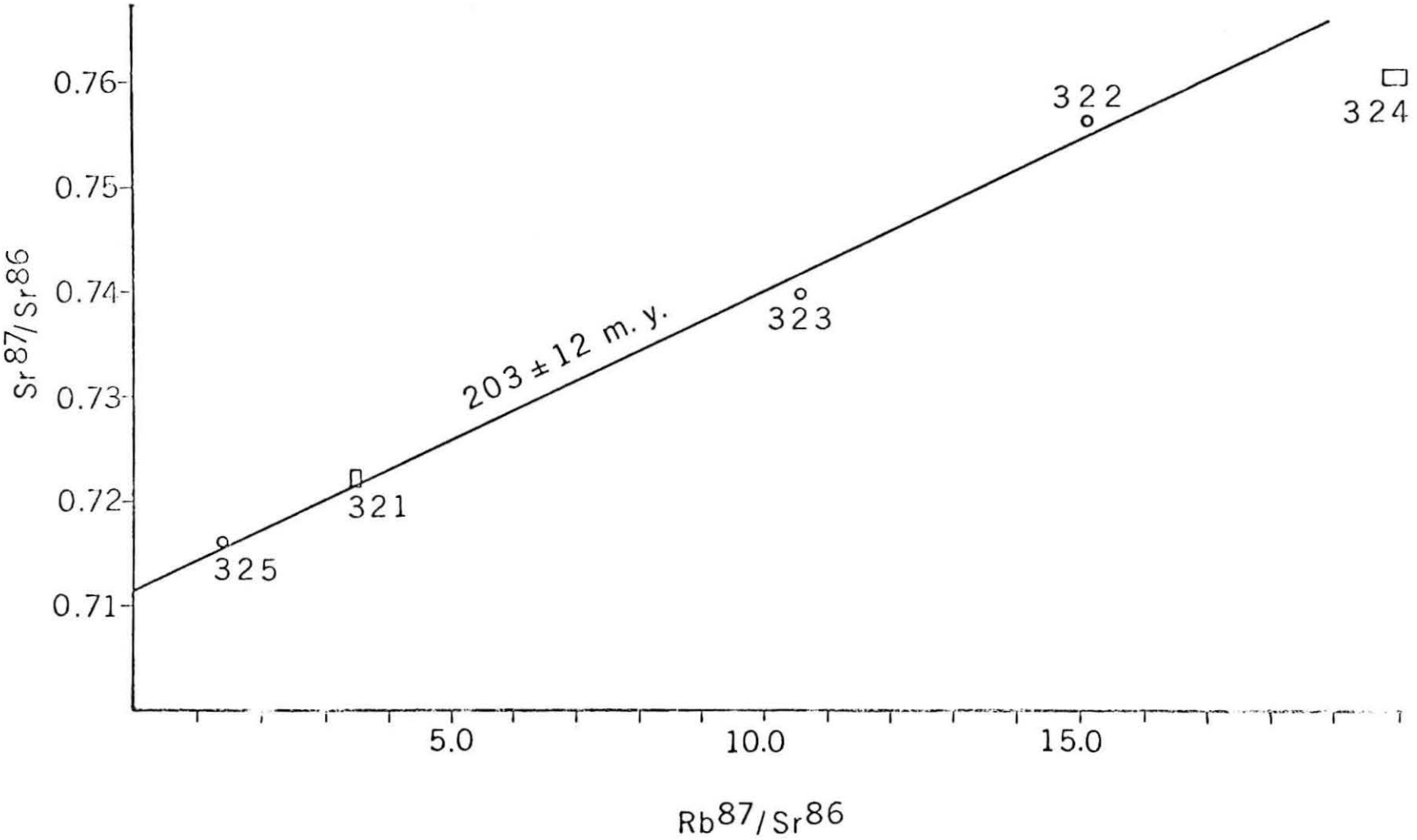

Figure 2. Rb-Sr Whole-Rock Isochron for Falla Tuffs.

Using the remaining four points, the slope of the isochron indicates an age of 203 ± 12 m.y. The intercept of the isochron with the ordinate axis gives an initial Sr^{87}/Sr^{86} ratio of 0.7118. The four points closely define an isochron with little scatter. The linear correlation coefficient is 0.99592. The isochron was calculated by the lease squares method. This age of 203 ± 12 m.y. falls within the Triassic period. It is not possible to be more precise than this, because of the uncertain age of the boundary of the Triassic period with both the Permian and the Jurassic periods.

The age for the Falla Formation tuffs is consistent with other radiometric evidence. D. H. Elliot (personal communication) has obtained six K-Ar ages for the overlying Kirkpatrick Basalt and the correlative Ferrar Dolerite. The mean value for these ages is 170 m.y. In addition, one dolerite boulder from the Prebble Formation has given a K-Ar age of 179 m.y.

The age of the Falla Formation, then, would appear to be very close to 200 m.y., and this age agrees with other radiometric evidence. This date provides a radiometric age for the fossil plant Dicroidium odontopteroides, and a lower limit for the age of the recently discovered labyrinthodont amphibian.

REFERENCES

Barrett, P. J.; Baillie, R. J.; and Colbert, E. H.; Triassic amphibian from Antarctica, Science, 161: 3840 (1968a), 460.

GEOCHRONOLOGY OF THE BASEMENT ROCKS OF THE CENTRAL TRANSANTARCTIC MOUNTAINS, ANTARCTICA

René Eastin

Excerpts from a dissertation submitted in partial fulfillment of the requirements of the Ph.D. degree, Graduate School, The Ohio State University, Columbus, Ohio

August, 1970

CHAPTER III

PENSACOLA MOUNTAINS

Physiography

The Pensacola Mountains are part of the Transantarctic Mountain chain and extend for 500 km between 40° and 70° W. longitude, and 82° and 86° S. latitude, near the southern edge of the Filchner Ice Shelf as shown in Figure 1. They are subdivided into the Patuxent, Neptune, and Forrestal Ranges and the Dufek Massif, with locations shown in Figure 21.

The Pensacola Mountains form a barrier to ice flowing from the polar plateau toward the coast. They reach elevations of more than 1000 m above the surrounding ice, dividing the flow of ice from the polar plateau into three large glaciers: (1) the Patuxent Ice Stream, 154 km wide, between the Patuxent Range and the Thiel Mountains, (2) the Academy Glacier, 60 km wide, between the Patuxent and Neptune Ranges, and (3) the Support Force Glacier, 122 km wide, between the Forrestal Range and Mt. Ferrara. The Patuxent and Neptune Ranges were once covered by glacier ice, as indicated by the presence of striated bedrock on the highest parts of the ranges and by thick moraines in the Patuxent Range (Schmidt and Ford, 1969).

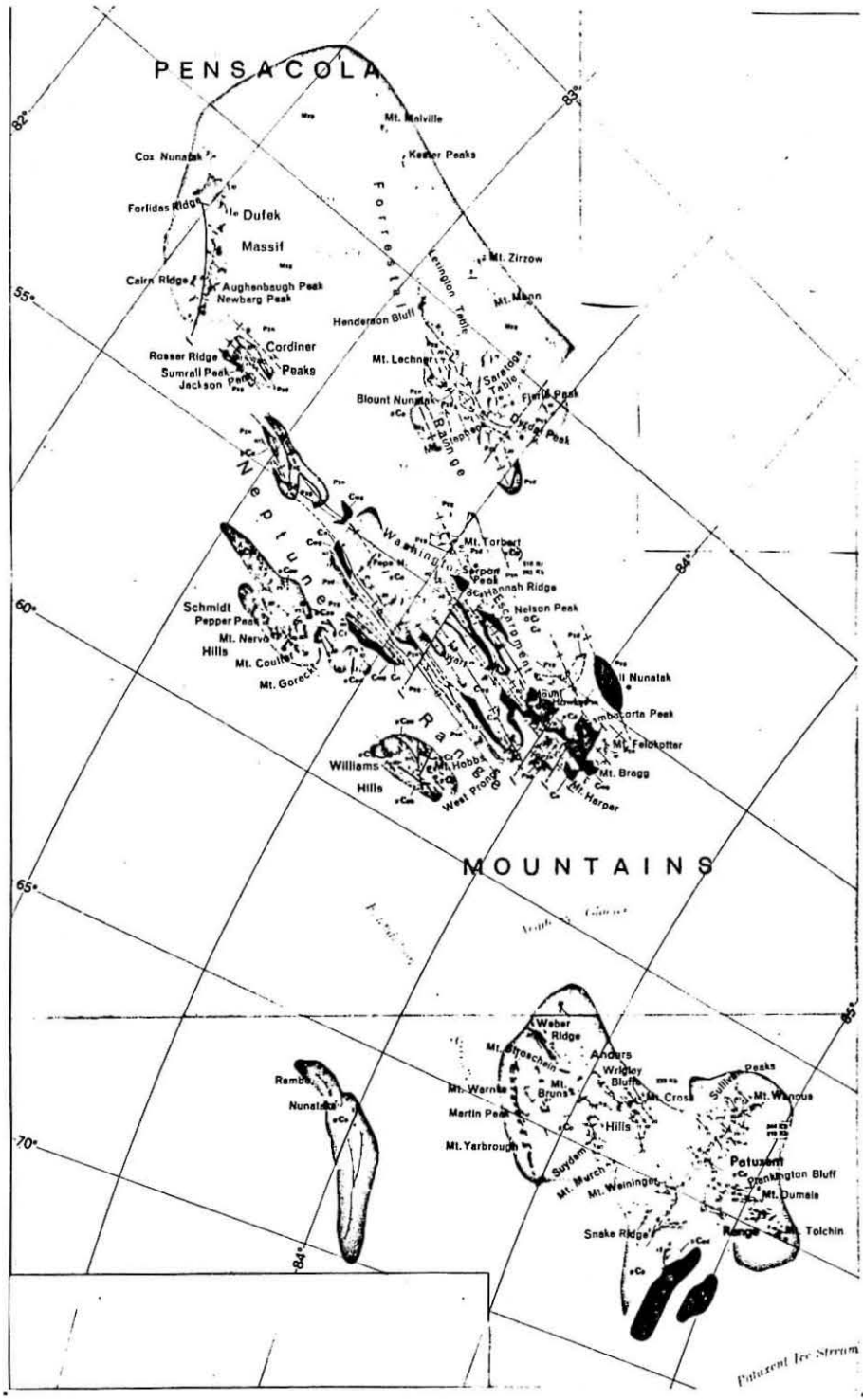

Figure 21. Geologic map of the Pensacola Mountains (from Schmidt and Ford, 1969).

History of Exploration

The Pensacola Mountains were first seen by man during a U.S. Navy transpolar reconnaissance flight in 1956 with W. M. Hawkes as pilot. Augenbaugh (1961) and Walker (1961) described the findings of the first visit to the mountains, after a reconnaissance of the Dufek Massif in December, 1957, as part of the United States' I.G.Y. program.

Following these early investigations, the U.S. Geological Survey carried out a reconnaissance geological and geophysical mapping program in the Pensacola Mountains during the period 1962-1966. Schmidt and Ford (1963) described the geology of the Patuxent Range, and Schmidt and others (1956) that of the Neptune Range. Williams (1969) has written a study of the petrography of the Upper Precambrian and Paleozoic sandstones of the Pensacola Mountains. The layered gabbro intrusion of the Dufek Massif and Forrestal Range has been described by Ford and Boyd (1968). Finally, an excellent summary and map of the geology of the Pensacola Mountains by Schmidt and Ford (1969) was published as part of the American Geographical Society's Antarctic Map Folio Series.

Stratigraphy and Structure

Ten sedimentary and volcanic rock formations have been recognized in the Pensacola Mountains. They are divided into three stratigraphic sequences, each bounded above by an angular unconformity. A columnar section from Schmidt and Ford (1969) is shown in Figure 22.

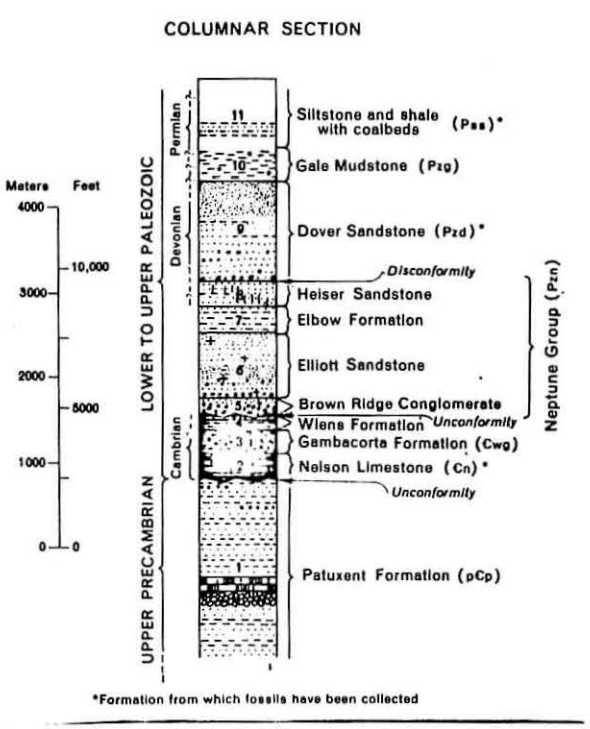

Figure 22. Stratigraphic column of the Neptune Range, Pensacola Mountains. The numbers refer to the geologic cross section, Figure 24. (From Schmidt and Ford, 1969)

The oldest sequence consists of the Patuxent Formation, estimated to be several tens of thousands of feet thick and probably of late Precambrian age. The middle sequence consists of the Nelson Limestone at the base, followed by volcanics of the Gambacorta Formation and the siltstone and sandstone of the Wiens Formation. This sequence, about 1,000 m in total thickness, is of the earliest Paleozoic age.

The rocks of the third sequence consist of six formations, totaling 4,000 m in thickness and ranging in age from Ordovician or Devonian to Permian. The oldest unit in this sequence is the Brown Ridge Conglomerate, a massive red poorly sorted coarse conglomerate, ranging from a feather edge up to 1000 m thick. The Elliott Sandstone, the next youngest unit, is a calcareous sandstone and conglomerate about 700 m thick. The Elbow Formation, a red siltstone and shale unit 300 m thick, overlies the Elliott Sandstone. Above the Elbow Formation is the Heiser Sandstone, a quartz sandstone about 300 m thick. These four formations are grouped by Schmidt and Ford (1969) as the Neptune Group; their upper contact is marked by a disconformity.

A quartz sandstone about 1200 m thick, called the Dover Sandstone, overlies the Neptune Group. It crops out in the Neptune and Forrestal Ranges, and may be the equivalent of a similar sandstone in the Patuxent Range that contains plant fossils of probable Late Devonian age (Schmidt and others, 1965).

The Dover Sandstone is separated from the overlying unit, the Gale Mudstone, by a probable disconformity. The Gale Mudstone is a black pebbly mudstone, probably a tillite and correlating with other

Late Paleozoic tillites of the Transantartic Mountains (Schmidt and others, 1965).

The youngest sedimentary rocks of the Pensacola Mountains crop out on the Pecora Escarpment, south of the Patuxent range, and in the southern Forrestal Range. These rocks are interbedded sandstones and shales, containing black carbonaceous and coal-bearing layers with a glossopterid flora of Permian age (Schopf, 1964). They are similar to Beacon Super-group rocks, but are not known to be in contact with other units in the Pensacola Mountains (Schmidt and Ford, 1969).

Part of this study has involved dating the Patuxent and Gambacorta Formations, the basalts, felsic flows, and diabase included in the Patuxent Formation, and the Serpan Granite and Gneiss. In order to interpret the results of the radiometric dates, these units are described in detail.

Patuxent Formation

The type section of the Patuxent Formation is in the Patuxent Range, where it makes up about 90 percent of the exposed bedrock. The formation is also well exposed throughout the Neptune Range, where it makes up about 40 percent of exposed bedrock. The unit may occur as far to the northeast as Mt. Spann in the Argentina Range.

The Patuxent Formation consists of grayish-green, rhythmically interbedded subgraywackes and slates. Detrital grains of quartz, rock fragments, and minor amounts of feldspar occur in a groundmass of fine-grained quartz, sericite, and chlorite. In the western part of the Neptune Range, in the Schmidt and William Hills, pillow lavas having

an aggregate thickness of 1000 m and basalt flows from 2 to 30 m thick are abundant, interbedded with the sandstones and slates. Sediments of the Patuxent Formation show graded bedding, load casts, current bedding, and channel fillings. Rock fragments in the sandstones consist of chert grains, shale, phyllite, sandstone, siltstone, and basalt (Williams, 1969).

The thickness of the Patuxent Formation is estimated to be several tens of thousands of feet. The uncertainty is due to the present occurrence of the formation of tight isoclinal folds and the absence of an exposed lower contact. The Patuxent Formation is unconformably overlain by the Middle Cambrian Nelson Limestone and has been thought to be late Precambrian in age by Schmidt (1965).

Nelson Limestone

The Nelson Limestone, the oldest unit of the second sequence, unconformably overlies the Patuxent Formation at an angle of nearly 90° at its type section, 2.4 km south of Nelson Peak on the Washington Escarpment in the Neptune Range (Figure 23). It is conformably overlain by the Gambacorta Formation. The contact between the two units is exposed on Wiens Peak. The Nelson Limestone crops out in the Patuxent Range, the Neptune Range, and the Schneider Hills, part of the Argentina Range northeast of the Forrestal Range.

The formation consists of dark-gray, thin and thick-bedded limestone with a red conglomerate. Total thickness is 180 to 240 m. Three different faunal groups of trilobites and brachiopods of Middle Cambrian age have been identified in the Nelson Limestone; in addition, an

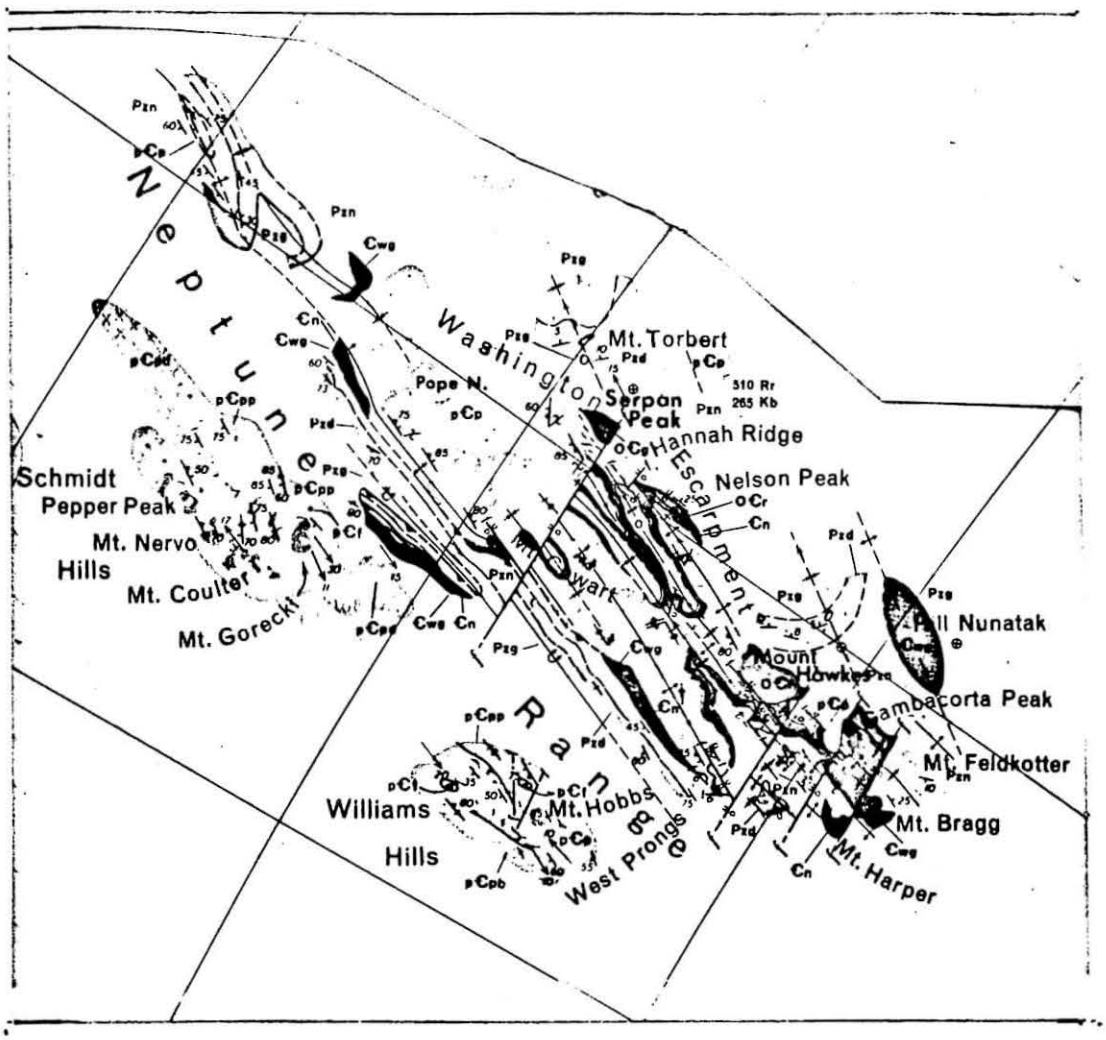

Figure 23. Geologic map of the Neptune Range, Pensacola Mountains (from Schmidt and Ford, 1969).

archaeocyathid of probable Early Cambrian age was found (Schmidt and others, 1965).

Gambacorta Formation

The Gambacorta Formation is a huge complex of lava and breccia flows, with a few ignimbrites. It is confined to the southern Neptune Range, reaching more than 900 m in thickness at Gambacorta Peak (Figure 23) and thinning outwards until it disappears within 5 to 10 km. The upper and lower contacts are exposed and the formation is in conformable succession with the Nelson Limestone below and the Wiens Formation above. The Gambacorta Formation has been divided into six members, as shown in Table 13 (Schmidt and others, 1965).

Wiens Formation

The type section of the Wiens formation is on Elliot Ridge in the southern part of the Neptune Range, to which the formation is limited, and conformably overlies the Gambacorta Formation. In places, the Wiens Formation intertongues with volcanic sedimentry beds of the upper Gambacorta. The formation is unconformably overlain by the Elliot Sandstone of the third sedimentary sequence.

The Wiens Formation consists of interlayered green and red-brown thin-bedded shale, siltstone, and fine sandstone, and contains several thin-bedded gray oolitic limestones. The formation is less than 300 m thick, and, together with the Gambacorta Formation, is probably Cambrian in age (Schmidt, 1965).

Table 13: Stratigraphy of the Gambacorta Formation, Neptune Range. (Schmidt, wirtten communication).

Member	Lithology	Sample Numbers
Elliott Rhyolite Breccia	Rhyolite breccia of the basal Elliot Sandstone	294
Upper Gambacorta	Mostly light green, thin and thick layered, flows and fluvial volcanics	
White Porphyry	Thick, rhyolitic, probably ash flow units with quartz and two feldspar phenocrysts (Feldspars commonly entirely altered)	
Hawkes Pyro-clastics	Thick dark green ignimbritic ash flow tuff units with phenocrystic quartz-Kspar-plagioclase clasts. Relatively little altered and consisting of several differentiation phases	348, 349 350, 351 292, 293
Johnson Porphyry	Thick, black ash flow unit with distinctive phantom or shadow feldspar phenocrysts	391
Red-Brown Member	Thin red-brown and purple agglomerates, breccias, pyro-clastites and flows; generally low potassium and with quartz and plagioclase phenocrysts	290 389, 390
Lower Gambacorta	Thin, mostly light green, pyroclastic (containing devitrified glass and pumice) tuffaceous and fluvial volcanic units. Commonly contaminated with limestone, probably from the underlying Cambrian Nelson Limestone	291

Igneous rocks

Diabase. Diabase sills 2 to 300 m thick are intruded into the Patuxent Formation in the Schmidt Hills of the western Neptune Range. The sills seem to have been folded at the time of initial deformation of the Patuxent formation and may thus be late Precambrian in age (Schmidt, 1965).

Felsic flows and intrusives. Felsic flows 2 to 100 m thick, and plugs about 30 to 55 m in diameter, are interbedded with and intruded into the Patuxent Formation in the Schmidt and Williams Hills of the Neptune Range. Together with the basalt flows and diabase sills of the Patuxent Formation, these felsic flows and plugs form a spilite-keratophyre suite penecontemporaneous with the eugeosynclinal deposition of the Patuxent Formation (Schmidt, written communication).

Hypabyssal rhyolitic porphyry. At Nelson Peak, Gambacorta Peak, and Mt. Hawkes in the eastern Neptune Range, hypabyssal rhyolitic porphyry in sills up to 300 m thick, and in irregularly shaped bodies up to 5 miles in diameter, intrudes rock units as young as the Wiens Formation. The porphyry is evidently older than the Brown Ridge conglomerate, because the conglomerate contains porphyry cobbles (Schmidt, 1965).

Serpan granite and gneiss. At Serpan Peak in the eastern Neptune Range a biotite granite gneiss is in intensely sheared contact with the Patuxent Formation. Vertical axial-plane cleavage of the Patuxent Formation may be parallel with the gneiss contact. Foliation in the gneiss also seems to parallel the contact.

Just east of Serpan Peak, in an area where gravity study indicates a large deep-seated low-density body, are boulders of coarse-grained biotite granite in moraine deposits. The restricted distribution of the boulders and their similarity in hand-specimen, chemical, and petrographic characteristics have led Schmidt (written communication) to suggest that they are derived from a large granite pluton hidden beneath the snow cover east of Serpan Peak.

Schmidt and others (1965) have reported two radiometric dates on specimens from the Serpan Granite: (1) a Rb-Sr whole-rock model date of 510 $\pm$ 30 m.y. and (2) a K-Ar biotite date of 265 $\pm$ 13 m.y. In addition, a lead-alpha date of 350 $\pm$ 40 m.y. on zircon from the same granite was reported recently (Schmidt, written communication). Along with this last analysis, Schmidt suggested that each date may have geologic meaning, the spread reflecting the effects of polymetamorphism.

Three regional metamorphic events are known from stratigraphic and structural relationships in the Pensacola Mountains:

(1) A pre-Middle Cambrian event which involved folding of the Patuxent Formation.

(2) A Cambro-Ordovician (about 500 m.y.) event, the Ross Orogeny, which involved folding of the second stratigraphic sequence, including the Middle Cambrian Nelson Limestone.

(3) A post-Permian event (225 m.y. or less), perhaps mid-Mesozoic, which involved folding of the third sequence, including Permian coal beds. Ford has recently defined this disturbance as the Weddell Orogeny (Schmidt, written communication).

The apparently close relationship between the gneiss of Serpan Peak and the supposed granite body allows three possible interpretations: (1) the gneiss is Precambrian crystalline basement, brought to the surface along a fault between the granite and the Patuxent Formation; (2) the gneiss is a mafic border phase, genetically related to the granite pluton; or (3) the gneiss is a zone of chemically altered sedimentary rock at the contact of the granite (Schmidt, written communication).

Schmidt (written communication) has suggested that the second interpretation is most probable: that the gneiss represents a foliated "protoclastic" border phase of the Serpan granite. Chemical analyses of the granite and gneiss are compared in Table 14. The gneiss samples contain less SiO_2, Na_2O, and K_2O_2 than the granites. However, the gneiss samples contain more Al_2O_3, Fe_2O_3, MgO, and CaO than the granites. It is not yet possible to determine the reason for this difference in chemistry, if in fact the granite and gneiss are co-magmatic. Another possibility exists: that the more mafic character of the gneiss is a result of partial assimilation of the adjacent Patuxent Formation. No chemical analyses of the Patuxent Formation are available at this time to test this possibility.

Besides the granite-gneiss relationship, there may be a genetic relationship between the Serpan Granite and the volcanics of the Gambacorta Formation. Schmidt and others (1965) suggested the possibility that the granite is older than the Elliott Sandstone. If this is true, the granite may intrude the Gambacorta Formation, underlying the

Table 14: Chemical Analyses of the Serpan Granite and the Serpan Gneiss, Neptune Range, Pensacola Mountains (from Schmidt, written communication)

	Serpan Granite		Serpan Gneiss	
	432	433	427	431
SiO_2	75.96	75.25	55.41	69.86
Al_2O_3	12.87	12.92	16.71	14.37
Fe_2O_3	.50	.55	3.32	.85
FeO	1.03	1.27	4.97	2.21
MgO	.09	.09	3.54	1.06
CaO	.59	.65	6.76	1.41
Na_2O	3.29	3.26	2.99	3.50
K_2O	4.78	4.92	2.60	4.39
H_2O+	.50	.59	1.38	1.21
H_2O-	.08	.09	.04	.07
TiO_2	.10	.12	1.30	.50
P_2O_5	.01	.01	.49	.15
MnO	.04	.05	.15	.08
CO_2	.02	.03	.05	.17
Cl	.01	.02	.02	.03
F	.02	.02	.16	.06
Subtotal	99.89	99.84	99.89	99.92
Less O	.01	.01	.07	.04
Total	99.88	99.83	99.82	99.88

Elliott Sandstone. The Gambacorta volcanics may then represent the beginning of an orogeny in Cambro-Ordovician time that ended with the intrusion of the Serpan Granite. Table 15 lists chemical analyses of samples of the Gambacorta Formation. Comparison with Table 14 shows a close similarity between these analyses and those for the Serpan Granite. If these two units are indeed co-magmatic, they could have identical initial Sr^{87}/Sr^{86} ratios. This hypothesis was tested and the results are discussed in the later section, Age Determinations (Summary).

Lamprophyre dikes. Several small dikes of porphyritic olivine-clinopyroexne-biotite lamprophyre a few cm to 1 m wide cut the Patuxent Formation in the Patuxent Range. Brecciation, viscous-flow structure, and lack of wall-rock alteration suggest that the dikes were intruded at relatively low temperatures. Potassium-argon dates of 219, 233, and 244 m.y. $\pm$ 5% on biotite from these dikes have been reported by Schmidt and Ford (1969).

Dufek Intrusion. Ford and Boyd (1968) have described the large stratiform mafic intrusion that makes up the Dufek Massif and most of the Forrestal Range. The intrusion consists of pyroxene gabbro interlayered with minor anorthosite and pyroxenite and capped with granophyre. The intrusion is exposed in two partial, nonoverlapping stratigraphic sections each about 2 km thick, one in the Dufek Massif and one in the Forrestal Range.

The estimated thickness of the intrusion is 7 km and the known areal extent is 8,000 km^2; magnetic anomalies indicate a much greater extent unexposed. Layering in the Dufek Massif is tilted gently

Table 15: Chemical analyses of the Gambacorta Formation, Neptune Range, Pensacola Mountains (from Schmidt, written communication)

Sample	351	294	292	293	348	349	350
SiO_2	74.10	73.71	76.98	76.88	74.71	73.27	73.71
Al_2O_3	12.46	14.12	12.06	11.95	12.68	12.63	12.65
Fe_2O_3	1.31	1.52	1.22	1.08	.94	.85	1.82
FeO	1.24	1.40	.27	.38	1.15	2.20	.61
MgO	.39	.38	.17	.08	.44	.54	.49
CaO	1.15	1.79	.19	.55	1.31	2.05	1.38
Na_2O	3.79	.91	2.21	3.31	3.47	3.36	3.33
K_2O	3.50	3.64	5.88	4.75	3.72	3.34	3.32
H_2O+	.85	1.67	.52	.32	.89	1.08	1.29
H_2O-	.04	.27	.08	.05	.05	.05	.12
TiO_2	.26	.11	.11	.28	.24	.34	,23
P_2O_3	.02	.02	.02	.07	.05	.06	.02
MnO	.06	.05	.01	.02	.05	.08	.07
CO_2	.59	.15	.01	.02	.27	.07	.75
Cl	.00	.02	.01	.01	.00	.01	.01
F	.03	.02	.02	.03	.03	.08	.04
Subtotal	99.79	99.78	99.76	99.76	100.00	100.01	99.84
Less O	.01	.01	.01	.01	.01	.03	.02
Total	99.78	99.77	99.75	99.75	99.99	99.98	99.82

southeastward. In the Forrestal Range, the layering forms a broad syncline. Neither the base nor the top are exposed, but a post-Permian age is indicated by metamorphic effects on nearby Permian carbonaceous beds.

Structure

Figure 24 is a diagrammatic geologic cross-section of the central Neptune Range (Schmidt and others, 1965) that illustrates the structure of the Pensacola Mountains, with the exception of the Dufek Massif. The structure of the Neptune Range can be divided into three parts coinciding with the three stratigraphic sequences, each bounded above by an angular unconformity.

The oldest sequence consists of the Patuxent Formation. These rocks are mostly isoclinally folded with nearly vertical axial-plane cleavage that strikes north in the Neptune Range, northeast in the Patuxent Range.

The second sequence consists of the Nelson Limestone, the Gambacorta Formation, and the Wiens Formation. Open, sinuous folds are symmetrical with wave lengths of about 9.6 km. Some smaller folds are disharmonic, asymmetrical, and locally overturned toward the west. Fold axes trend northerly and plunge gently to the south.

The Beacon rocks of the third sequence have likewise been deformed into broad open folds, trending northerly in the central Neptune Range and in the Forrestal Range. The rocks of the third sequence dip gently east on the plateau of the eastern Neptune Range and are horizontal in the northeastern part. Along a major structural discontinuity,

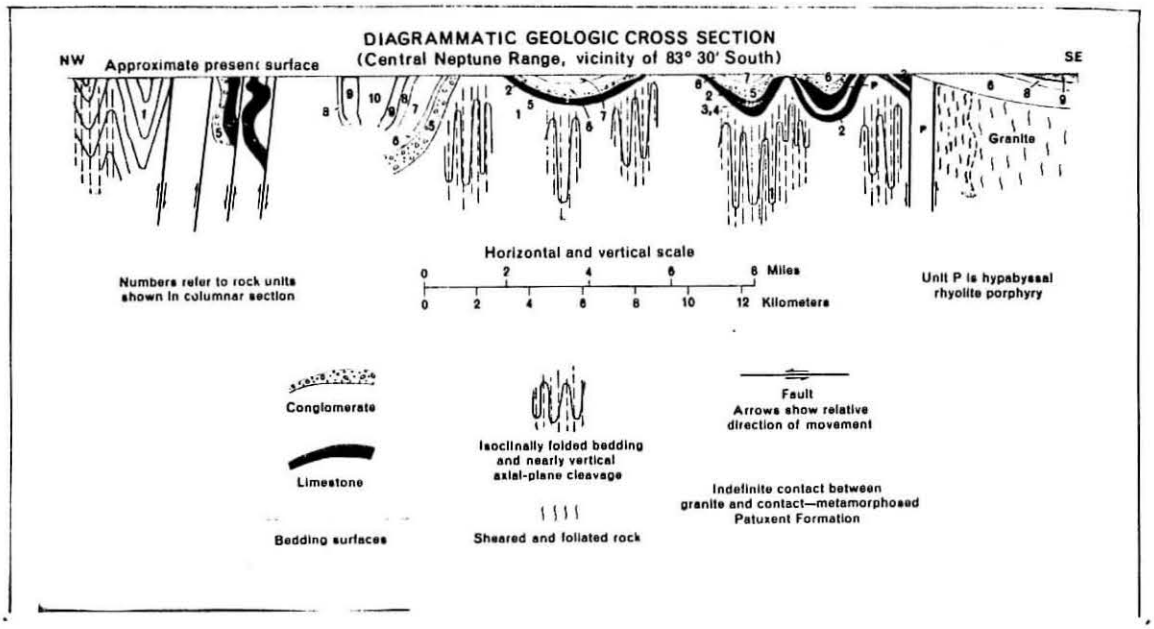

Figure 24. Structure cross section of the Neptune Range, Pensacola Mountains (from Schmidt and Ford, 1969).

probably a fault zone, in the west central Neptune Range, the rocks of the third sequence are nearly vertical or slightly overturned to the west (Schmidt and others, 1965).

The Dufek Intrusion has been uplifted along high-angle faults bordering the southeastern edge of the Filchner Ice Shelf. A similar fault zone of probable large displacement may be the reason for the present height of the Pensacola Mountains (Schmidt and Ford, 1969).

Age Determinations

An attempt was made to date seven rock units of the Pensacola Mountains: the Patuxent Formation; the diabase sills, the basalt flows, and the felsic flows interlayered with it; the Gambacorta Formation; and the Serpan Granite and Gneiss. These units are part of the first and second stratigraphic sequences and have been folded at least twice. The Patuxent Formation has been metamorphosed to the chlorite grade and all the other units have been altered to varying degrees.

Gambacorta Formation

Eleven samples, representing four members (see Table 13) of the Gambacorta Formation have been analyzed for dating. Two additional samples have been included: (1) 294, a rhyolite breccia at the base of the Elliot Sandstone that is part of the Beacon Supergroup sequence above the Gambacorta and (2) 356, a hypabyssal rhyolite porphyry from a plug at Pope Nunatak in the north-central Neptune Range. The analytical data are summarized in Table 16.

Table 16: Rb and Sr Analytical Data for the Gambacorta Formation

Sample	Rb (ppm)$_a$	Sr (ppm)$_a$	Rb^{87}/Sr^{86} ± error	$(Sr^{87}/Sr^{86})_b$ ± 2σ
290	262.6	168.4	4.525	0.7311
	261.1	169.0	4.478	0.7319
avg.	261.9	168.7	4.502 ± 0.023	0.7315 ± 0.0008
291	115.2	241.5	1.381	0.7207 ± 0.0009
	114.2	244.4	1.353	
	114.7	243.0	1.367 ± 0.014	
292	130.0	166.0	2.270 ± 0.028	0.7214 ± 0.0018
293	144.3	136.5	3.064 ± 0.038	0.7286 ± 0.0012
294	140.6	132.2	3.085 ± 0.038	0.7292 ± 0.0014
348	131.1	121.2	3.136 ± 0.039	0.7291 ± 0.0012
349	121.7	170.5	2.066 ± 0.026	0.7221
				0.7211
				0.7216 ± 0.0010
350	128.5	107.3	3.474 ± 0.043	0.7333 ± 0.0013
351	106.3	112.6	2.736 ± 0.034	0.7286 ± 0.0010
356	136.8	132.7	2.987 ± 0.037	0.7274 ± 0.0008
389	158.7	83.90	5.498 ± 0.069	0.7495 ± 0.0008
390	135.8	193.2	2.035 ± 0.025	0.7223 ± 0.0007
391	94.57	173.1	1.582 ± 0.020	0.7160 ± 0.0005

[a] by isotope dilution

[b] corrected for isotope fractionation by assuming $Sr^{86}/Sr^{88} = 0.1194$

The Gambacorta Formation is probably Middle to Late Cambrian in age, as indicated by stratigraphic relationships. The Hawkes member of the Gambacorta conformably overlies the Middle Cambrian Nelson Limestone in many places. The Gambacorta Formation is well exposed between the Nelson Limestone and the Elliot Sandstone, which is probably Ordovician in age (Schmidt, written communication).

The Rb and Sr analytical data are plotted in an isochron diagram in Figure 25. Clearly, the points are scattered and do not fit a single isochron. That this scatter is real is indicated by the precision of the measurements; samples 290 and 291 were analyzed in duplicate and in both analyses the Rb^{87}/Sr^{86} ratios differed by less than 2%. Duplicate measurements of the Sr^{87}/Sr^{86} ratio in samples 290 and 349 show differences of about 0.1%.

There might be several reasons for such nonlinearity: (1) different degrees of contamination by crustal rocks; (2) different initial Sr^{87} Sr^{86} ratios; (3) the lack of whole-rock closed systems due to metamorphism and alteration since deposition; and (4) the fact that different units of the Gambacorta might be of significantly different age.

Contamination by surficial rocks on which the volcanic flows were extruded must be considered a possibility. Sample 291 from the Lower Gambacorta member, for example, is probably contaminated by the underlying Nelson Limestone. Other samples, however, cannot be explained in this way. Although the Hawkes member is commonly intensely altered and contaminated with calcite near the Nelson Limestone, the samples selected by Schmidt were supposedly not from such disturbed and altered outcrops.

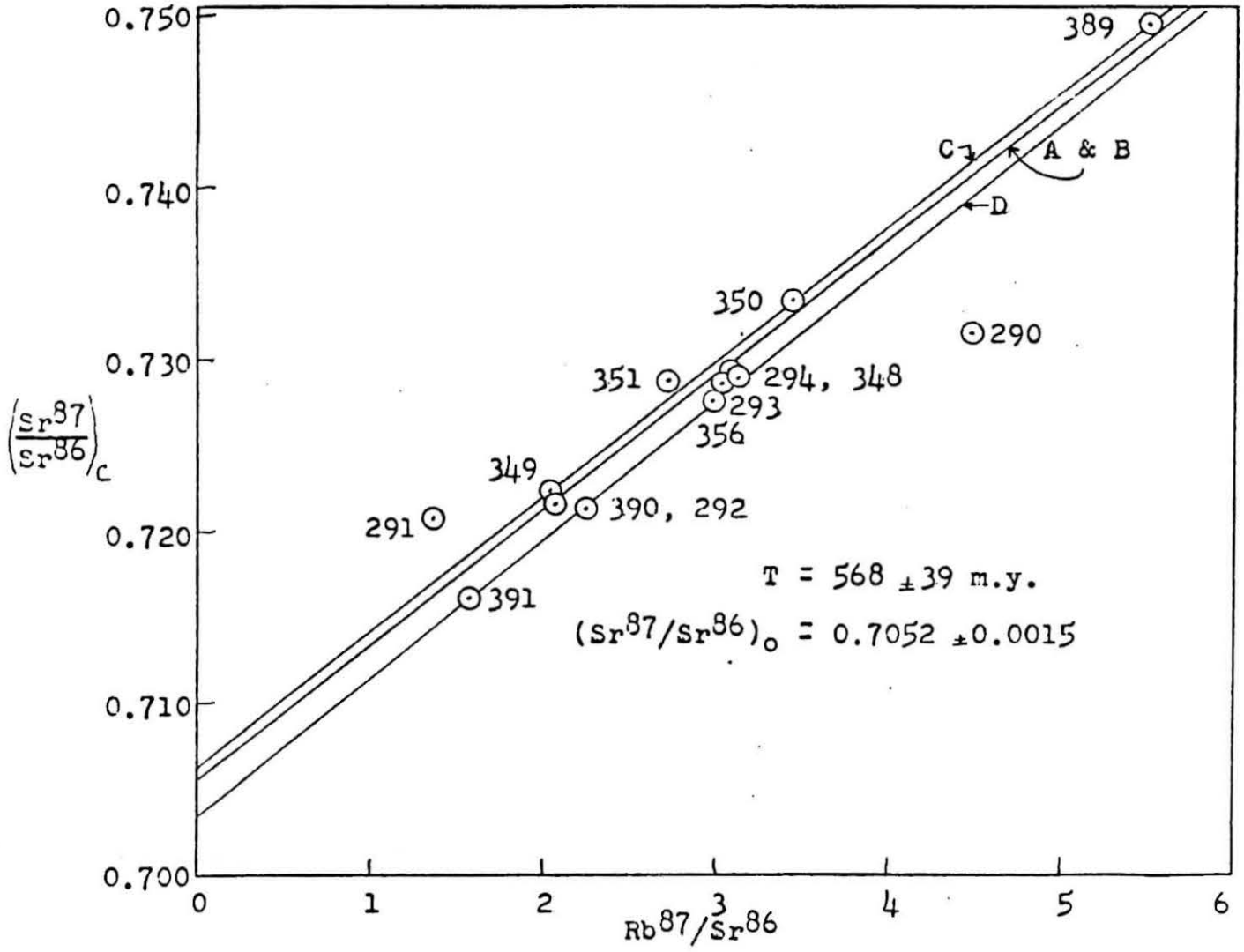

Figure 25. Isochron diagram for the Gambacorta Formation, Neptune Range.

Thin-section analyses of the samples of the Gambacorta Formation, however, show extensive contamination by xenoliths in varying degrees of alteration (Shultz, written communication). Sample 349 from the Hawkes member, for example, has small xenoliths of arenaceous limestone and fine-grained graphic granite. Xenoliths of crustal rock would be enriched in Rb and radiogenic Sr^{87}; their presence in random fashion and in various lithologic types could produce the scatter shown in Figure 25.

The second possibility of explaining the observed scatter is that the flows and pyroclastic units are not co-magmatic. This situation could occur in two ways: (1) the flows and pyroclastics originated at the same time, but from different magma sources, some perhaps containing more crustal-derived matter than others and thus having higher Sr^{87}/Sr^{86} ratios (2) the units may be of different age, which is the fourth possibility for producing the observed scatter. Both of these conditions would be indicated by isotopic homogeneity of the initial Sr^{87}/Sr^{86} ratios within each stratigraphic unit. Two units are represented by more than one sample. Samples 290, 390, and 389 from the Red-Brown Member are only co-linear if 290 is omitted (isochron B in Figure 25). The six samples from the Hawkes Pyroclastics (292, 293, 348, 349, 350, 351) define isochron A, but are also not co-linear. The nearly identical positions of isochrons A and B and the scatter of points defining isochron A seem to indicate that the Red-Brown and Hawkes Members do not have characteristic initial Sr^{87}/Sr^{86} ratios.

The third suggested possibility is varying degrees of alteration during the several metamorphic events since deposition of the Gambacorta Formation in the Cambrian. All thin sections described by Schultz show alteration effects. Sample 290 is a greatly altered rhyolite, showing abundant hematite (as do many other samples), which suggests iron metasomatism. Alteration effects common in other samples are: (1) embayed and rounded quartz grains (2) K-feldspar altered to clay, epidote, and sericited, and replaced by hematite (3) plagioclase partially altered to sericite and epidote (4) anphibole altered to chlorite, sphene, and carbonate. Together with contamination by xenoliths of crustal rocks, metamorphism provides ample reason for the scatter shown in Figure 25.

If an isochron is fitted to all thirteen samples the calculated date is 493 ± 53 m.y. This date is compatible with stratigraphic relationships, but the poor degree of fit is unacceptable. Isochron A is calculated for twelve points, 290 is omitted, and indicates a date of 568 ± 39 m.y. with an initial Sr^{87}/Sr^{86} ratio of 0.7052 ± 0.0015.

If a procedure is followed like that described in the "isochron analysis" section, it may be possible to reduce the error of the age determination and to indicate a more realistic variation of the initial Sr^{87}/Sr^{86} ratio. Samples from the Hawkes Member and the Red-Brown Member (except 290) define isochrons B and C respectively (isochron B is not drawn, but is very close to A). Samples 292, 356, and 391 define isochron D. Isochron B indicates a date of 572 ± 81 m.y. with an initial Sr^{87}/Sr^{86} ratio of 0.7051 ± 0.0032. Isochron C indicates a date of

563 $\pm$ 2 m.y. and an initial Sr^{87}/Sr^{86} ratio of 0.7063 $\pm$ 0.0001. Isochron D produces a date of 580 $\pm$ 5 m.y. and has an initial Sr^{87}/Sr^{86} ratio of 0.7032 $\pm$ 0.0001. These three isochrons are parallel, within the limits of error, to isochron A, defined by all the samples (except 290).

All of these dates are consistent with the stratigraphic age of the Gambacorta Formation and account for 12 of the 13 samples; the highly altered sample, 290, does not fit an isochron that is compatible with stratigraphic information. By this method the best possible radiometric determination of the age of the Gambacorta Formation is a weighted average of the dates of isochrons B, C, and D: 573 $\pm$ 81 m.y. The range of initial Sr^{87}/Sr^{86} ratios is from 0.7031 to 0.7083.

In this case the method of multiple isochrons has not reduced the error of the age determination. The error of isochron A fitted through all the points (except 290) is 7%; the error of the weighted average isochron is 14%. The range of initial Sr^{87}/Sr^{86} ratios for the two methods is only slightly different, 0.7037 to 0.7067 for isochron A and 0.7031 to 0.7083 for the weighted average isochron. Separation of the Gambacorta Formation samples on the basis of stratigraphy is not sufficient to reduce the error of the age determination.

In summary, the rocks of the Gambacorta Formation do not form a single isochron because they have not remained closed systems to Rb and Sr since their extrusion as lava and pyroclastics. Contamination has probaly occurred by inclusion of xenoliths of crustal rocks or post-depositional alteration, or both. The best estimate of the age of these volcanics is 568 $\pm$ 39 m.y.

Serpan granite and gneiss

Eight samples of the Serpan gneiss from Serpan Peak in the northeast Neptune Range were analyzed for dating. The analytical data are summarized in Table 17 together with data for two specimens of Serpan granite from moraine deposits near Serpan Peak.

The gneiss samples vary from a dark dioritic phase with abundant hornblende, sphene and chloritized biotite to a leucocratic phase in which the biotite is also altered to chlorite. One of the granite samples is a white biotite granite, the other is a red variety.

The data for the Serpan gneiss are plotted in an isochron diagram in Figure 26. As with the Gambacorta Formation no single linear array is apparent. An isochron fitted to all eight samples indicates an age of 674 ± 55 m.y. with an initial Sr^{87}/Sr^{86} ratio of 0.7054 ± 0.0006. This isochron has not been drawn on Figure 26 because the scatter of the data suggests that multiple isochrons may be more accurate representatives of the age of these rocks.

If, as Schmidt has suggested, the gneiss represents a border phase of the Serpan Granite, then the chemical differences between the two shown in Table 14 indicate that assimilation of country rock (probably the Patuxent Formation) has occurred. This assimilation may be responsible for the scatter of points on the isochron diagram. If the gneiss samples are assumed to be the same age, then parallel isochrons fitted to subsets of the data will reduce the uncertainty in the calculated age due to the presence of more than one initial Sr^{87}/Sr^{86} ratio.

Table 17: Rb and Sr Analytical Data for the Serpan Granite and Gneiss, Neptune Range

Sample	Rb (ppm)[a]	Sr (ppm)[a]	Rb^{87}/Sr^{86} ± error	$(Sr^{87}/Sr^{86})_b$ ± 2σ
Serpan Granite				
432	280.2	66.6	11.64 ± 0.19	0.7933 ± 0.0030
433	266.2	60.9	11.87 ± 0.18	0.7934 ± 0.0026
USGS[d]	278.0[c]	54.4[c]	14.74	0.8154 -
Serpan Gneiss				
424	161.2	452.4	0.9623 ± 0.0149	0.7153 0.7153 0.7153 ± 0.0002
425	156.6	314.5	1.347 ± 0.021	0.7153 0.7161 0.7157 ± 0.0008
426	87.2	823.2	0.2842 ± 0.0044	0.7078 0.7078 0.7078 ± 0.0002
427	98.4	654.7	0.4096 ± 0.0066	0.7087 ± 0.0022
428	164.0	440.6	1.020 ± 0.016	0.7130 ± 0.0018
429	89.2	628.1	0.3826 ± 0.0061	0.7094 ± 0.0014
430	205.5	175.2	3.155 ± 0.048	0.7304 0.7318 0.7311 ± 0.0014
431	170.6	397.3	1.157 ± 0.018	0.7162 ± 0.0017

[a] By x-ray fluorescence

[b] Corrected for fractionation by assuming $Sr^{86}/Sr^{88} = 0.1194$

[c] By isotope dilution

[d] Schmidt, written communication

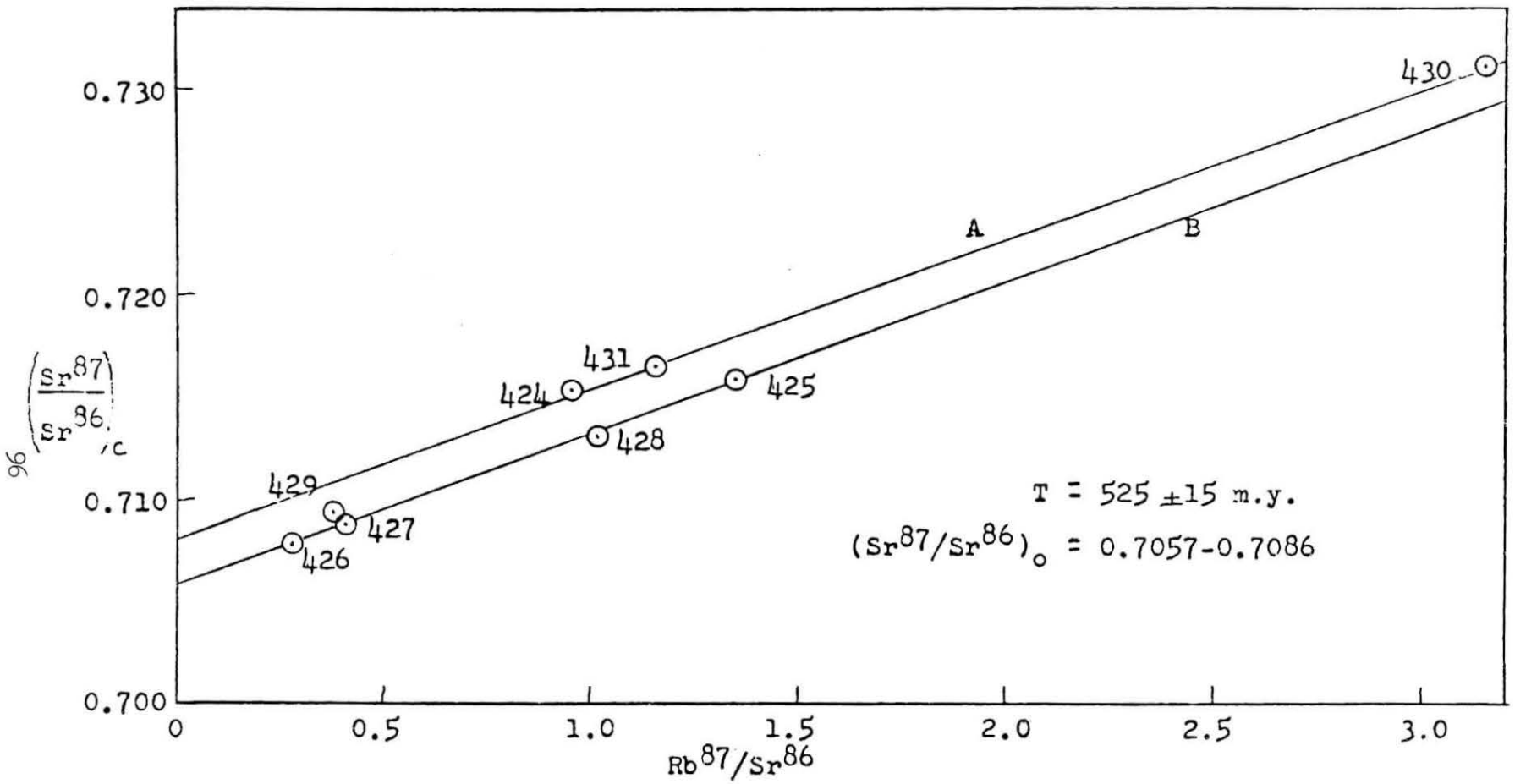

Figure 26. Isochron diagram for the Serpan Gneiss, Neptune Range, Pensacola Mountains.

Isochron A in Figure 26 is defined by samples 424, 430, and 431. It indicates a date of 516 $\pm$ 14 m.y. with an initial Sr^{87}/Sr^{86} ratio of 0.7084 $\pm$ 0.0002. Isochron B, defined by samples 425, 426, 427, and 428, indicates a date of 531 $\pm$ 5 m.y. with an initial Sr^{87}/Sr^{86} ratio of 0.7057 $\pm$ 0.0. The best estimate of the age of these rocks is a weighted average of these two isochrons: 525 $\pm$ 15 m.y. with a range of initial Sr^{87}/Sr^{86} ratios of 0.7057 to 0.7086.

Analytical data for the Serpan Granite have been plotted in Figure 27. The two samples of granite analyzed at The Ohio State University (432, 433) are combined in this plot with the granite sample dated by the U.S. Geological Survey (U.S.G.S.). An isochron fitted to these three samples indicates an age of 530 $\pm$ 34 m.y.; the initial Sr^{87}/Sr^{86} ratio is 0.7064 $\pm$ 0.0061. This age is identical within the limits of analytical error to the model age calculated by the U.S.G.S. for one sample of the Serpan Granite. The large uncertainty in the initial Sr^{87}/Sr^{86} ratio is due to the position of the data points, far from the Sr^{87}/Sr^{86} coordinate and because the two samples analyzed at O.S.U. plot very close together, but are not identical, producing some uncertainty in what otherwise would be a two-point isochron.

The age calculated for the Serpan Granite is also identical within the limits of error to the age of the Serpan Gneiss. The initial Sr^{87}/Sr^{86} ratio of the Serpan Granite is within the range of initial ratios calculated for the Serpan Gneiss. These results, together with the field relationship, support Schmidt's suggestion that the gneiss and granite are co-magmatic. A pooled isochron, Figure 28, using all

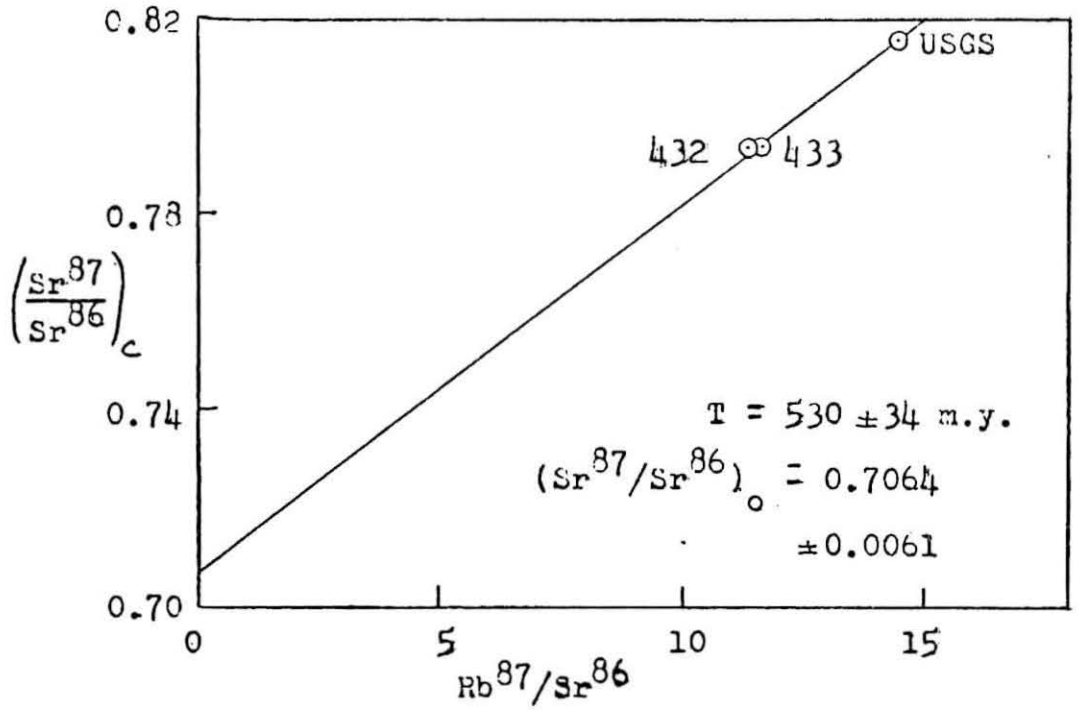

Figure 27. Isochron diagram for the Serpan Granite, Neptune Range.

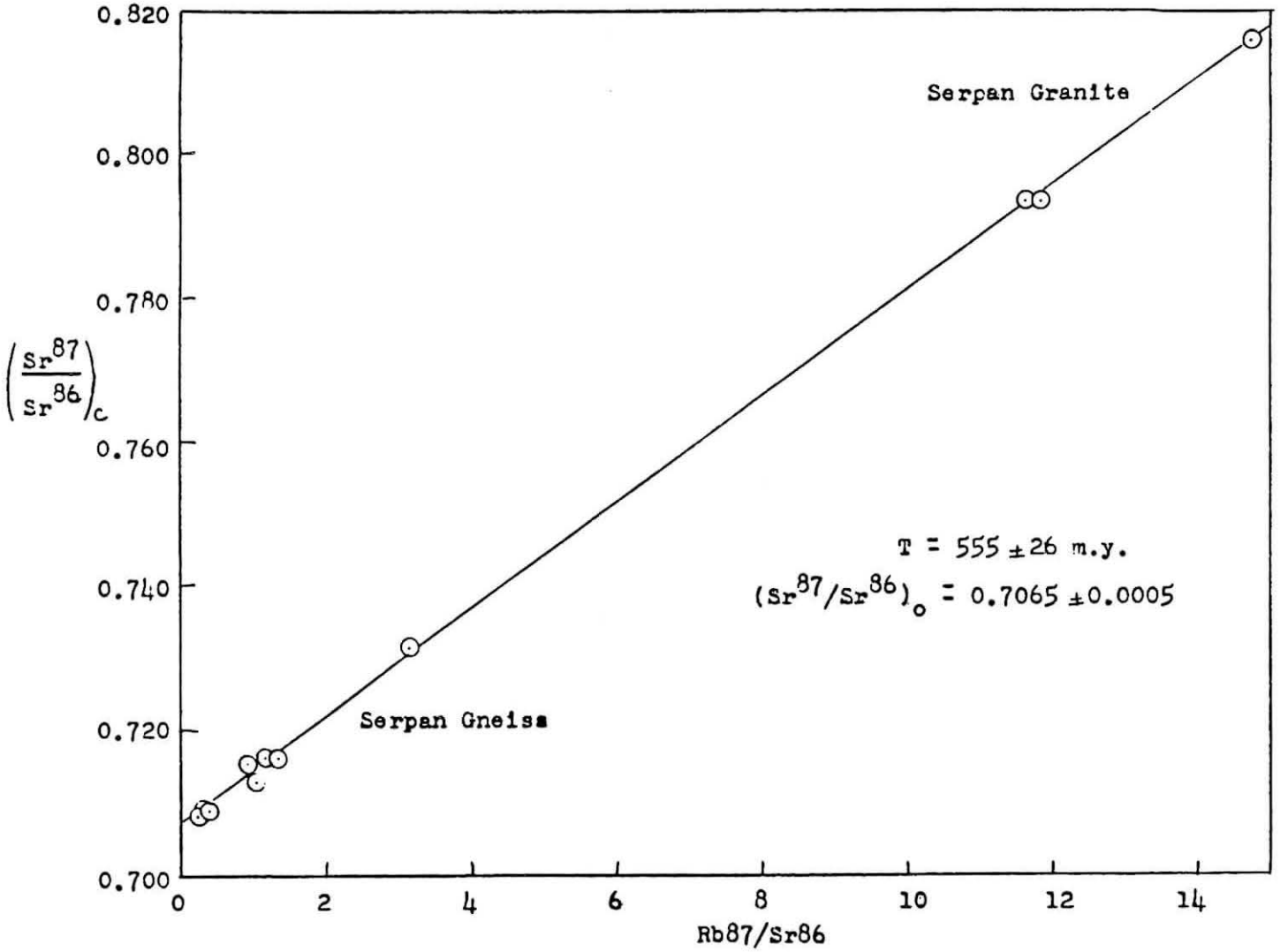

Figure 28. Isochron diagram for the Serpan Granite and Gneiss, Neptune Range.

eleven samples yields probably the best estimate of the age of the Serpan Granite and Gneiss: 555 $\pm$ 26 m.y., with $(Sr^{87}/Sr^{86})_o$ = 0.7065 $\pm$ 0.0005.

Felsic flows and plugs

Nine samples of felsic flows and plugs deposited with and intruded into the Patuxent Formation in the Neptune Range have been analyzed for an age determination. Analytical data for these samples are listed in Table 18.

Three samples are rhyolites collected from Gorecki nunatak in the Schmidt Hills (352, 354, 358). They occur in a large block that does not show the otherwise pervasive isoclinal folding of the Patuxent Formation, but are in a massive breccia containing limestone fragments that are anomalous to the Patuxent Formation.

Five samples are from the Williams Hills. Samples 434, 435, 353, and 355 are rhyolites which occur near vertical dips in isoclinally folded Patuxent Formation. Specimen 357 is a felsic welded tuff and is from an outcrop which does not show folding.

The analytical data for these felsic rocks are plotted in Figure 29. It is clear by inspection that these samples do not define a single isochron. However, four samples, 354, 357, 358, and 434, do define an isochron which is labeled A. It indicates an age of 1210 $\pm$ 76 m.y. and an initial Sr^{87}/Sr^{86} ratio of 0.7052 $\pm$ 0.0008. This age is compatible with the field evidence that the Patuxent Formation is older than Cambrian. In fact, because the felsic flows are interbedded with the sediments, the age of the flows is a good estimate of the time of

Table 18: Rb and Sr Analytical Data for Felsic Flows and Plugs of the Patuxent Formation, Neptune Range

Sample	Rb (ppm)[a]	Sr (ppm)[a]	Rb^{87}/Sr^{86} ± error	$(Sr^{87}/Sr^{86})_b$ ± (2 σ)
352	78.99	299.4	0.7482 ± .0157	0.7158c
	76.43	302.1		0.7122
avg.	77.71	300.8		0.7126 ± 0.0008
353	264.2	111.8	6.903 ± .029	0.7567
	264.5	111.0		0.7546
	264.4	111.4		0.7553
				0.7555 ± 0.0024
354	36.00	318.2	0.3276 ± .0041	0.7111 ± 0.0010
355	116.4	81.23	4.094 ± .071	0.7444
	113.9	82.27		0.7439
	115.2	81.75		0.7442 ± 0.0006
357	2.7c	42.17	0.1299 ± .0384	0.7088
	1.82	38.80		0.7052
	1.82	40.49		0.7070 ± 0.0036
358	102.6	484.4	0.6136 ± .0077	0.7145 ± 0.0014
434	44.8d	116.5d	1.048 ± .017	0.7231 ± 0.0008
435	1.5d	81.6d	0.0557 ± .00464	0.7181
				0.7161
				0.7174 ± 0.0023

[a]By isotope dilution unless otherwise noted.

[b]Corrected for fractionation by assuming $Sr^{86}/Sr^{88} = 0.1194$

[c]Not included in the average.

[d]By x-ray fluorescence.

deposition of the Patuxent Formation.

Four samples do not fit isochron A. Taken together, these samples define an isochron which produces a date of 585 $\pm$ 92 m.y. with an initial Sr^{87}/Sr^{86} ratio of 0.7026 $\pm$ 0.0041. The high initial ratio and the probability that the felsic flows of isochron A are 1210 m.y. old suggests that this date is a reset date due to a metamorphic event, perhaps during the Ross Orogeny.

The reasons why the four rocks of isochron A appear to have escaped the effects of a later metamorphic event are not clear. Geography does not seem to have been a factor. Two of the samples of isochron A are from the Schmidt Hills (354, 358) and two others are from the Williams Hills (353, 434). The degree of metamorphism may have been a factor; three of the samples of isochron A are from outcrops which Schmidt noted as not showing the typical isoclinal folding of the Patuxent Formation (354, 358, 357). However, sample 434 was folded and sample 352, although not folded, does not lie on isochron A.

The large error of the 585 m.y. date and the scatter of the data suggest that the method of multiple isochrons may reduce this uncertainty. Isochron B is constructed through the points for samples 352 and 353. It yields a date of 500 $\pm$ 8 m.y. and an initial ratio of 0.7074 $\pm$ 0.0002. It is parallel to the 585 $\pm$ 91 m.y. isochron within the limits of error. Isochron C is defined by 355 and 435 and is closely parallel to isochron B. It indicates a date of 475 $\pm$ 2 m.y. and an initial ratio of 0.7171 $\pm$ 0.0001. The weighted average date for these two isochrons is 488 $\pm$ 6 m.y. The range of initial Sr^{87}/Sr^{86} ratios is

from 0.7072 to 0.7172. This result is taken as the best date for the four reset samples. It has a significantly lower associated error than the combined isochron and indicates better the scatter of the data because it indicates a larger range of the initial Sr^{87}/Sr^{86} ratio.

In summary, the felsic flows deposited with the Late Precambrian Patuxent Formation may be as old as 1210 ± 76 m.y. however, a Cambro-Ordovician period of volcanism and granitic intrusion has reset some of the felsic flows to the time of this orogeny. The best estimate of this Cambro-Ordovician event, using data from the felsic flows, is 488 ± 6 m.y.

Patuxent Formation

Eleven samples of metasedimentary rocks from the Late Precambrian Patuxent formation were analyzed: 2 subgraywackes, 5 siltstones and shales and 4 slates. These analyses are listed in Table 19. All of these rocks are from the Patuxent Range, unlike the other rock units dated which are from the Neptune Range.

The Patuxent Formation samples were chosen by Schmidt from outcrops in the Patuxent Range so as to be relatively free from alteration by intrusives (Schmidt, personal communication). The rocks are all from different outcrops, scattered throughout the range.

The Patuxent Formation in the Neptune Range contains abundant diabase and basalt, plus the felsic flows and plugs discussed above. In the Patuxent Range, however, the only intrusions are a few small Lamprophyre dikes (232 m.y.), small, probably late Precambrian diabase sills 40 km from a sample site, and a small late Precambrian or early

Table 19: Rb and Sr Analytical Data for the Patuxent Formation, Patuxent Range

Sample	Rb $(ppm)_a$	Sr $(ppm)_a$	Rb^{87}/Sr^{86} $\pm$ error	$(Sr^{87}/Sr^{86})_b$ $\pm 2\sigma$
436	195.0	103.6	5.103 ± 0.079	0.7430 ± 0.0019
437	184.8	65.2	7.704 ± 0.118	0.7639 ± 0.0026
438	102.9	193.2	1.452 ± 0.023	0.7253 ± 0.0025
439	228.7	50.0	$12,498 \pm 0.193$	0.7815 ± 0.0038
440	106.8	98.4	2.936 ± 0.046	0.7315
			avg.	0.7304
				0.7309 ± 0.0011
441	256.5	87.1	8.009 ± 0.123	0.7596 ± 0.0020
442	225.5	36.6	16.735 ± 0.261	0.8083
				0.8091
				0.8087 ± 0.0008
443	-	-	1.671 ± 0.029	0.7272 ± 0.0026
444	153.6	176.0	2.471 ± 0.038	0.7328 ± 0.0016
445	-	-	2.253 ± 0.035	0.7283 ± 0.0036
446	115.5	229.2	1.369 ± 0.021	0.7225 ± 0.0022

[a] By x-ray fluorescence.

[b] Fractionation corrected by assuming $Sr^{86}/Sr^{88} = 0.1194$

Paleozoic rhyolite porphyry 60 km from a sample site. Hopefully, therefore, these samples of the Patuxent Formation would have a radiometric age compatible with their stratigraphic position unconformably beneath the Middle Cambrian Nelson Limestone. They have, however, been regionally metamorphosed.

The analytical data for the Patuxent Formation are plotted in an isochron diagram in Figure 30. Two linear arrays are formed. The distinction as to which line a sample is on does not have any apparent basis in lithology or geographic location. Samples 437 and 444 form isochron A, for which a date of 436 $\pm$ 12 m.y. has been calculated; the initial Sr^{87}/Sr^{86} ratio is 0.7173 $\pm$ 0.0006. The remaining nine samples form an isochron, labeled B, which produces a date of 402 $\pm$ 4 m.y. with an initial Sr^{87}/Sr^{86} ratio of 0.7146 $\pm$ 0.0004. A combined isochron with all eleven samples indicates a date of 395 $\pm$ 10 m.y., identical within the limits of analytical error to the date of isochron B. If samples 437 and 444 are considered anomalous, isochron B can be considered to be the best determination of a radiometric date on the Patuxent Formation. This date is not an indication of the time of deposition, but is a reset date produced by the last metamorphic event which affected the Patuxent Formation in the Patuxent Range.

Basalt and diabase

It was hoped that analysis of the basalt flows and diabase sills deposited with and intruded penecontemporaneously into the Patuxent Formation would permit the accurate dating of the associated sediments. To this end, six diabase samples from the Schmidt Hills and four basalt

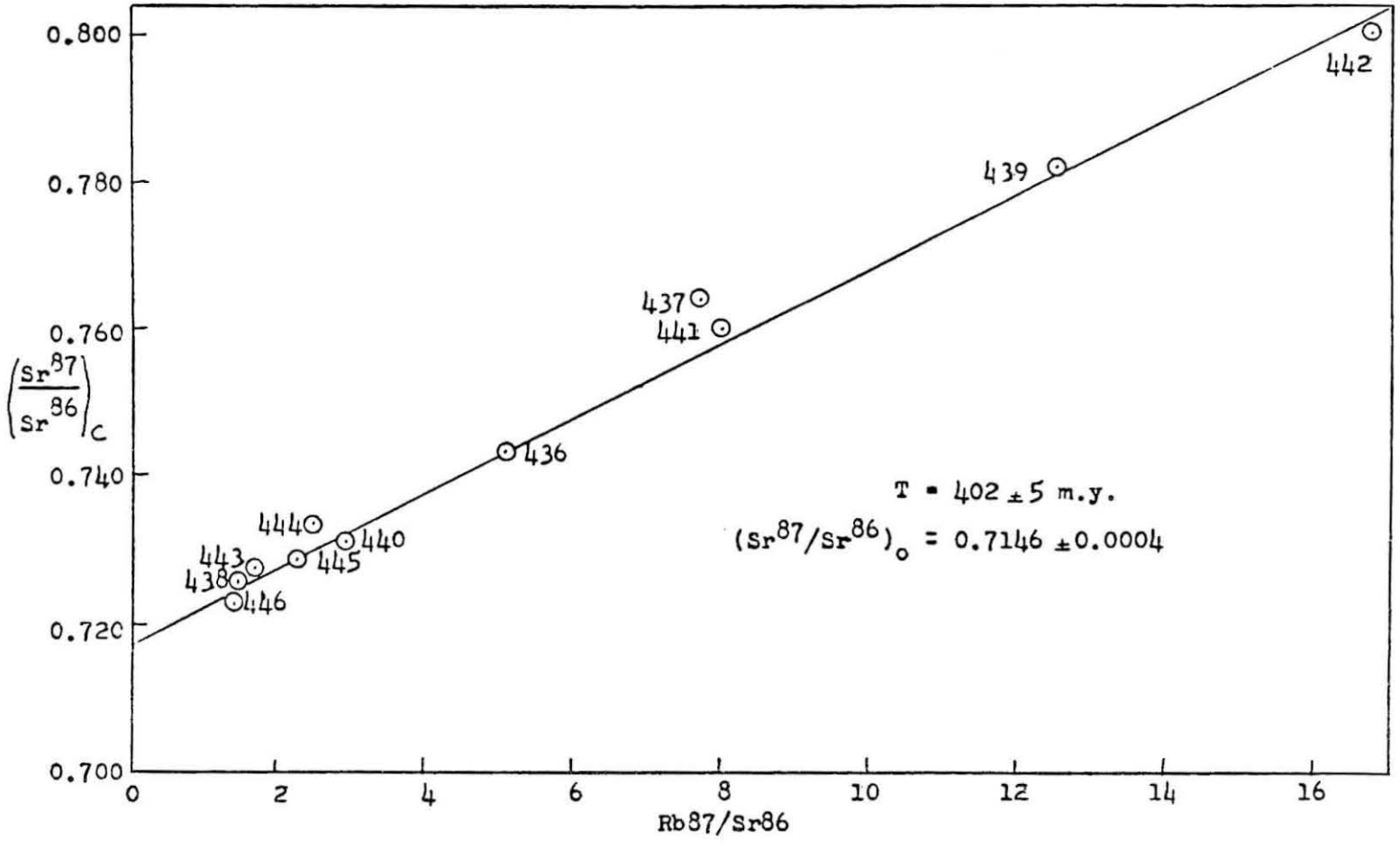

Figure 30. Isochron diagram for the Patuxent Formation, Patuxent Range.

samples from the Williams Hills were analyzed (these outcrop areas are in the western Neptune Range). The analytical data are listed in Table 20 and plotted in an isochron diagram in Figure 31.

As expected for such basic rocks, the values of Rb^{87}/Sr^{86} ratios are quite low (less than 0.7 overall, less than 0.25 for most samples) and their range is small. No apparent isochrons are formed; the samples are not dateable because of low Rb/Sr ratios and insufficient enrichment in radiogenic Sr^{87}.

If the rock systems have not been re-homogenized in Rb and Sr since their original formation, it is possible to calculate maximum and minimum dates of origin. Isochron A in Figure 31 has been drawn as a minimum age limit for the diabase sills and isochron B was drawn as a maximum age limit. Between these two slopes are all possible isochrons for these data, assuming that sample 421 is not anomalous. One of this set of isochrons may indicate the true date of origin for the diabase sills.

Isochron A indicates a minimum date of 760 m.y. with an initial Sr^{87}/Sr^{86} ratio of 0.7067. Isochron B yields a maximum date of 1267 m.y. and an initial Sr^{87}/Sr^{86} ratio of 0.7020. A good estimate of the age of these rocks is obtained by isochron C, which is defined by samples 418, 419, 420, and 421, all from the same sill. The date produced from this calculation is 778 ± 59 m.y. The initial Sr^{87}/Sr^{86} ratio is 0.7065 ± 0.0003. The conclusion that the diabase sills are Precambrian is compatible with the stratigraphic age of the Patuxent Formation.

Table 20: Rb and Sr Analytical Data for Diabase and Basalt of the Patuxent Formation, Neptune Range

Sample	Rb (ppm)$_a$	Sr (ppm)$_a$	Rb^{87}/Sr^{86} ± error	$(Sr^{87}/Sr^{86})_b$ ±2σ
Diabase				
418	12.1	198.0	0.1768 ± 0.0030	0.7079 ± 0.0013
419	8.0	203.6	0.1131 ± 0.0068	0.7077 ± 0.0014
420	2.7	223.8	0.0342 ± 0.0011	0.7071 ± 0.0011
421	66.1	273.9	0.6647 ± 0.0107	0.7138 ± 0.0013
422	9.4	212.9	0.1208 ± 0.0030	0.7061 ± 0.0019
423	23.4	267.4	0.2370 ± 0.0058	0.7062 ± 0.0020
Basalt				
414	8.1$_c$	100.3$_c$	0.1830 ± 0.0070	0.7078 ± 0.0011
415	10.1$_c$	207.6$_c$	0.1371 ± 0.0081	0.7079 ± 0.0018
416	13.0	244.1	0.1415 ± 0.0041	0.7061 ± 0.0024
417	11.1	194.5	0.1655 ± 0.0114	0.7077 ± 0.0016

[a]By x-ray fluorescence unless noted otherwise.

[b]Fractionation corrected assuming $Sr^{86}/Sr^{88} = 0.1194$

[c]By isotope dilution.

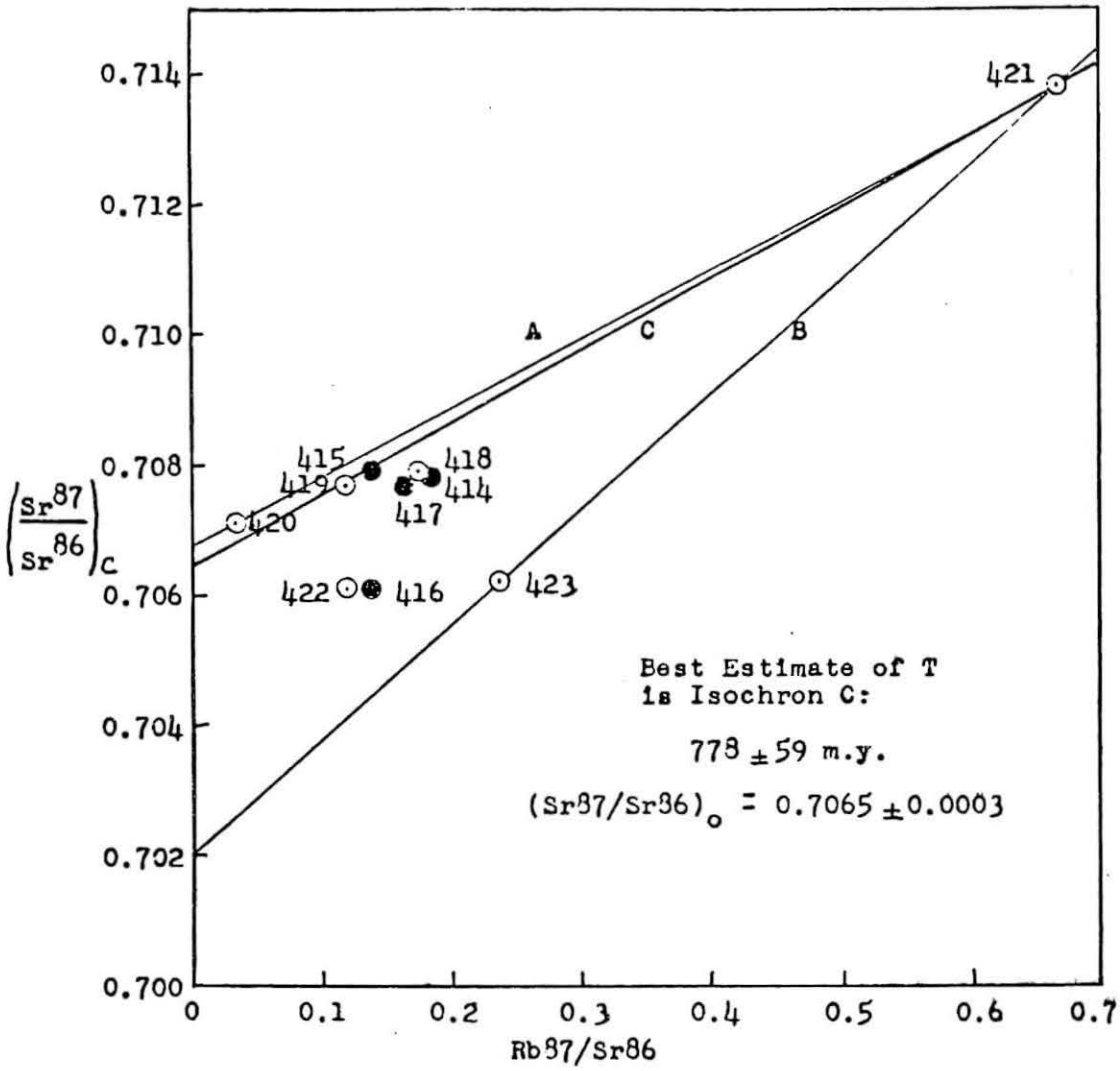

Figure 31. Isochron diagram for diabase and basalt of the Patuxent Formation, Neptune Range.

There is some indication that the diabase samples have retained some original stratigraphic characteristics with regard to the Sr^{87}/Sr^{86} ratios. Samples 418, 419, 420, 421 all come from the same sill (60 m thick) at Gorecki Nunatak. They are numbered in order, from the base to 15 cm below the sill top. Schmidt noted that there was no mega- or micro-evidence of contamination with the surrounding Patuxent Formation, but sample 421 may owe its relatively high Sr^{87}/Sr^{86} ratio to the nearness of the contact and resulting assimilation effects. The remaining two diabase samples, 422, 423 are from the interior of a sill 80 to 110 m thick, at Nunatak #10 and appear to have different Sr^{87}/Sr^{86} ratios from the Gorecki Nunatak samples. Unfortunately, this interpretation is merely conjecture and cannot be used to support the belief that the age estimate is reliable.

The four basalt samples are all from different outcrops in the Williams Hills. Clearly, inspection of Figure 31 shows that the basalt flows do not form an isochron.

Summary

Age determinations on two igneous units which are part of the Patuxent Formation have indicated dates which are compatible with the Precambrian stratigraphic age of the Patuxent Formation: (1) Four samples of felsic flows are dated at 1210 ± 76 m.y. (2) Diabase sills intruding the Patuxent metasediments are estimated to be about 778 m.y. old. These dates are summarized in Table 21.

Prior to the deposition of the Middle Cambrian Nelson Limestone, the Patuxent Formation sediments and included igneous rocks were

Table 21: Summary of Age Determinations for the Pensacola Mountains

Rock Unit		Age (m.y.)	$(Sr^{87}/Sr^{86})_a$
Gambacorta Fm. plus Serpan Granite and Gneiss		510 ± 35	0.7080 ± 0.0024
Serpan Granite and Gneiss		555 ± 26	0.7065 ± 0.0005
Serpan Gneiss	A.	516 ± 14	0.7084 ± 0.0002
	B.	531 ± 5	0.7057 ± 0.0
wt. avg.		525 ± 15	0.7057 - 0.7086
Serpan Granite		530 ± 34	0.7064 ± 0.0061
Gambacorta Formation	A[b]	568 ± 39	0.7052 ± 0.0015
	B.	572 ± 81	0.7051 ± 0.0032
	C.	563 ± 2	0.7063 ± 0.0001
	D.	580 ± 5	0.7032 ± 0.0001
wt. avg.		573 ± 81	0.7031 - 0.7083
Diabase	A.	760	0.7067
	B.	1267	0.7020
	C.	778 ± 59	0.7065 ± 0.0003
Felsic Flows	A[b]	1210 ± 76	0.7052 ± 0.0008
	B.	500 ± 8	0.7074 ± 0.0002
	C.	475 ± 2	0.7171 ± 0.0001
wt. avg.		488 ± 6	0.7072 - 0.7172
Patuxent Formation		402 ± 5	0.7146 ± 0.0004

[a] Initial ratio.

[b] Omitted from average and considered best estimate of the age.

intensely folded and subjected to mild regional metamorphism. This event has not been detected by the age measurements.

The next event, in Cambro-Ordovician time, is as well recorded in the Pensacola Mountains as it is throughout most of the Transantarctic Mountain chain: The Ross Orogeny. This orogeny in the Pensacola Mountains is represented by the intrusion of the Serpan Granite, together with a mafic border phase, the Serpan Gneiss, at 555 ± 26 m.y. The granitic intrusive activity may have been contemporaneous with extensive volcanism, represented by the Gambacorta Formation which was dated at 568 ± 39 m.y.

The possibility, suggested by Schmidt, that the Serpan Granite and the Gambacorta Formations are co-magmatic appears to be consistent with the Rb and Sr isotopic analyses. Figure 32 is an isochron diagram on which are plotted the combined data for the Serpan Granite and Gneiss and the Gambacorta Formation. The individually determined ages for the three igneous units are idential, within the limits of analytical error. The initial Sr^{87}/Sr^{86} ratios are also identical within the limits of error. The chemical analyses of the Serpan Granite and Gambacorta Formation listed in Tables 14 and 15 show strong similarities and also support the hypothesis that these two rocks are co-magmatic.

Metamorphism during the Ross Orogeny re-set some of the felsic flows of the Patuxent Formation to a date of 488 ± 6 m.y. The Patuxent Formation itself remained an open system to Rb and Sr much longer; the date of 401 ± 5 m.y. for the Patuxent Formation in the Patuxent Range is the youngest event detected. However, this date may be related to

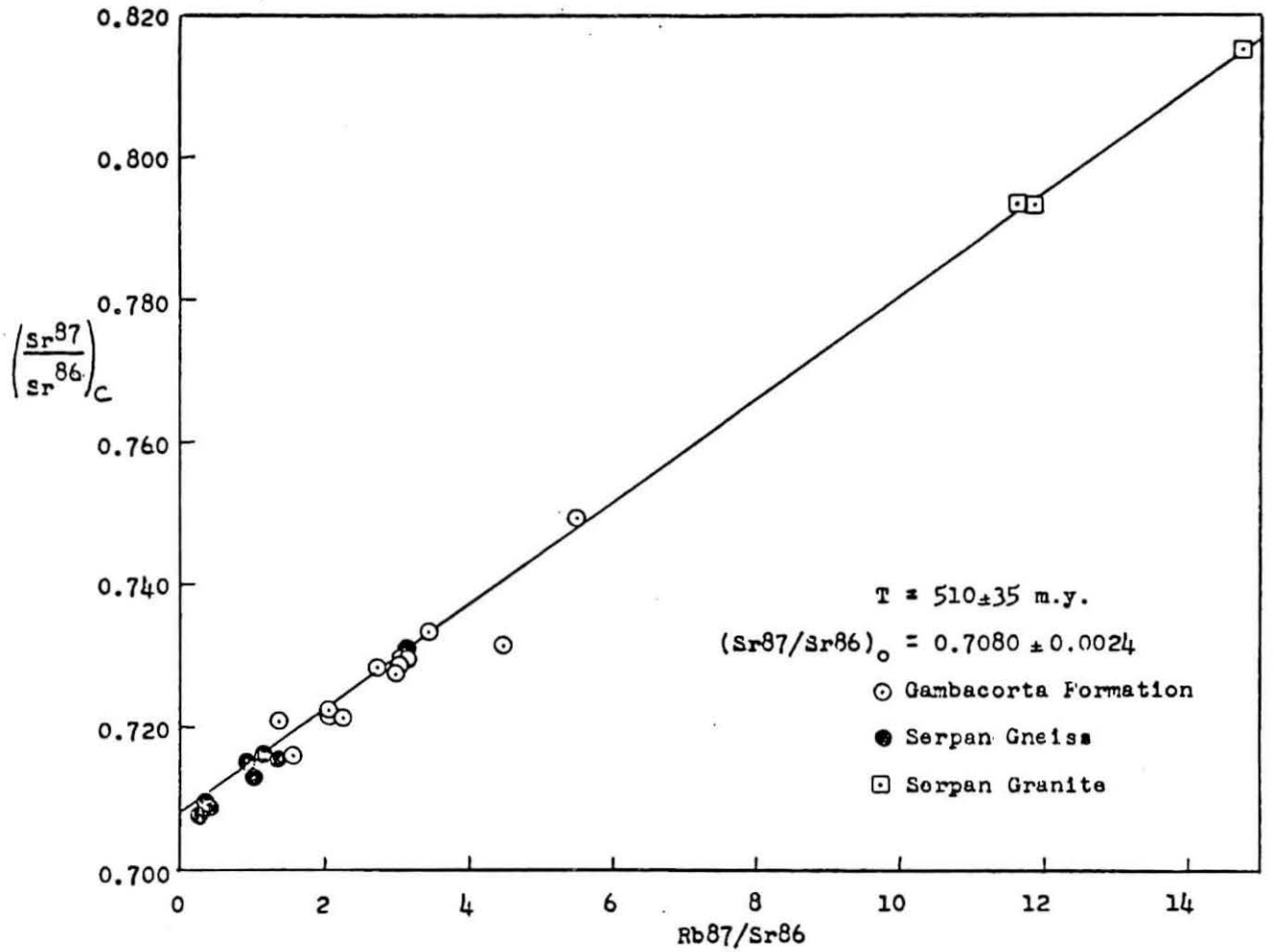

Figure 32. Pooled isochron for the Gambacorta Formation, Serpan Granite, and Serpan Gneiss, Neptune Range.

the different geographic locality of the Patuxent Formation samples. Unfortunately, this formation was not dated in the Neptune Range. It is possible that the Ross Orogeny persisted longer in the Patuxent Range than in the Neptune Range, 100 km away.

CHAPTER IV

THIEL MOUNTAINS

Introduction

The Thiel Mountains, at latitude 85° S. and longitude 90° W., lie about midway along the 85° S. parallel between the Ohio Range of the Horlick Mountains and the Patuxent Range of the Pensacola Mountains (see Figures 1 and 33). They were originally thought to be part of the Horlick Mountains until mapping by the Horlick Mountains traverse party in December 1959 showed that they formed a separate range.

U.S. Geological Survey field parties did reconnaissance mapping in the Thiel Mountains in January, 1961, and from November 1961 to January 1962. The results of these investigations have been reported by Ford (1964), Aaron and Ford (1964), Anderson (1963), Ford and Aaron (1962), Ford and others (1963), and Schmidt and Ford (1969).

General Geology

The Thiel Mountains consist predominantly of a large still-like body of cordierite-hypersthene quartz-monzonite porphyry, which is intruded by several granite plutons. In addition to the igneous rocks there are relatively minor amounts of thermally-metamorphosed clastic sedimentary rocks. Radiometric age determinations summarized by Schmidt and Ford (1969) and listed in Table 22 indicate late Precambrian

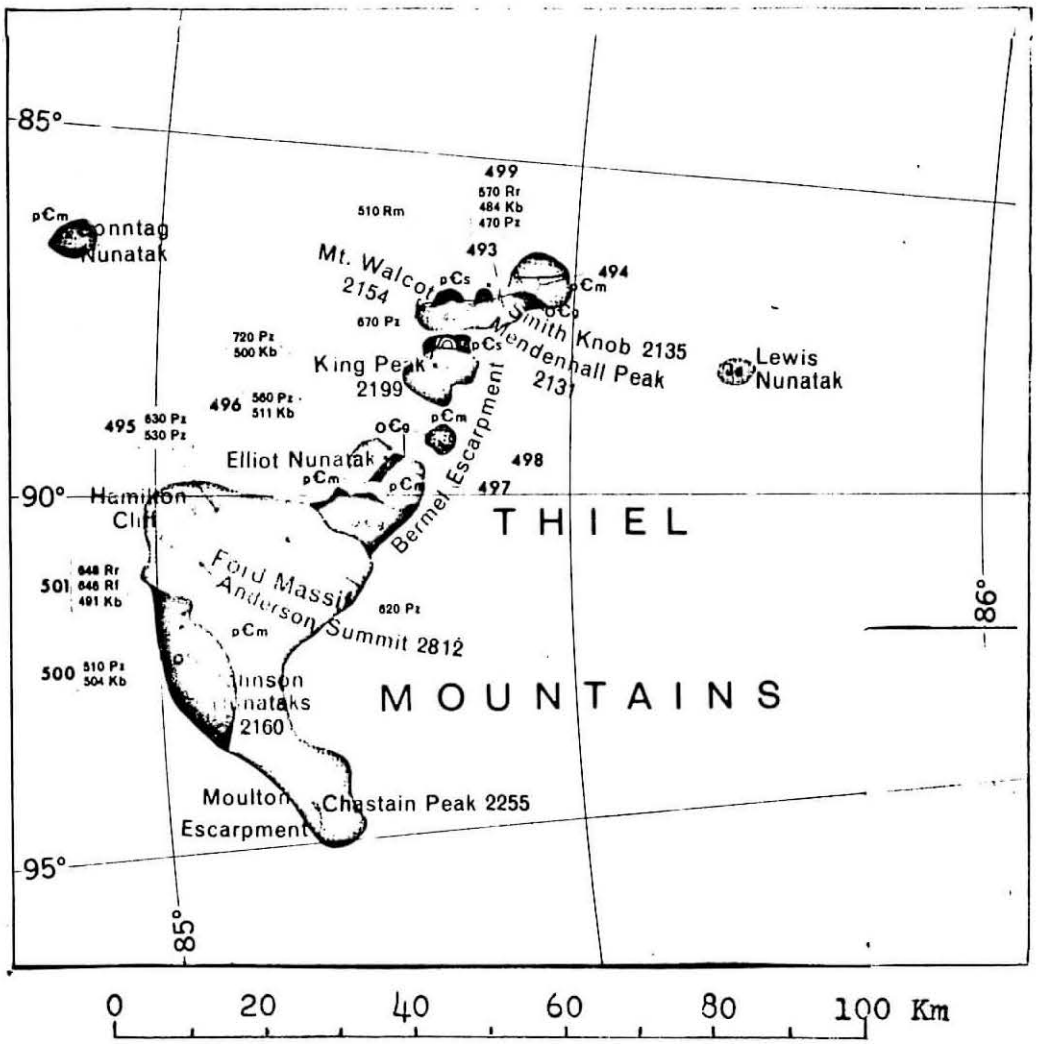

Jd	Diabase	Jurassic ?
OCg	Granitic Rock	Upper Cambrian to Lower Ordovician
pCm	C-H-Q monzonite porphyry	Precambrian
pCs	Metasedimentary Rocks	Precambrian

Figure 33. Geologic map of the Thiel Mountains (from Schmidt and Ford, 1969).

Table 22: Published Age Determinations for the Thiel Mountains, Antarctica

Location	Method & Material	Age (m.y.)	Reference
A. Cordierite-hypersthene quartz-monzonite porphyry			
85° 10' S. 90° 30' W.	Pb-alpha: Zircon	620 ± 70	2
85° 5' S.	Pb-alpha: Zircon		
	non-magnetic	630 ± 70	2
	magnetic	530 ± 60	2
85° 19' S. 87° 50' W.	Pb-alpha: zircon	670 ± 50	1
B. Granodiorite			
85° 17' S. 89° 20' W.	Pb-alpha: zircon	720 ± 90	3
	K-Ar: biotite	500 ± 5%	3
85° 2' S. 91° 37' W.	Rb-Sr: whole rock	648 ± 85	3
	Rb-Sr: K-feldspar	646 ± 85	3
	K-Ar: biotite	491 ± 5%	3
85° 27' S. 87° 00' W.	Rb-Sr: whole rock	570 ± 70	3
	K-Ar: biotite	484 ± 5%	3
	Pb-alpha: zircon	470 ± 50	1
85° 17' S. 89° 30' S.	Pb-alpha: zircon	560 ± 60	1
	K-Ar: biotite	511 ± 5%	3

Table 22 (Continued)

Location	Method & Material	Age (m.y.)	Reference
85° 2' S. 91° 45' W.	Pb-alpha: zircon	510 ± 50	3
	K-Ar; biotite	504 ± 5%	3

References:
1. Ford, 1964.
2. Ford, et al., 1963.
3. Schmidt and Ford, 1969.

to Early Paleozoic ages for the bedrock of the Thiel Mountains.

Metasediments

The oldest rocks of the Thiel Mountains are low-grade thermally metamorphosed thin-bedded clastic sedimentary rocks. They crop out in the easternmost nunataks of the Thiel Mountains, and consist of spotted hornfelses, impure marbles, sandstones, and siltstone. These beds total about 100 m in thickness and are nearly horizontal. Thin sills or flows of dacite are concordantly intercalated with the metasediments. The metasediments are of unknown age, but are late Precambrian or older because they are intruded by the cordierite-hypersthene quartz-monzonite porphyry for which Schmidt and Ford (1969) reported a late Precambrian age.

Cordierite-Hyperstene Quartz-Monzonite Porphyry

The principal rock of the Thiel Mountains is a medium-grained dark-gray cordierite-hypersthene quartz-monzonite. It crops out throughout the 200 km^2 area of the Thiel Mountains and shows no foliation or layering in most exposures. At one locality faint layering in the porphyry defines a broad, open anticline with a minimum amplitude of 500 m, and at another locality a gneissic texture may be related to magmatic flowage (Ford, 1964).

About 60 percent of the porphyry is composed of large, angular phenocrysts of plagioclase and angular to rounded and embayed phenocrysts of quartz ranging from 2 to 6 mm in size. These are set in a very fine-grained holocrystalline groundmass of anhedral quartz and alkali feldspar. Smaller phenocrysts of potassium feldspar, hypersthene,

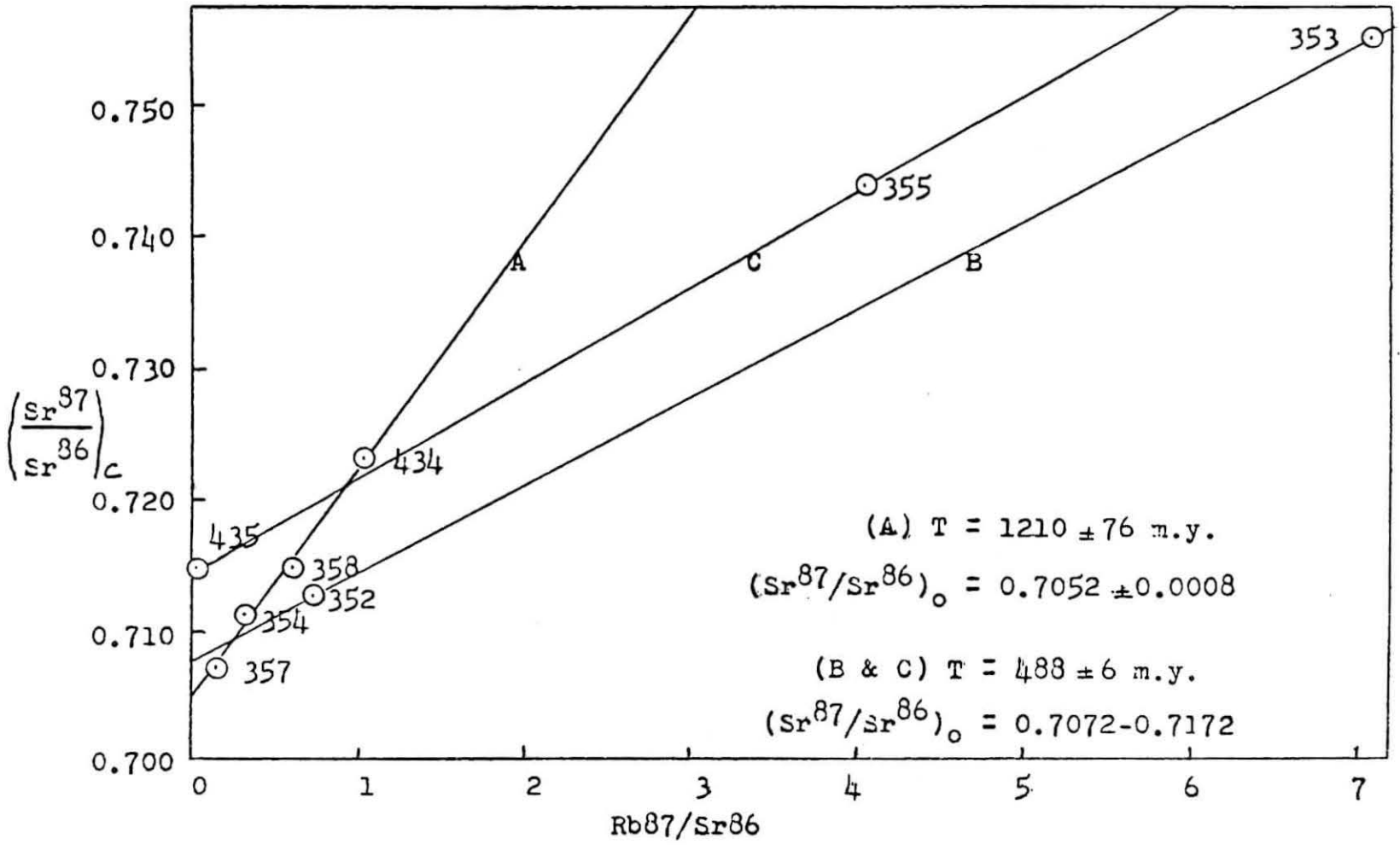

Figure 29. Isochron diagram for the felsic flows of the Patuxent Formation, Neptune Range.

and cordierite are also present (Ford, 1964).

Table 22 lists dates obtained by the lead-alpha method on zircons from the hypersthene quartz-monzonite porphyry. There is reasonably good agreement for a late Precambrian-Cambrian age.

Although the presence of cordierite might suggest a metamorphic origin of the porphyry, an igneous origin is clearly indicated, according to Ford (1964) and Vance (1962), by abundant euhedral or fragmented plagioclase phenocrysts showing delicate oscillatory zoning, as well as by large quartz phenocrysts showing considerable resorption effects. There is no clear evidence, however, whether the porphyry is volcanic or hypabyssal in nature. The very fine-grained groundmass may be the result of rapid cooling on extrusion at the surface. But many other characteristics favor an intrusive origin, perhaps as a large sill: the absence of bedding, the vertical and lateral homogeneity, the absence of individual flow units, and the uniform chemical composition.

In his description of the porphyry, Ford (1964) noted the presence of granulite inclusions containing cordierite and hypersthene. He suggested that these inclusions are metamorphic xenoliths from original cordierite and hypersthene granulites (charnockites) and that their presence may explain the uniform and widespread presence of cordierite and hypersthene within this rock.

Biotite Granite and Quartz Monzonite

Several large masses of light-colored granitic rock intrude the porphyry. These have been dated as Cambrian to Early Ordovician in age (see "granodiorite" in Table 22). The granitic intrusives are granodioritic to quartz monzonitic in modal and chemical composition.

The intrusive character of the granitic rock is shown by contact breccia, with blocks of altered porphyry included in the granitic rock; by granite dikes and pegmatites in the porphyry; and by recrystallization effects in porphyry samples collected near the contacts (Ford, 1964).

Age Determinations

Samples of the cordierite-hypersthene quartz-monzonite porphyry and the granitic rocks that intrude it were analyzed for dating.

Cordierite-Hypersthene Quartz-Monzonite Porphyry

Four samples of the principal rock of the Thiel Mountains were analyzed for dating by the Rb-Sr whole-rock isochron method. The locations of these samples (493, 494, 495, 496) are shown on the map of the Thiel Mountains, Figure 33. Analytical data for these four porphyry samples are given in Table 23 and plotted in Figure 34.

The four porphyry samples form a line whose slope indicates an age of 632 $\pm$ 102 m.y., with an initial Sr^{87}/Sr^{86} ratio of 0.7086 $\pm$ 0.0059. Unfortunately, the similarity of the Rb/Sr ratios of these samples does not allow the isochron to be determined with more adequate precision and leads to the large uncertainty ($\pm$ 16%) of the date. The numerical value of this date is, however, in agreement with the dates reported by Schmidt and Ford (1969) shown in Table 22.

Biotite Granite and Quartz Monzonite

The granitic rocks that intrude the cordierite-hypersthene quartz-monzonite porphyry are represented by two specimens of biotite granite 497 and 498, and three specimens of quartz monzonite, 499,

Table 23: Analytical Data for Rocks from the Thiel Mountains, Antarctica

Sample	Rb (ppm)$_a$	Sr (ppm)$_a$	Rb^{87}/Sr^{86} ± error	$(Sr^{87}/Sr^{86})_b$ ± 2σ
Cordierite-hypersthene quartz-monzonite porphyry				
493	197.2	127.4	4.191 ± .065	0.7447 ± .0027
494	191.6	130.1	3.941 ± .060	0.7427 ± .0018
495	211.6	112.6	5.134 ± .078	0.7544 ± .0036
496	184.4	126.4	3.835 ± .059	0.7433 ± .0018
Biotite granite				
497	153.7	154.4	2.722 ± .043	0.7325 ± .0017
498	185.2	155.6	3.276 ± .050	0.7355 ± .0026
Quartz monzonite				
499	303.7	66.0	12.62 ± .20	0.7913 ± .0028
500	147.2	91.9	4.386 ± .069	0.7446 ± .0014
501	147.5	102.3	3.930 ± .060	0.7417 ± .0007

[a] By x-ray fluorescence.

[b] Fractionation corrected assuming $Sr^{86}/Sr^{88} = 0.1194$

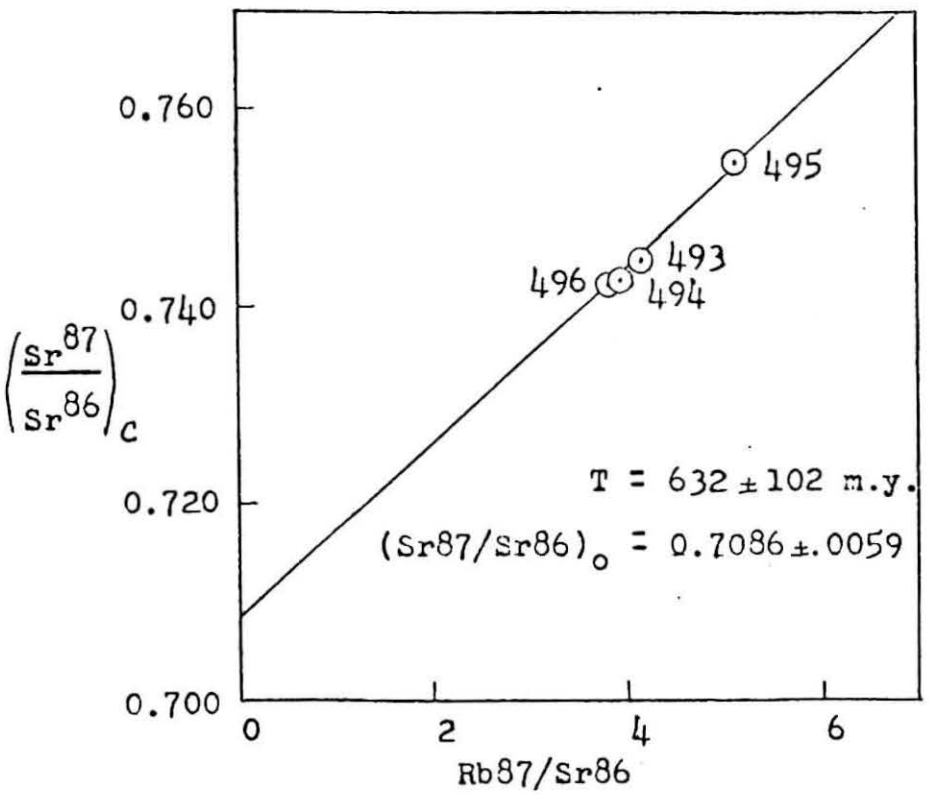

Figure 34. Isochron diagram for the Cordierite, hypersthene quartz-monzonite porphyry, Thiel Mountains.

500, and 501. Analytical data for these samples are given in Table 23 and plotted in Figure 35. The three quartz-monzonite samples define a good isochron, labeled A, indicating an age of 409 $\pm$ m.y. with an initial Sr^{87}/Sr^{86} ratio of 0.7194 $\pm$ 0.0003.

The two samples of biotite granite, 497 and 498, are very similar in Rb/Sr ratios and a reliable isochron cannot be drawn. Instead, model dates have been calculated assuming an initial Sr^{87}/Sr^{86} ratio of 0.7194. This initial ratio is the same as that for the porphyritic quartz-monzonite, considered to be approximately contemporaneous with the biotite granite by Ford (1964). Another reason for choosing 0.7194 and an initial ratio for the biotite granites rather than 0.7100 (which is commonly estimated for granitic rocks) is that the line formed by the two points, 497 and 498, intersects the Sr^{87}/Sr^{86} coordinate at 0.7180.

The model dates calculated in this way are 346 $\pm$ 3 m.y. for 498 and 352 $\pm$ 3 m.y. for 497. These dates are close enough to be considered one result. An average date of 349 m.y. has therefore been taken to be the best estimate of the age of the biotite granite. This isochron is labeled B in Figure 35.

Summary

The isochron age of 632 m.y. for the cordierite-hypersthene quartz-monzonite porphyry (Table 24) is in agreement with dates calculated by other methods for this rock. The intrusion of this rock may indicate the presence in the Thiel Mountains of the late Precambrian Beardmore Orogeny, defined by Grindley and McDougall (1969) for the central Transantarctic Mountains.

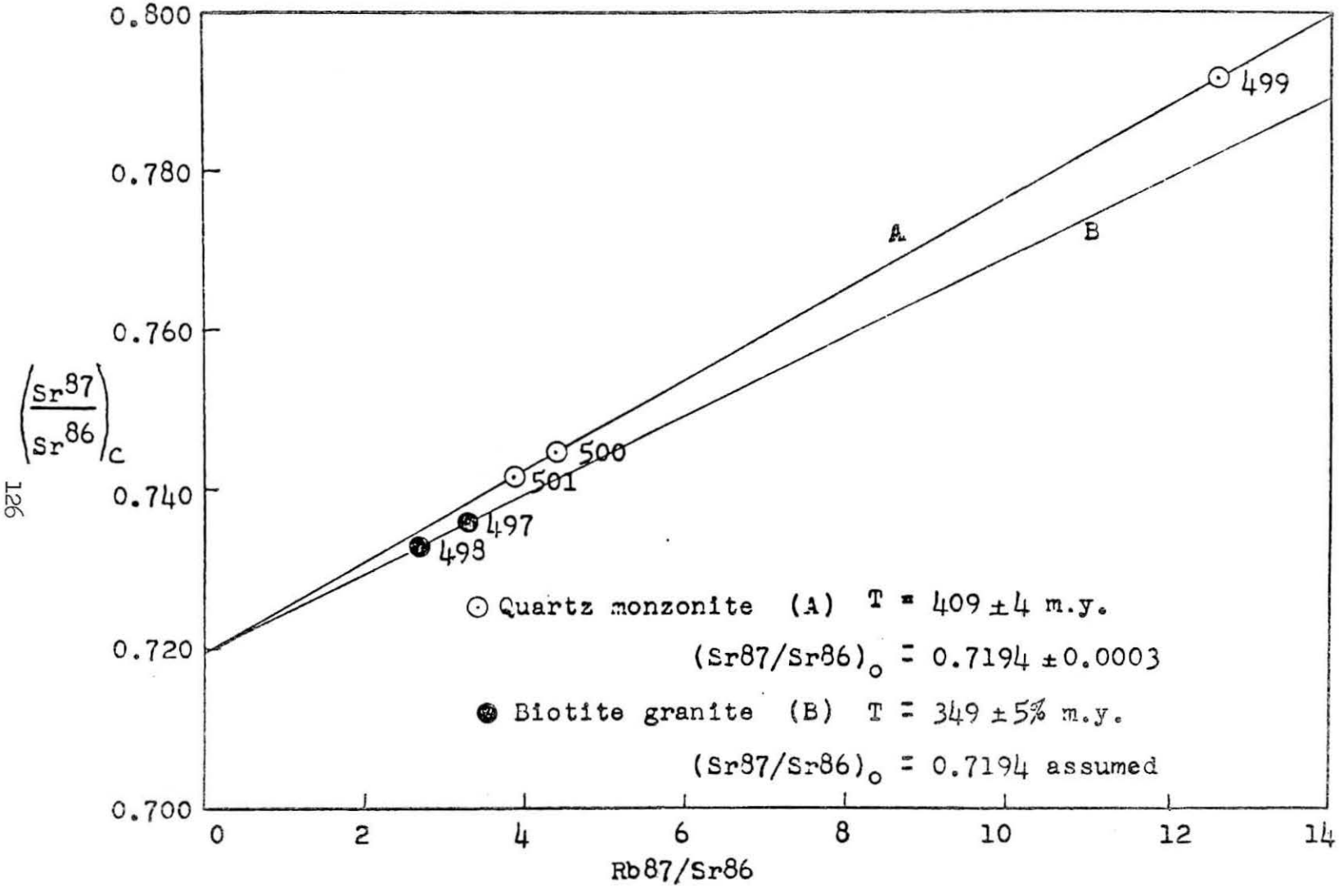

Figure 35. Isochron diagram for granitic rocks from the Thiel Mountains.

Table 24: Summary of Age Determinations for the Thiel Mountains

Rock Unit		Age	$(Sr87/Sr86)_o \pm \sigma$
Biotite Granite	497	352 ± 3 m.y.	0.7194 (assumed)
	498	346 ± 3	0.7194 (assumed)
	avg.	$349 \pm 5\%$	
Quartz monzonite		409 ± 4	0.7194 ± 0.0003
Cordierite-hypersthene quartz-monzonite porphyry		632 ± 102	0.7086 ± 0.0059

The model ages of 346 and 352 m.y. and the isochron age of 409 m.y. determined for the granitic rocks are in agreement with their intrusive relationship into the late Precambrian porphyry. The ages of the granitic rocks are younger than the period characteristic of the Ross Orogeny, 520 to 450 m.y., and may not be related to it.

CHAPTER V

NILSEN PLATEAU

Introduction

The Nilsen Plateau is part of the Queen Maud Mountains, located along the Antarctic coast near the southernmost extension of the Ross Ice Shelf as shown in Figure 36. The plateau is located at 86°30'S. latitude and 160°W. longitude, on the west side of the Amundsen Glacier, 100 km inland from the Ross Ice Shelf. The Faulkner Escarpment, the western boundary of the Nilsen Plateau, overlooks tributary glaciers leading to Scott Glacier.

A systematic geological investigation of the Nilsen Plateau was carried out by an expedition of The Institute of Polar Studies, The Ohio State University, during the 1963-64 field season. The geology of the crystalline basement complex was described by McLelland (unpublished manuscript).

General Geology

The Queen Maud Mountains, of which the Nilsen Plateau is a part, consist of flat-lying clastic sedimentary rocks overlying with angular conformity a basement complex made up of granitic intrusives and minor amounts of metamorphosed sedimentary and volcanic rock.

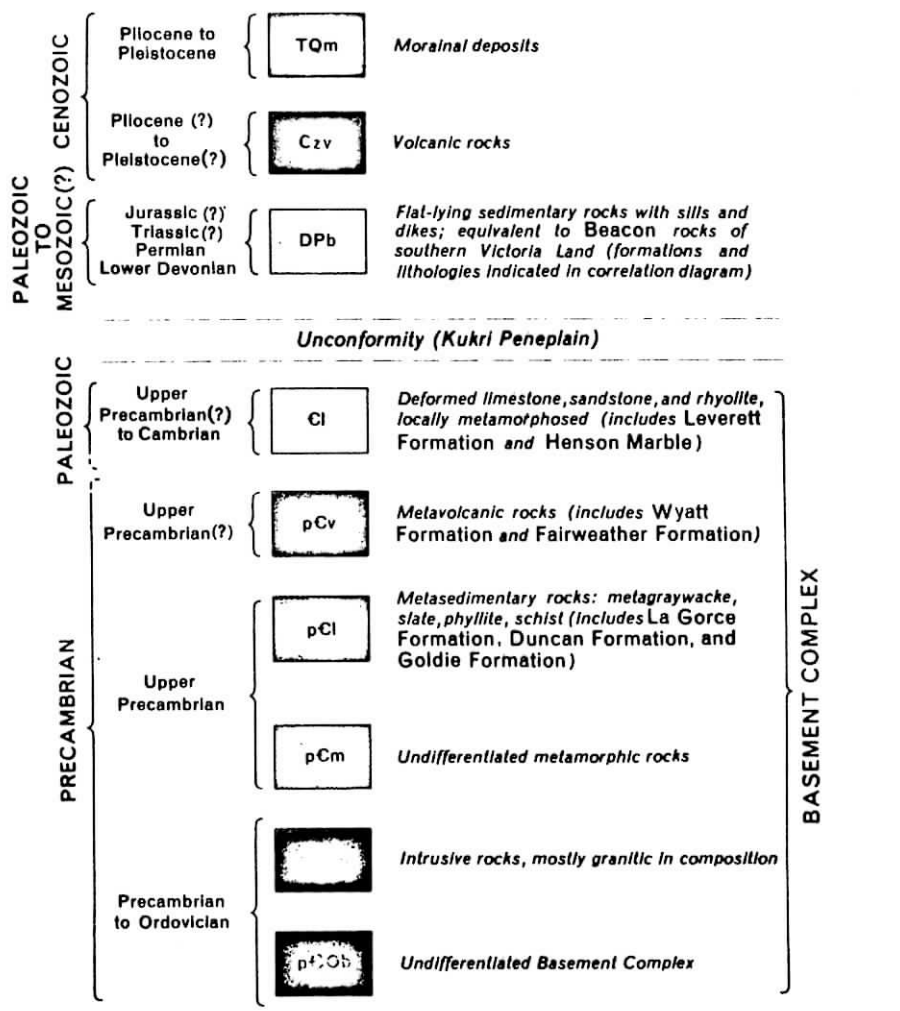

Figure 36. Geologic map of the eastern Queen Maud Mountains and Horlick Mountains (from Mirsky, 1969).

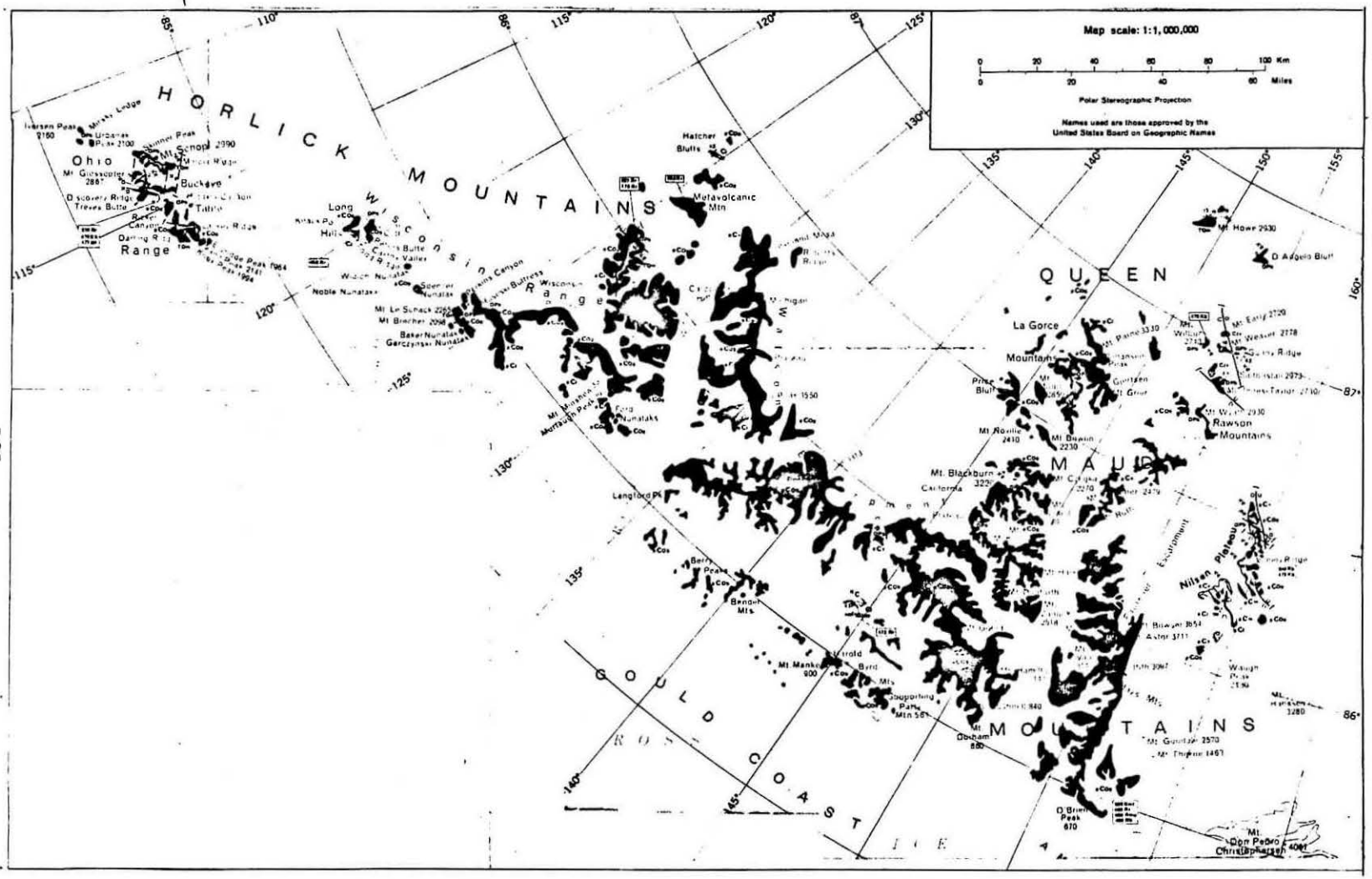
Map scale: 1:1,000,000
0 20 40 60 80 100 Km
0 20 40 60 Miles
Polar Stereographic Projection
Names used are those approved by the United States Board on Geographic Names
HORLICK MOUNTAINS
Ohio Range
Wisconsin Range
QUEEN MAUD MOUNTAINS
La Gorce Mountains
Rawson Mountains
GOULD COAST
Mt. Schopf
Buckeye
Tillite
Metavolcanic Mtn
Mt. Blackburn
Nilsen Plateau
Mt. Don Pedro Christophersen

The basement rocks of the Nilsen Plateau are described by McLelland (unpublished manuscript). Most of the basement consists of a composite batholith composed of three major granitic plutons: the Lonely Ridge Granodiorite, the South Quartz Monzonite, and the Cougar Canyon Quartz Monzonite. Another pluton, the North Quartz Monzonite, is exposed just north of the main outcrops of the Nilsen Plateau (Figure 37 and Table 25). Minor outcrops of metamorphosed sedimentary and volcanic rocks, which have been intruded by granitic rocks of the batholith, occur in scattered localities along the escarpment (McLelland, unpublished manuscript).

An erosion surface with relief up to 110 feet separates the basement complex from the overlying sediments. This surface is known as the Kukri Peneplain in the Western Queen Maud Mountains and in Victoria Land. The flat-lying sedimentary sequence is 600 to 1200 m thick and is mostly of Permian age, correlative with the Beacon rocks of Southern Victoria Land.

The basal unit of the sedimentary sequence is a tillite belonging to the Scott Glacier Formation. The glacial deposits are overlain by a sequence of clastic sediments which include coal and carbonaceous beds containing the Glossopteris flora (Queen Maud Formation). The sedimentary rocks are intruded by abundant diabase sills which are considered correlative with the Ferrar Dolerites of Jurassic age in Victoria Land (Mirsky, 1969). The upper beds of the youngest rocks, the Nilsen Formation (Table 25), may extend into the Early Triassic (Long, unpublished manuscript). Volcanic rocks of Pleistocene to Recent age occur 50 km south of the Nilsen Plateau (Mirsky, 1969).

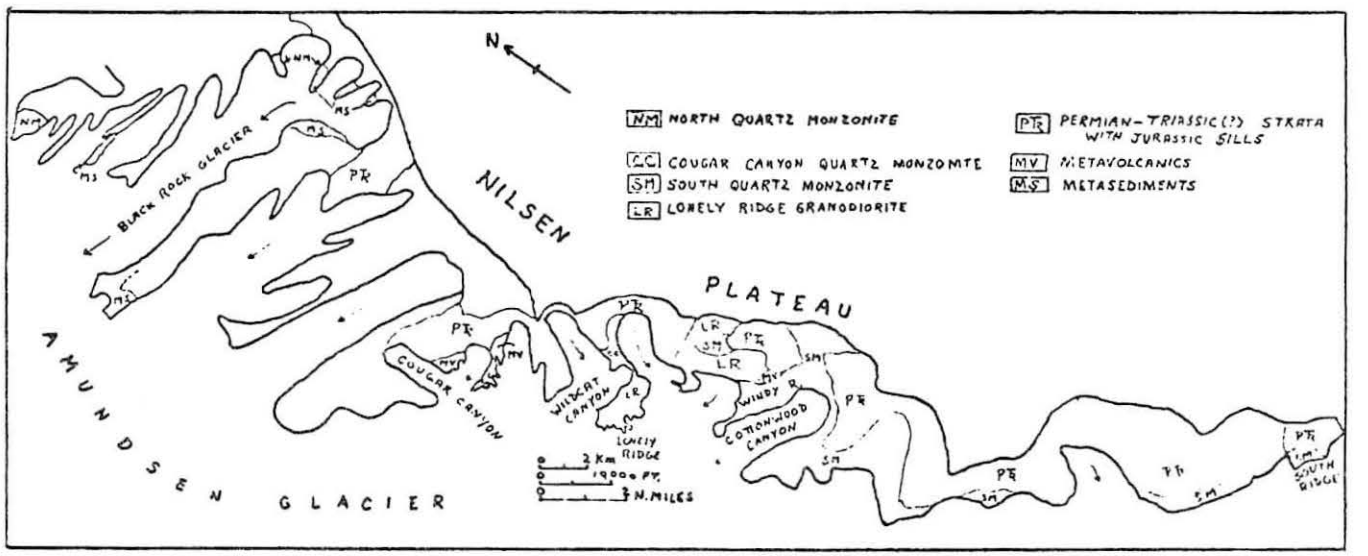

Figure 37. Geologic map of the Nilsen Plateau (after McLelland).

Table 25: Stratigraphy of the Nilsen Plateau, Queen Maud Mountains, Antarctica

	Stratified Rocks	Lithology	Intrusives
Jurassic			Diabase
Permian to Early Triassic (?)	Nilsen Formation:	Sandstone, conglomerate	
Permian	Queen Maud Formation:	Sandstone, Siltstone, Shale coal	
	Amundsen Formation:	Sandstone	
Late Paleozoic, Permian (?)	Roaring Valley Formation:	Shale	
	Scott Glacier Formation:	Tillite	
	unconformity		
?			North Quartz Monzonite
Early Paleozoic (?)			Cougar Canyon Quartz Monzonite
			South Quartz Monzonite
Precambrian	(Metavolcanics		Lonely Ridge Granodiorite
	(Metasediments		

(From Mirsky, 1969, and McLelland, unpublished manuscript)

Metasedimentary Rocks

The oldest rocks in the Nilsen Plateau are metasedimentary rocks which crop out along Black Rock Glacier (Figure 37) and are composed of interbedded metagreywacke and slate. Neither top nor bottom of the 330 m section is exposed. The beds are asymmetrically folded along north-south horizontal axes with a wavelength of about 1½ km (McLelland, unpublished manuscript).

The metagreywacke occurs in beds ½ to 3 m thick and consists of fine, subangular grains of quartz and albite, with minor K-feldspar and epidote, in a matrix of biotite, sericite, and a little chlorite. The beds of slate are less than 15 cm thick and consist of very fine-grained biotite and sericite with slightly larger quartz lenses and grains of euhedral pyrite.

The only exposure of the contact between metasedimentary rocks and the granitic plutons is on the southwest side of Lonely Ridge, where metasedimentary rocks occur as xenoliths in the Lonely Ridge Granodiorite. A Rb-Sr date on biotite from the Lonely Ridge granodiorite indicates an age of 846 $\pm$ 35 m.y. (McLelland, published manuscript) and provides a minimum date for the metasedimentary rocks.

McLelland (unpublished manuscript) and Minshew (1967) have correlated the metasedimentary rocks of the Nilsen Plateau with the Late Precambrian La Gorce Formation in the Scott Glacier area of the Queen Maud Mountains.

Metavolcanic Rocks

Metavolcanic rocks crop out at the southern end of the Nilsen Plateau, in the Cougar Canyon-Airstrip Ridge area, and also in the Black Rock Glacier area. The metavolcanic unit consists of quartz, albite, biotite, and minor K-feldspar phenocrysts 1 to 5 mm in size set in a very fine-grained groundmass of quartz, albite, and K-feldspar. The albite phenocrysts are partially altered to chlorite, sericite, and magnetite, and much of the groundmass is altered to sericite, epidote, chlorite, and calcite (McLelland, unpublished manuscript).

An outcrop in the Black Rock Glacier area shows that the metavolcanics are discordant to the underlying metasedimentary rocks, with a chilled zone in the metavolcanics at the contact. In the same area, the metavolcanic rocks are intruded by the North Quartz Monzonite. No other contacts with granitic rocks in the area are exposed (McLelland, unpublished manuscript).

Both McLelland and Minshew (1967) have correlated the metavolcanic rocks of the Nilsen Plateau with the Wyatt Formation. The Wyatt Formation was defined by Minshew (1967) for exposure at Mt. Wyatt in the Scott Glacier area of the Queen Maud Mountains. Although the Wyatt Formation is exposed in the Wisconsin Range (Murtaugh 1969) and the Scott Glacier area in an attitude stratigraphically above the metasedimentary rocks of the La Gorce Formation, the Nilsen Plateau is the only area where the contact is exposed.

Igneous Rocks

Lonely Ridge Granodiorite

The Lonely Ridge Granodiorite crops out in an area 2½ km wide and 8 km long between Lonely Ridge and the east side of Cottonwood Canyon. The dark, medium-grained rock consists of plagioclase (An 33 to An 45), quartz, biotite, and microcline-perthite, with minor hornblende (McLelland, unpublished manuscript).

The granodiortie has been cataclastically deformed, producing gneissose textures of narrow bands, containing augen of quartz and feldspar up to 10 mm in width. Bands of extreme deformation up to 9 m wide occur throughout the granodiorite. These blastomylonite bands and the gneissose foliation strike N.40°W. $\pm$ 10° with an approximately vertical dip (McLelland, unpublished manuscript).

Along its northern border, the Lonely Ridge Granodiorite is in fault contact with the Cougar Canyon Quartz Monzonite. However, the South Quartz Monzonite has extended apophyses into the Lonely Ridge Granodiorite. In adition, large slabs of the granodiorite are included in the main body of the South Quartz Monzonite near their contact (McLelland, unpublished manuscript).

South Quartz Monzonite

The South Quartz Monzonite forms the major part of the basement complex in the southern end of the Nilsen Plateau. The rock is light-gray or greenish-gray, medium to coarse-grained, and locally porphyritic in texture. It consists of microcline-perthite, quartz, and plagioclase, with minor amounts of biotite and muscovite. The South

Quartz Monzonite also shows some cataclastic effects, although on a smaller scale than does the Lonely Ridge Granodiorite. On Lonely Ridge, the quartz monzonite intrudes granodiorite and metasedimentary rocks and is itself intruded by dikes of aplite and pegmatite (McLelland, unpublished manuscript).

A similar quartz monzonite occurs as tabular and lens-shaped bodies within the Lonely Ridge Granodiorite adjacent to its contact with the South Quartz Monzonite. McLelland has designated this rock as a border phase of the South Quartz Monzonite, although no actual gradation between the two is known.

Cougar Canyon Quartz Monzonite

The Cougar Canyon Quartz Monzonite is porphyritic, with phenocrysts of microcline-perthite up to 60 mm long in a medium to coarse-grained groundmass of quartz, plagioclase, microcline, and biotite. The groundmass shows cataclastic textures. The contacts of thus plutonic unit are not exposed, but another similar unit, McLelland's Unit U-1, intrudes a small apophysis of South Quartz Monzonite. This relationship may mean that the Cougar Canyon Quartz Monzonite is younger than both the Lonely Ridge Granodiorite and the South Quartz Monzonite (McLelland, unpublished manuscript).

North Quartz Monzonite

The fourth pluton described by McLelland, the North Quartz Monzonite, is not in contact with the three plutons just described. Stocks of this quartz monzonite intrude metavolcanic rocks in the northern Nilsen Plateau, adjacent to Amundsen Glacier. The North

Quartz Monzonite is porphyritic, with large K-feldspar phenocrysts in a medium to coarse-grained groundmass of smoky quartz, plagioclase, and biotite. Some phenocrysts show rapakivi rims of albite. The North Quartz Monzonite is not appreciably deformed, which may mean that it is younger than the three other units of the batholith.

Age Determinations

Four rock units were analyzed for dating. These are the metamorphosed sedimentary rocks, the metavolcanic rocks, the Lonely Ridge Granodiorite, and the South Quartz Monzonite.

Metasedimentary rocks

Six metasedimentary rock samples were available for analysis. Three of these are metagreywackes, 472, 473, and 475. Two samples are quartzites, 474 and 476. Sample 471 is a phyllite. All the samples except 471 are from the head of Black Rock Glacier (Figure 37). The phyllite, 471, is from Lonely Ridge (Figure 41), where a lens of metasedimentary rock occurs as a xenolith within the South Quartz Monzonite and Unit 1 of the Cougar Canyon Quartz Monzonite.

Analytical data for the six metasedimentary rocks are listed in Table 26 and plotted in an isochron diagram in Figure 38. Four of these samples form an isochron which indicates an age of 728 ± 27 m.y. and an initial Sr^{87}/Sr^{86} ratio of 0.7117 ± 0.0005.

The two remaining samples, 471 and 473, define a line whose slope indicates a date of 485 m.y. with an initial ratio of 0.7173 ± 0.0005. The origin of sample 471 from a xenolith within two

Table 26: Analytical Data for Metasedimentary Rocks from the Nilsen Plateau, Queen Maud Mountains, Antarctica

Sample	Rb (ppm)$_a$	Sr (ppm)$_a$	Rb^{87}/Sr^{86} $\pm$ error	$(Sr^{87}/Sr^{86})_b$ $\pm$ 2 σ
471	245.9	36.7	$19.07 \pm .29$	$0.8464 \pm .0012$
472	113.2	171.9	$1.798 \pm .028$	$0.7297 \pm .0012$
473	153.3	138.4	$3.012 \pm .046$	$0.7377 \pm .0026$
474	97.7	219.4	$1.208 \pm .019$	$0.7244 \pm .0024$
475	108.9	175.3	$1.703 \pm .027$	$0.7293 \pm .0012$
476	59.8	154.0	$1.074 \pm .017$	0.7228
				0.7224
				avg. $0.7226 \pm .0004$

[a] By x-ray fluorescence.

[b] Fractionation corrected assuming $Sr^{86}/Sr^{88} = 0.1194$.

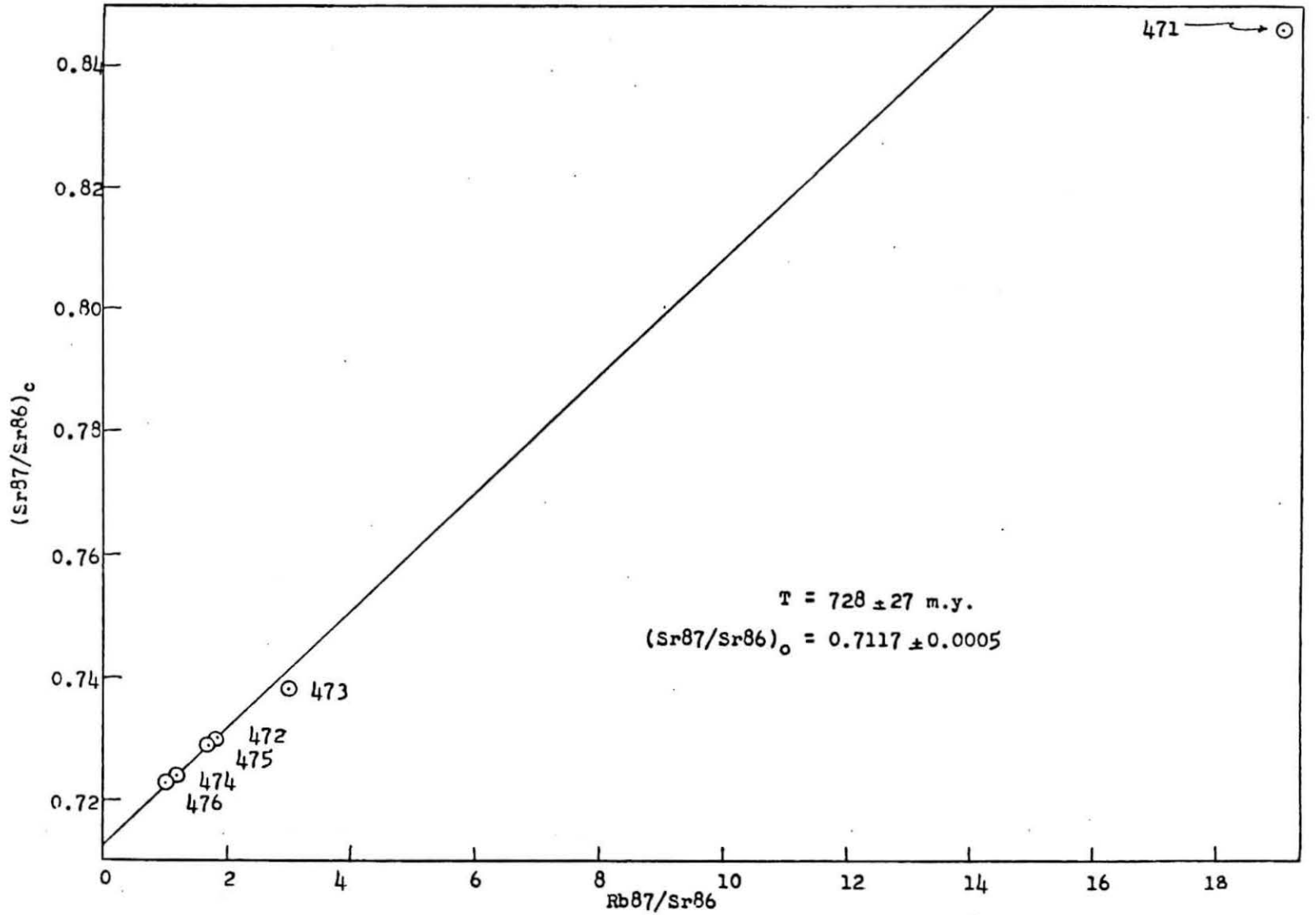

Figure 38. Isochron diagram for the metasedimentary rocks, Nilsen Plateau.

granitic rocks suggests that it may have been isotopically rehomogenized by the intrusives. The reason for sample 473's nonconformity with the age of the other samples from Black Rock Glacier is not clear.

The 728 m.y. age of the metasedimentary rocks is a minimum estimate of the time of deposition of the original sediment. The isochron result indicates when the metasediments were last homogenized in regard to Rb and Sr. Two samples were reset by a still later event, dated at 485 m.y.

Metavolcanic rocks

Nine samples of metavolcanic rocks from the Nilsen Plateau have been analyzed for dating. The analytical data are listed in Table 27 and plotted in Figure 39. Sample 470 is from an outcrop at South Ridge. The remaining samples are from an area at the head of Cougar Canyon, about 30 km from South Ridge.

An isochron fitted to all nine points yields a date of 466 $\pm$ 26 m.y. with an initial Sr^{87}/Sr^{86} ratio of 0.7179 $\pm$ 0.0021. Two points, 463 and 461, lie outside the limits of error for this isochron and were omitted from a recalculated best-fit line. The isochron which results from omission of 461 and 463 indicates an apparent age of 486 $\pm$ 10 m.y. with an initial Sr^{87}/Sr^{86} ratio of 0.7150 $\pm$ 0.0007.

Because the metavolcanic rocks were regarded by McLelland as equivalent to the Wyatt Formation for which an age of 633 m.y. was reported by Montigny and Faure (1969), the isochron date of 486 m.y. for the metavolcanic rocks is regarded as a reset date. The metavolcanics may be about the same age as the metasediments, but a more accurate estimate of their age is not possible. The only igneous rock observed

Table 27: Analytical Data for Metavolcanic Rocks from the Nilsen Plateau, Queen Maud Mountains, Antarctica

Sample	Rb (ppm)$_a$	Sr (ppm)$_a$	Rb^{87}/Sr^{86} $\pm$ error	$(Sr^{87}/Sr^{86})_b$ $\pm 2\sigma$
461	219.2	87.7	$6.806 \pm .107$	$0.7636 \pm .0006$
462	-	-	$5.628 \pm .087$	$0.7527 \pm .0016$
463	67.1	159.3	$1.147 \pm .018$	$0.7292 \pm .0018$
464	-	-	$5.873 \pm .093$	$0.7554 \pm .0028$
465	128.2	121.2	$2.887 \pm .044$	$0.7344 \pm .0014$
466	120.1	147.3	$2.199 \pm .035$	$0.7307 \pm .0032$
467	205.9	85.4	$6.539 \pm .102$	$0.7583 \pm .0028$
469	-	-	$6.047 \pm .094$	$0.7560 \pm .0022$
470	-	-	$6.399 \pm .111$	$0.7589 \pm .0014$

[a]By x-ray fluorescence.

[b]Fractionation corrected assuming $Sr^{86}/Sr^{88} = 0.1194$.

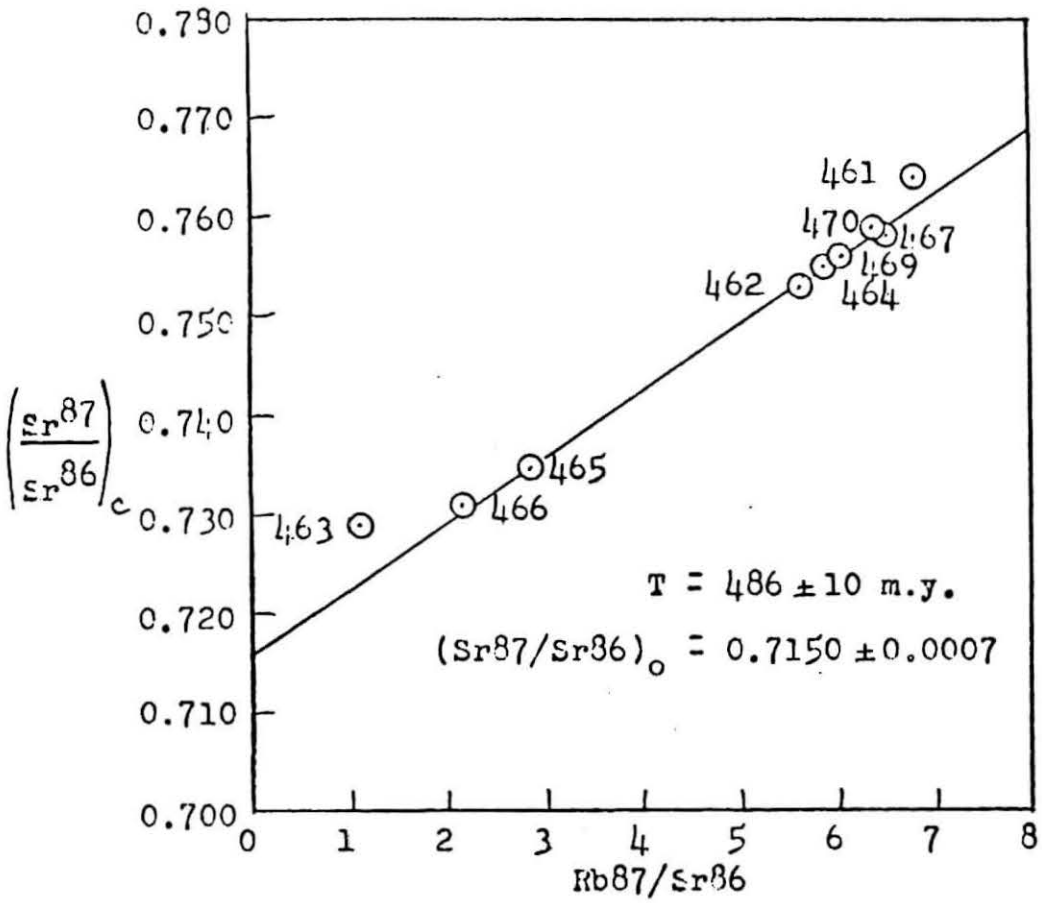

Figure 39. Isochron diagram for the metavolcanic rocks, Nilsen Plateau.

by McLelland to be intrusive into the metavolcanics is the North Quartz Monzonite, which he believed to be the youngest pluton in the basement complex possibly of post-Ross Orogeny origin. The Lonely Ridge Granodiorite, which was found to be late Precambrian in age, intrudes the metasedimentary rocks and may also intrude the metavolcanics. If this relationship is assumed to be true, it is another reason to classify the metavolcanic date of 486 m.y. as being reset.

It is interesting that the metasedimentary rocks were not completely reset by later metamorphic events as the metavolcanics were. Ordinarily, sedimentary rocks, having a high clay content, are susceptible to Rb and radiogenic Sr^{87} loss from clay minerals during metamorphism. Volcanic rocks, on the other hand, contain most of their Rb and Sr^{87} in feldspars which are more retentive minerals. In this case, however, the sediments were originally sandstones and greywackes, high in feldspar and low in clay minerals. The one phyllite of the metasedimentary suite was reset as expected. The metavolcanics are described by McLelland as being much altered to sericite and chlorite. If during an early metamorphism (perhaps at 728 m.y.), the volcanics were recrystallized, then a later event at about 486 m.y. would more easily reset their radiometric age. The two reset metasediments also indicate this later event, at 485 m.y.

Lonely Ridge Granodiorite

Seven samples of the Lonely Ridge Granodiorite were analyzed for dating. The data are listed in Table 28 and plotted in Figure 40. All of the samples are from Lonely Ridge (shown in Figure 41) or nearby, an area in which McLelland (unpublished manuscript) found complex

Table 28: Analytical Data for the Lonely Ridge Granodiorite, Nilsen Plateau, Queen Maud Mountains, Antarctica

Sample	Rb (ppm)$_a$	Sr (ppm)$_a$	Rb^{87}/Sr^{86} $\pm$ error	$(Sr^{87}/Sr^{86})_b$ $\pm 2\sigma$
477	70.4	182.1	$1.052 \pm .017$	$0.7206 \pm .0018$
478	88.7	163.6	$1.487 \pm .025$	$0.7242 \pm .0018$
479	99.3	231.4	$1.161 \pm .019$	$0.7216 \pm .0018$
480	114.5	161.2	$1.946 \pm .031$	$0.7284 \pm .0036$
481	120.8	138.6	$2.398 \pm .038$	0.7300 0.7309 avg $0.7305 \pm .0009$
482	337.6	12.9	71.52 ± 1.42	1.164 1.164 $1.164 \pm .000$
483	396.5	5.4	270.7 ± 6.6	2.225 1.000c 2.159 $2.192 \pm .066$
502 biotite$_d$	414.4	31.7	39.55 -	1.183 -

[a] By-x-ray fluorescence.

[b] Fractionation corrected assuming $Sr^{86}/Sr^{88} = 0.1194$.

[c] Omitted from average calculation.

[d] Analyzed by Isotopes, Inc., Westwood, N.J., (McLelland, unpublished manuscript).

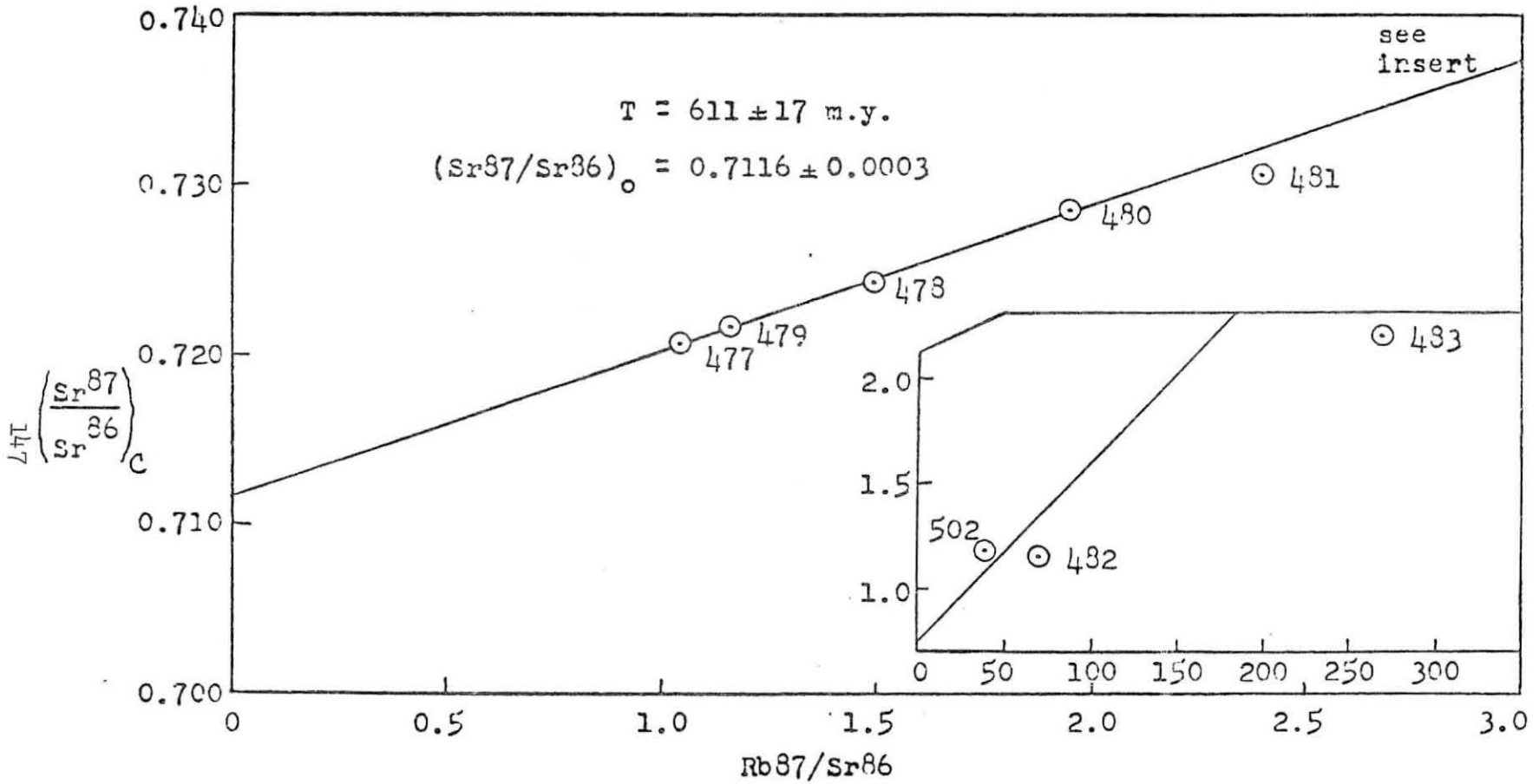

Figure 40. Isochron diagram for the Lonely Ridge Granodiorite, Nilsen Plateau.

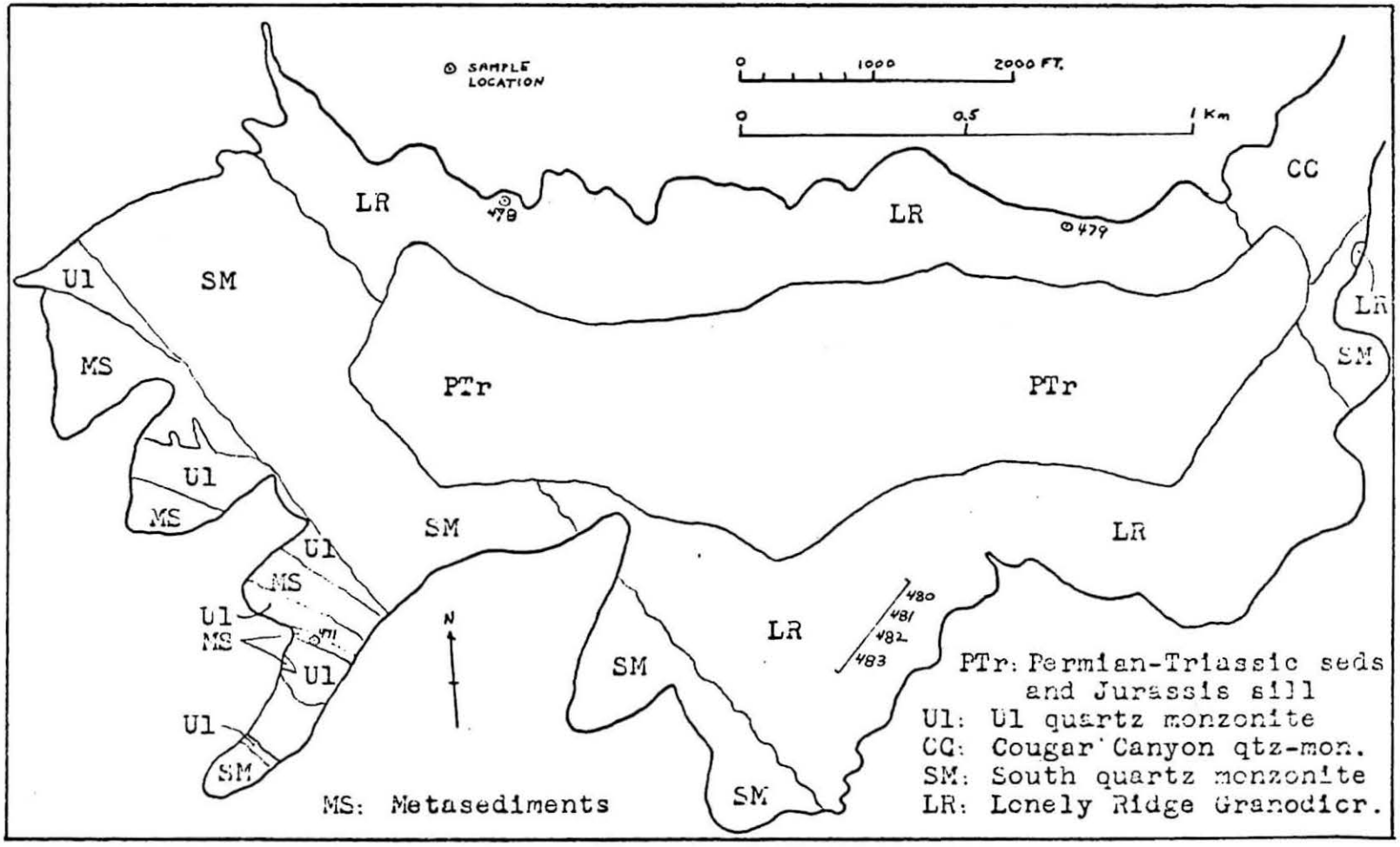

Figure 41. Geologic map of Lonely Ridge, Nilsen Plateau (after McLelland).

intrusive relationships among the several granitic rocks of the batholith.

Only four of the seven samples fit an isochron within experimental error. The isochron formed by these four points, 477, 478, 479, and 480, indicates an age of 611 $\pm$ 17 m.y. with an initial Sr^{87}/Sr^{86} ratio of 0.7116 $\pm$ 0.0003.

Two of the samples (482, 483) which do not fit this isochron are greatly enriched in Rb and radiogenic Sr^{87}. These samples, and perhaps to a lesser degree sample 481, have not remained closed systems to Rb and Sr and are not suitable for dating. By assuming n initial Sr^{87}/Sr^{86} ratio of 0.704, model ages were calculated for these three samples. The model age for the least affected sample, 481, is 789 m.y. and is a maximum estimate of the age of this rock. The model ages for 482 and 483 are 461 m.y. and 394 m.y. respectively. These two rocks would be expected to indicate a Precambrian model age similar to that for 481, but their degree of alteration in Rb and Sr content makes interpretation of their anomalously young model ages a matter of conjecture.

The Late Precambrian-Early Cambrian age of 611 m.y. calculated for the Lonely Ridge Granodiorite is consistent with its intrusive relationship into the metasedimentary rocks, for which an age of 728 m.y. was calculated. An age of 611 m.y. for the Lonely Ridge Granodiorite is not compatible with the model age of 846 m.y. for biotite from one sample of this rock reported by McLelland (unpublished manuscript).

The biotite sample is numbered 502 and is also plotted in Figure 40. Because the best age consistent with the isochron data is 611 m.y., the model age based on the biotite sample must be in error.

The cause of this anomalous result is probably the initial Sr^{87}/Sr^{86} ratio of 0.712 which was assumed in order to calculate the model age. It is possible that sample 502, like 482 and 483, is greatly enriched in radiogenic Sr^{87}. The biotite therefore may have had a much higher initial Sr^{87}/Sr^{86} ratio than 0.712. A hypothetical isochron for separated minerals from sample 502 would presumably indicate a post-611 m.y. event when that sample was re-homogenized with regard to Rb and Sr.

South Quartz Monzonite

Six samples of the South Quartz Monzonite were selected for isochron analysis. The data for these rocks are listed in Table 29 and plotted in an isochron diagram in Figure 42. Samples 506 and 511 are from the southwest wall of Cottonwood Canyon. Samples 507, 508, and 509 are from Windy Ridge. Sample 513 is from an outcrop about half way to South Ridge.

Five points fit an isochron within experimental error. This isochron indicates an age of 452 ± 14 m.y. for the South Quartz Monzonite. The initial Sr^{87}/Sr^{86} ratio is 0.7248 ± 0.0037. Sample 508 does not fit this isochron and a model age has been calculated for this rock by assuming an initial Sr^{87}/Sr^{86} ratio of 0.704. This calculation results in a date of 405 m.y.

Sample 508, like sample 482 and 483 of the Lonely Ridge Granodiorite, appears to be enriched in Rb and depleted in normal Sr and does not lie on an isochron. These rock samples evidently have not remained closed to Rb and Sr since intrusion of their respective plutons.

Table 29: Analytical Data for the South Leuco Quartz Monzonite, Nilsen Plateau, Queen Maud Mountains, Antarctica

Sample	Rb (ppm)$_a$	Sr (ppm)$_a$	Rb^{87}/Sr^{86} ± error	$(Sr^{87}/Sr^{86})_b$ ± 2σ
506	306.1	24.8	34.37 ± .54	0.9483 ± .0042
507	318.3	18.5	49.59 ± .76	1.042 ± .004
508	370.3	8.3	134.7 ± 2.9	1.404
				1.494
				avg. 1.464 ± .090
509	117.0	95.9	3.346 ± .052	0.7397 ± .0041
511	238.9	82.2	7.931 ± .123	0.7760 ± .0015
513	306.0	20.4	41.64 ± .68	0.9737 ± .0041

[a]By x-ray fluorescence.

[b]Fractionation corrected assuming $Sr^{86}/Sr^{88} = 0.1194$

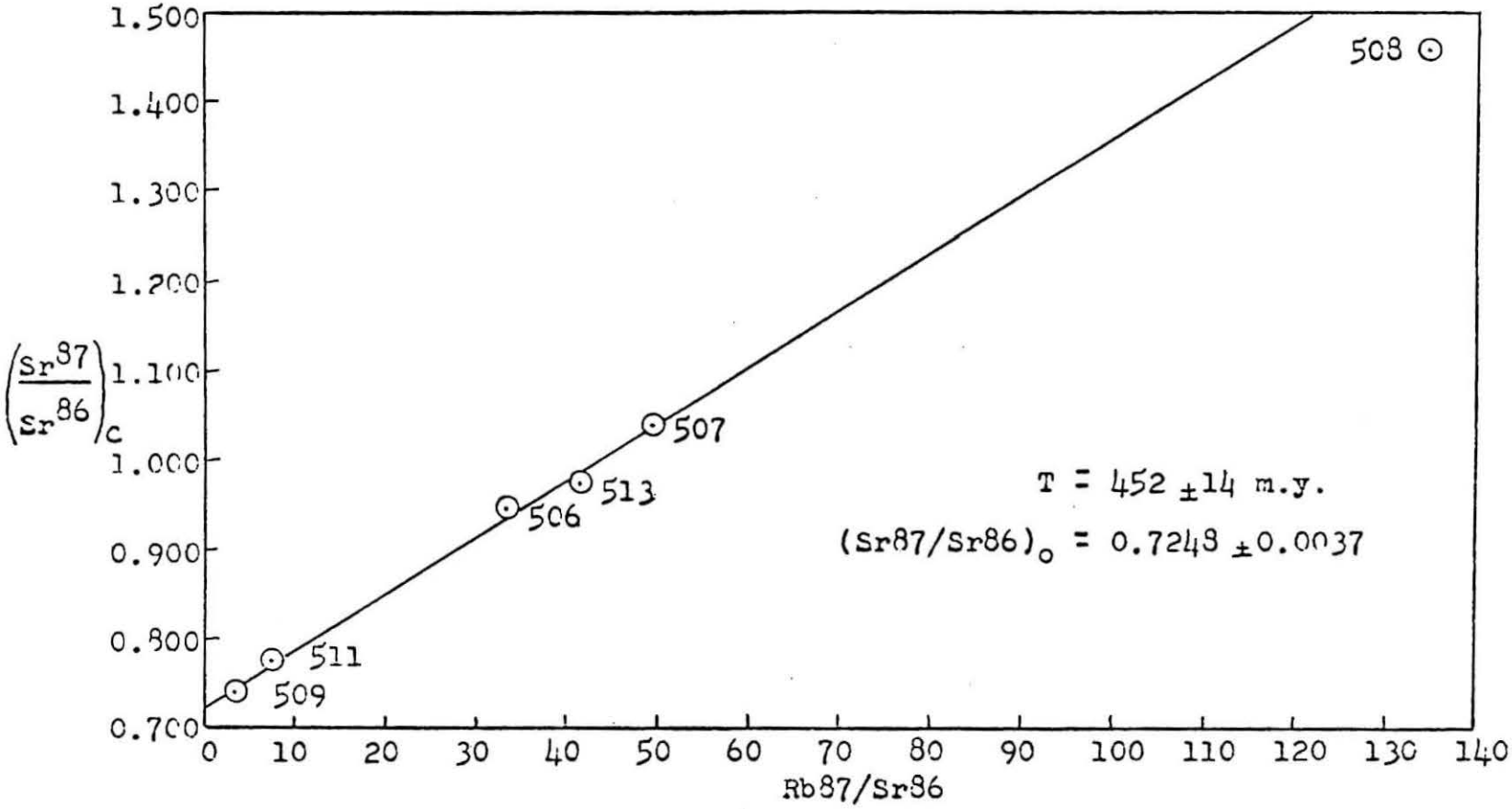

Figure 42. Isochron diagram for the South Quartz Monzonite, Nilsen Plateau.

Summary

Table 30 summarizes the age determinations for the Nilsen Plateau. The metasedimentary, rocks which are the stratigraphically oldest rocks in the Nilsen Plateau, have produced the oldest isochron age, 728 m.y. This age represents the time when these rocks were last metamorphosed and became isotopically homogenized and closed systems to Rb and Sr. The calculated age of 728 m.y. is a minimum estimate of the time of deposition of the sediments. It may reflect a partial resetting of the metasediments due to intrusion by the Lonely Ridge Granodiorite.

The isochron age of the Lonely Ridge Granodiorite is 611 m.y. This age is a revision of the 846 m.y. model date for this pluton reported by McLelland (unpublished manuscript). The intrusion of the Lonely Ridge Granodiorite and the isotopic homogenization of the metasediments of the Nilsen Plateau appear to represent the Beardmore Orogeny (680-621 m.y.) in this area.

The metavolcanics which overlie the metasedimentary rocks are probably equivalent to the Late Precambrian Wyatt Formation of the Scott Glacier area and are probably older than the isochron date of 486 m.y. This date is regarded as a reset date and, together with two samples of metasediments dated at 485 m.y., may reflect intrusion by the younger plutons of the basement complex. One of these plutons, the South Quartz Monzonite, was found to have an age of 452 m.y. and may have been emplaced during the Ross Orogeny.

Table 30: Summary of Age Determinations for the Nilsen Plateau, Queen Maud Mountains, Antarctica

Rock Unit	Age (m.y.) $\pm$ error	$(Sr^{87}/Sr^{86})_o$ $\pm \sigma$
South Quartz Monzonite	452 ± 14	0.7248 ± 0.0037
Lonely Ridge Granodiorite	611 ± 17	0.7116 ± 0.0003
Metavolcanic rocks	486 ± 10	0.7150 ± 0.0007
Metasedimentary Rocks	728 ± 27	0.7117 ± 0.0005

CHAPTER VIII

CONCLUSIONS

The ages that have been determined for the rock units analyzed in this study are listed in Table 36 and arranged in a correlation chart in Table 37. The earliest event detected is the crystallization of the felsic flows interbedded with the sediments of the Patuxent Formation in the Neptune Range of the Pensacola Mountains. The age of these flows and the time of deposition of the Patuxent Formation is 1210 ± 76 m.y. The Patuxent Formation is therefore one of the oldest rocks in the Transantarctic Mountains.

The presence of rocks older than 1000 m.y. in the Transantarctic Mountains has only recently been reported. Grindley and McDougall (1969) reported an average date of 1020 m.y. by the K-Ar method on hornblende from amphibolite and pegmatite of the Nimrod Group at the head of Nimrod Glacier. They interpreted these dates as marking the end of regional metamorphism during the Nimrod Orogeny which they postulated may have produced the several occurrences of high-grade metamorphic rocks that have been reported in the Shackleton Range (Stephenson, 1966), the Wisconsin Range (Murtaugh, 1969), and Victoria Land. The age of the Nimrod Group was determined by Gunner and Faure (1970), who reported a Rb-Sr whole-rock isochron age of 1980 m.y. for these rocks. They may be even older.

Table 36: Summary List of Age Determinations

Location	Rock Unit	Age (m.y.)
Pensacola Mountains	Gambacorta Formation	568 ± 39
	Serpan Granite and Gneiss	555 ± 26
	Diabase	778 ± 59
	Felsic flows	488 ± 6 (a)
	" "	1210 ± 76
	Patuxent Formation	402 ± 5 (a)
Thiel Mountains	Biotite Granite	350 ± 20
	Quartz monzonite porphyry	409 ± 4
	Cordierite-hypersthene quartz monzonite porphyry	632 ± 102
Nilsen Plateau	South Quartz Monzonite	452 ± 14
	Lonely Ridge Granodiorite	611 ± 17
	Metavolcanics	486 ± 10(a)
	Metasediments	728 ± 27 (a?)
Coats Land	Littlewood Volcanics	1001 ± 16
Western Queen Maud Land	Trollkjellrygg Volcanics	856 ± 30

[a]Reset date

Table 37: Correlation Chart of Basement Rock Units Dated From The Central Transantarctic Mountains

Geological Period	Age M. Yrs.	Orogeny	Western Queen Maud Land	Coats Land	Pensacola Mountains	Thiel Mountains	Horlick Mountains	Wilson Plateau Scott Glacier Area	Nimrod Glacier
Carboniferous						~~~?~~~	Beacon	Beacon	Beacon
Devonian					Beacon (?)	350 Biotite Granite	Group	Group	Group
Silurian	400				402 Patuxent Fm. reset	409 Qtz-Mon Porph.			
Ordovician		Ross					472 Rhyolite	452 South Qtz-Mon.	456 Nimrod Group reset$_d$
					488 Patuxent Fm. flows reset		479 Qtz-Mon. $_b$ 498 Rhyolite	486 Metavolcanics reset	
	500				555 Serpan Granite and Gneiss				
Cambrian					568 Gambacorta Fm.				
					Nelson Ls.		Leverett Fm.	Leverett Fm.	Shackleton Ls.
	600					~~~?~~~			
		Beardmore				632 C-M-Q Monzonite Porphyry	627 Granodiorite$_b$ 633 Wyatt Fm. reset$_c$	611 Lonely Ridge Granodiorite	600 Nimrod Group reset$_d$
	700							Metavolcanics	
Pre-						Metasediments	La Gorce Fm.	728 Metasediments	
					778 Patuxent Fm. diabase sills				
	800								
cambrian			856 Trollkjell-rygg vols.						
			~~?~~~?~~~						
	1000	Nimrod	1030 Jorgen Intrusion$_a$	1001 Littlewood Vols.					1020 Nimrod Group (K-Ar horn.)$_e$
					1210 Patuxent Fm. flows dep.				
	1700	Vestfold (first)	1700 Borg Intrusions$_a$						
			~~?~~~						1980 Nimrod Group$_d$
	2000		Ahlmannryggen Group						

a. Allsopp and Neethling, 1970.

b. Faure and others, 1968.
c. Montigny and Faure, 1969.

d. Gunner and Faure in press.
e. Grindley and McDougall, 1969.

507 (64)
South Quartz Monzonite, Windy Ridge, Similar to 506, pink variety, weak gneissic foliation.

508 (94)
South Quartz Monzonite, Windy Ridge. Similar to 506.

509 (103)
South Quartz Monzonite, Windy Ridge. Similar to 506, but with weak gneissic foliation.

511 (148)
South Quartz Monzonite (granite?), southwest of Cottonwood Canyon. Phenocrysts of K-feldspar (up to 1" long) in medium-grained groundmass of quartz, biotite, and plagioclase.

513 (233)
South Quartz Monzonite, halfway to South Ridge. Similar to 506.

Coats Land

O.S.U. No.

235 Rhyolite or rhyodacite, Littlewood Nunataks, Coats Land. Small plagioclase phenocrysts (1-5 mm) in a dark-red aphanitic groundmass. Collected by N. B. Aughenbaugh and described in Aughenbaugh and others (1965).

367 Rhyolite or rhyodacite, Littlewood Nunataks, Coats Land. Similar to 235. Collected by J.C. Behrendt.

405 (Instituto Antarctico Argentino No. CE.75.533)
Rhyolite (?), Bertrab Nunatak, Coats Land. Described as: "Graphic granite; microcline and some plagioclase grains are idiomorphic, somewhat altered to kaolin, calcite, and iron oxide. Biotite has altered to chlorite."

406 (CE.75.534)
Rhyolite (?), Bertrab Nunatak, Coats Land. Similar to 405.

407 (CE.75.535)
Andesite (?), Bertrab Nunatak, Coats Land. Described by Instituto Antarctico Argentino as "Micro trondjemite: quartz with undulating extinction, plagioclase (olig.-andes.), turbid because of advanced state of alteration. Abundant biotite altered to chlorite. Alotriomorphic hornblende."

408 (CE.75.536)
Andesite (?), Bertrab Nunatak, Coats Land. Described as "microdiorite."

409 (CE.75.537)
Rhyolite (?) Bertrab Nunatak, Coats Land. Described as "graphic granite, groundmass too fine for minerals to be determined."

Western Queen Maud Land: Samples made available by D. C. Neethling, Antarctic Division of Geological Survey, Republic of South Africa.

O.S.U. No.

484 (Neethling's Lab. No. 1, Field No. U3)
Basalt, Trolkjellrygg Group, Lower Member, Utkikken, W. Queen Maud Land. Very fine-grained, medium gray.

485 (Lab No. 2, Field No. SL1)
Basalt, Trollkjellrygg Group, Transitional or Middle Member, Nunatak 820. Dark gray, fine grained.

486 (Lab No. 6, Field No. SN 20)
Basalt, Trollkjellrygg Group, Upper Mem., Snokallen. Similar to 485.

487 (Lab No. 9, Field No. SJ11)
Basalt, Trollkjellrygg Group, Upper Mem., Snokjerringa, Similar to 485.

488 (Lab No. 10, Field No. SJ22)
Basalt, Trollkjellrygg Group, Upper Mem., Snokjerringa. Similar to 485.

489 (Lab No. 12, Field No. B8)
Basalt, Trollkjellrygg Group, Upper Mem., Bolten. Dark red-brown, small phenocrysts of olivine and pyroxene.

490 (Lab No. 16, Field No. SN5)
Basalt, Trollkjellrygg Group, Upper Mem., Snokallen. Similar to 485.

491 (Lab No. 17, Field No. SN39)
Basalt, Trollkjellrygg Group, Upper Mem., small Nunatak southeast of Snokallen. Similar to 489.

492 (Lab No. 19, Field No. SN6)
Basalt, Trollkjellrygg Group, Upper Mem., Snokallen. Similar to 485.

BIBLIOGRAPHY

Adie, R.J., (ed.), 1964, Antarctic Geology: New York, Interscience, 758 p.

Adler, I., 1966, X-Ray Emission Spectrography In Geology: New York, Elsevier, 258 p.

Aldrich, L.T., Wetherill, G.W., Tilton, G.R., Davis, G.L., 1956, Half-life of Rb^{87}: Phy. Rev., v. 103, pp. 1045-1047.

Allsopp, H.L., and Neethling, D.C., 1970, Rb-Sr isotopic ages of Precambrian intrusives from Queen Maud Land, Antarctica: Earth & Planet. Sci. Let., v. 8, pp. 66-70.

Angino, E.E., and Turner, M.D., 1964, Antarctic orogenic belts as delineated by absolute age dates: in Antarctic Geology, R.J. Adie (ed.), North-Holland, Amsterdam, pp. 551-556.

Aughenbaugh, N.B., Lounsbury, R.W., and Behrendt, J.C., 1965, The Littlewood Nunataks, Antarctica: Jour. Geol., v. 73, pp. 889-894.

Beck, M.E. Jr., Ford, A.B., Boyd, W.W. Jr., 1968, Paleomagnetism for a stratiform intrusion in the Pensacola mountains, Antarctica: Nature, v. 217, pp. 534-535.

Behrendt, J.C., Meister, L., and Henderson, J.R., 1966, Airborne geophysical study of the Pensacola mountains of Antarctica: Science, v. 153, pp. 1373-1376.

Butt, B.C., 1962, The geology of the Straumsnutane and Istind Nunataks, Western Droning Maud Land: Rept. Geol. Survey South Africa, unpublished.

Capurro, L.R.A., 1955, Expedicion Argentina al Mar de Weddell: Ministerio de Marina, Direccion General de Navegacion e Hidrografia, pp. 129-131.

Cordini, I.R., 1959, El conocimiento geologico de la Antarctica: Instituto Antartico Argentino, Pub. No. 6, pp. 141-145.

Craddock, C., Gast, P.W., Hanson, G.M., and Linder, H., 1964, Rb-Sr ages from Antarctica: Geol. Soc. America Bull., v. 75, pp. 237-240.

Damon, P., et al., 1966, Correlation and chronology of ore deposits and volcanic rocks: U. Arizona, Ann. Prog. Rept. No. C OO-689-60.

Deutsch, S., Picciotto, E.E., and Reinharz, M., 1961, Age measurements on Antarctica rocks (Queen Maud Land): Nature, v. 191, pp. 1286-1287.

Doering, W.P., 1968, A rapid method for measuring the Rb/Sr ratio in silicate rocks: U.S. Geol. Survey Prof. Paper 600-C, pp. 164-168.

Eastin, R., 1970, The age of the Littlewood Volcanics of Coats Land, Antarctica: (abstr.) Program, North-central Sect., Geol. Soc. Amer., v. 2, No. 6, p. 386.

Eastin, R., Faure, G., and Neethling, D.C., in press, The age of the Trollkjellrygg Volcanics of Western Queen Maud Land, Antarctica: Ant. Jour. U.S.

Eastin, R., Faure, G., Schultz, C.H., and Schmidt, D.L., 1969, Rb-Sr ages of the Littlewood Volcanics and of the acid volcanic rocks of the Neptune Range, Pensacola Mountains, Antarctica: (Abstr.) Program, North-central Sect., Geol. Soc. Amer., Part 6, p. 13.

Faure, G., and Hurley, P.M., 1963, The isotopic composition of Sr in oceanic and continental basalts: application to the origin of igneous rocks: Jour. Petrology, v. 4, pp. 31-50.

Faure, G., Hill, R.L., Eastin, R., and Montigny, R.J., 1968, Age determination of rocks and minerals for the Transantarctic mountains: Ant. Jour. U.S., v. 3, No. 5, pp. 173-175.

Faure, G., Murtauch, J.G., and Montigny, R.J.E., 1968, The geology and geochronology of the basement rocks of the Central Transantarctic Mountains: Canad. Jour. Earth Sci., v. 5, p. 555-560.

Fenton, M.D., 1969, The evolution of the isotope composition of terrestrial Sr: unpublished PhD. dissertation, The Ohio State University, Columbus, Ohio.

Ford, A.B., 1964, Cordierite-bearing hypersthene-quartz-monzonite-porphyry in the Thiel mountains and its regional importance: in Antarctic Geology, R.J. Adie (ed.), Interscience, New York, pp. 429-441.

Ford, A.B., and Boyd, W.W. Jr., 1968, The Dufek intrusion, a major stratiform gabbroic body in the Pensacola Mountains, Antarctica: XXIII International Geol. Cong., v. 2, pp. 213-228.

Ford, A.B., and Boyd, W.W. Jr., 1969, Chemical trends in the Dufek intrusion, Pensacola mountains: Ant. Jour. U.S., v. 4, pp. 202-203.

Grindley, G.W., 1963, The geology of the Queen Alexandra range, Beardmore glacier, Ross dependency, Antarctica; with notes on the correlation of Gondwana sequences: N. Z. Jour. Geol. Geophys., v. 6, pp. 307-347.

Grindly, S.W., McGregor, V.R., and Walcott, R.I., 1964, Outline of the geology of the Rimrod-Beardmore-Axel-Heiberg glacier region, Ross dependency: in Antarctic Geology, R. J. Adie (ed.), North-Holland, Amsterdam, pp. 206-219.

Grindley, G.W., and Warren G., 1964, Stratigraphic nomenclature and correlation in the western Ross sea region: in Antarctic Geology, R.J. Adie (ed.), North-Holland, Amsterdam, pp. 314-333.

Grindly, G.W., and Laird, M.G., 1969, Geology of the Shackleton coast: Sheet 15, Amer. Geog. Soc., Antarctic Map Folio 12.

Grindley, G.W., and McDougall, I., 1969, Age and correlation of the Nimrod Group and other Precambrian rock units in the Central Transantarctic Mountains, Antarctica: N.Z. Jour. Geol. & Geophys., v. 12, pp. 391-411.

Gunn, B.M., and Warren, G., 1962, Geology of Victoria Land between the Mawson and Mulock Glaciers, Antarctica: Bull. N.Z. Geol. Surv., v. 71, p. 1-157.

Gunn, B.M., and Walcott, R.I., 1962, The geology of the Mt. Markham region, Ross dependency, Antarctica: N.Z. Jour. Geol. & Geophys., v. 5, pp. 407-426.

Gunner, John, and Faure, Gunter, (in press), Rubidium-strontium geochronology of the Nimrod Group, Central Transantarctic Mountains.

Hower, J., 1959, Matrix corrections in the x-ray spectographic trace element analysis of rocks and minerals: Amer. Mineral., v. 44, pp. 19-32.

Klimov, L.M., Ravich, M.G., and Soloviev, D.S., 1964, Geology of the Antarctic platform: in Antartic Geology, R. J. Adie (ed.) North-Holland, Amsterdam, pp. 681-691.

Long, W.E., 1967, Stratigraphy of the Thorvald Nilsen mountains, Antarctica: Unpublished.

Mack, M., and Spielberg,N., 1958, Statistical factors in x-ray intensity measurements: Spectrochim. Acta, v. 12, pp. 169-178.

McDougall, I., in press, K-Ar dates on minerals from dolerites from western Queen Maud Land, Antarctica: Symposium on Gondwana Stratigraphy, Buenos Aires, 1967.

McGregor, V.R., and Wade, R.A., 1969, Geology of the western Queen Maud Mountains: Sheet 16, Amer. Geog. Soc., Antarctic Map Folio 12.

McLelland, D., 1967, Geology of the basement complex, Thorvald Nilsen Mountains, Antarctica: Unpublished M.S. Thesis, University of Nevada, Reno.

Minshew, V.H., 1965, Potassium-argon age from a granite at Mount Wilbur, Queen Maud Range, Antarctica: Science, v. 150, pp. 741-743.

Minshew, V.H., 1967, Geology of the Scott Glacier and Wisconsin Range areas, central Transantarctic Mountains, Antarctica: Inst. of Polar Studies Rept. 22, The Ohio State University Res. Found., Columbus.

Mirsky, A., 1969, Geology of the Ohio Range-Liv Glacier area: Sheet 17, Amer. Geog. Soc., Antarctic Map Folio 12.

Montigny, R., and Faure, G., 1969, Contribution au probleme de l'homogeneisation isotopique du strontium des roches totales au cours du metamorphisme: Cas du Wisconsin Range, Antarctique: C.R. Acad. Sci. Paris, t.268, p. 1012-1015.

Murtaugh, J.G., 1969, Geology of the Wisconsin Range batholith, Transantarctic Mountains: N.Z. Jour. Geol. & Geophys., v. 12, pp. 526-550.

Neethling, D.C., 1964, The geology of the Zukkertoppen Nunataks, Ahlmannryggen, western Dronning Maud Land, Antarctica: in Antarctic Geology, R.J. Adie (ed.), North-Holland, Amsterdam, pp. 379-389.

Neethling, D.C., 1969, Geology of the Ahlmann Ridge, western Queen Maud Land: Sheet 7, Amer. Geog. Soc., Antarctic Map Folio 12.

Nicolaysen, L.O. 1961, Graphic interpretation of discordant age measurements on metamorphic rocks: in Geochronology of Rock Systems, Annals, F.N. Furnus and J.L. Kulp (eds.) Acad. Sci., New York, v. 91, pp. 198-206.

Norrish, K., and Chappell, B.W., 1967, X-ray fluorescence spectrography: in Physical Methods in Determinative Mineralogy, Zussman, J. (ed.), New York, Academic Press, 514 p.

Picciotto, E., and Coppez, A., 1963, Bibliographie des mesures d'ages absolus en Antarctique: Soc. Geol. Belg., Ann., v. 85, pp. 263-308.

Powell, J.L., Skinner, W.R., and Walker, D., 1969, Whole rock Rb-Sr age of metasedimentary rocks below the Stillwater Complex, Montana: Geol. Soc. America Bull., v. 80 pp. 1605-1612.

Reynolds, R.C., 1963, Matrix corrections in trace element analysis by x-ray fluorescence: estimation of the mass absorption coefficient by Compton scattering: American Mineral., v. 48, pp. 1133-1143.

Roots, E.F., 1953, Preliminary note on the geology of western Dronning Maud Land: Norsk Geol. Tids, v. 32, pp. 18-33.

Roots, E.F., 1969, Geology of western Queen Maud Land: Sheet 6, Amer. Geog. Soc., Antarctic Map Folio 12.

Solter, D.D., 1966, Distribution of rubidium, strontium, zirconium, and iron of Porphyry Mountain and age of the Silver Plumme granite, Jamestown, Colorado: unpublished M.S. Thesis, Geology Department, The Ohio State University.

Schmidt, D.L., 1969, Precambrian and lower Paleozoic igneous rocks, Pensacola Mountains, Antarctica: Ant. Jour. U.S., v. 4, pp. 203-204.

Schmidt, D.L., and Ford, A.B., 1969, Geology of the Pensacola and Thiel Mountains: Sheet 5, Amer. Geog. Soc., Antarctic Map Folio 12.

Schopf, J.M., 1964, Paleobotanical studies in Antarctica: Geol. Soc. Amer. Spec. Papers 76, Abstr. 1963, p. 317.

Stephenson, P.J., 1966, Geology l Theron Mountains, Shackleton Range and Whichaway Nunataks: Trans-Antarctic Exped. 1955-58, Sci. Rep., v. 8, 78 pp.

Vance, J.A., 1962, Zoning in igneous plagioclase: normal and oscillatory zoning: Amer. Jour. Sci., v. 260, pp. 746-760.

Warren, G., 1969, Geology of the Terra Nova Bay - McMurdo Sound Area, Victoria Land: Sheet 14, Amer. Geog. Soc., Antarctic Map Folio 12.

Webb, P.N., 1962, Isotope ages of Antarctic rocks - a summary: N.Z. Jour. Geol. & Geophys., v. 5, pp. 790-796.

Williams, P.L., 1969, Petrology of upper Precambrian and Paleozoic sandstones in the Pensacola mountains, Antarctica: Jour. Sed. Petrology, v. 39, pp. 1455-1465.

York, D., 1966, Least-squares fitting of a straight line: Canadian Jour. Physics, v. 44, pp. 1079-1086.

York, D., 1967, The best isochron: Earth & Planet, Sci. Let., v. 2, pp. 479-482.

Because of the great age of the Nimrod Group, they can no longer be regarded as being contemporaneous with the Patuxent Formation. Roots (1969) had suggested a correlation of the Patuxent Formation with the Ahlmannrygg Group in Western Queen Maud Land. However, Allsopp and Neethling (1970) reported an age of 1700 m.y. for the Borg Intrusives which cut the Ahlmannrygg Group. The sediments of the Ahlmannrygg Group are therefore older than 1700 m.y. and older than the Patuxent Formation.

The Patuxent Formation may, however, coincide with a period of sedimentation represented by the Turnpike metamorphics in the Shackleton Range (Stephenson, 1966), metasediments in the Thiel Mountains (Ford, 1964), and the LaGorce, Duncan, Goldie, and Cobham Formations of the Horlick and Queen Maud Mountains (Mirsky, 1969, and Grindley and McDougall, 1969).

The metasediments of the Nilsen Plateau, probable equivalents of the LaGorce Formation, were found to have an age of 728 ± 27 m.y. This is the first age determination of these rocks which is in agreement with their stratigraphic position. Even so, the indicated age represents the time when the rocks were isotopically homogenized and closed to Rb and Sr. Deposition of the sediments probably took place earlier.

The next event determined by this study is the extrusion of the Littlewood Volcanics in Coats Land at 1001 ± 16 m.y. This event, together with an age of 1030 m.y. reported by Allsopp and Neethling (1970) for the Jorgen syeno-diorite of Western Queen Maud Land and the 1020 m.y. date on hornblende from the Nimrod Group (Grindley and McDougall, 1969), appear to indicate the widespread nature of the

Nimrod Orogeny. Angino and Turner (1964) termed a related event on the East Antarctic Shield the Bunger Orogeny. In Western Queen Maud Land, the crystallization of the Trollkjellrygg Volcanics at 856 $\pm$ 30 m.y. and a date of 825 m.y. by the K-Ar method on plagioclase from the Borg Intrusives (McDougall, in press) may indicate a later phase of the Bunger Orogeny.

It is not clear whether the Nimrod Orogeny affected the Pensacola Mountains. Although the best estimate of the age of the diabase sills intruding the Patuxent Formation is 778 $\pm$ 59 m.y., the sills may be as old as 1267 m.y. In either case, because the sills are folded along with the intruded sediments, it is not possible to pinpoint the time of folding as part of the Nimrod ($\sim$ 1000 m.y.) or the Beardmore ($\sim$ 625 m.y.) Orogenies. The limiting dates of folding of the Patuxent Formation are 1210 m.y. (the felsic flows) and about 550 m.y. (the Middle Cambrian Nelson Limestone).

In the Nilsen Plateau an undetermined interval of time separates the metasediments and the discordantly overlying metavolcanics. The Wyatt Formation, probably correlative to the metavolcanics of the Nilsen Plateau, was found to have an age of 633 m.y. in the Wisconsin Range by Montigny and Faure (1969). If the 728 m.y. age of the metasediments and the 633 m.y. age of the Wyatt Formation are not reset dates, they may indicate the actual interval of time between deposition of the two units.

However, there is evidence of the Beardmore Orogeny (620 - 680 m.y.) in both the Nilsen Plateau and the Wisconsin Range. The age of the Lonely Ridge Granodiorite of the Nilsen Plateau is 611 $\pm$ 17 m.y.

This corresponds to the age reported by Faure and others (1968) of 627 ± 22 m.y. for a granodiorite pluton intruding the metamorphic rocks of the Wisconsin Range. The cordierite-hypersthene quartz-monzonite porphyry of the Thiel Mountains was found to have an age of 632 ± 102 m.y. It also intrudes metasedimentary rocks. These plutons may have produced reset radiometric dates on the metamorphosed sedimentary and volcanic rocks that were intruded. No events during this period were detected in the Pensacola Mountains, but the isoclinal folding and low-grade metamorphism of the Patuxent Formation may have occurred at this time (Schmidt and others, 1965).

Gunner and Faure (1970) recorded a date of about 600 m.y. from metasedimentary rocks of the Nimrod Group at the head of Nimrod Glacier, indicating a metamorphic event at the time of the Beardmore Orogeny. Their Rb-Sr analyses did not, however, detect the Nimrod Orogenic period reported by Grindley and McDougall (1969) from K-Ar analyses on hornblende.

Following the Beardmore Orogeny, a period of erosion lowered the land surface. A marine transgression then resulted in deposition of a widespread limestone unit containing Middle Cambrian fossils. This is the Nelson Limestone in the Pensacola Mountains (Schmidt and others, 1965), part of the Leverett Formation in the Scott Glacier area (Mirsky, 1969), and the Shackleton Limestone of the western Queen Maud Mountains (McGregor and Wade, 1969).

The next event is the Ross Orogeny, a period of thermal metamorphism, granitic intrusion (the Granite Harbour Intrusives) and volcanism, in Cambro-Ordovician time. The Ross Orogeny in the

Pensacola Mountains is recorded by the intrusion of the Serpan Granite and Gneiss at 555 ± 26 m.y., and volcanic activity represented by the Gambacorta Formation whose age is 568 ± 39 m.y. Most of the felsic flows of the Patuxent Formation were isotopically rehomogenized at this time and record a reset date of 488 ± 6 m.y. The thermal effects of the Ross Orogeny in the Patuxent Range of the Pensacola Mountains did not subside until the end of the Silurian; the reset date of 402 m.y. for the Patuxent Formation indicates this cooling period.

The Thiel Mountains apparently were also active at this time. The age of 409 m.y. for the quartz-monzonite porphyry that intrudes the cordierite-hypersthene quartz-monzonite porphyry coincides with the Ross Orogeny. Model ages calculated for the biotite granite indicate that it is about 350 m.y. old and probably contemporaneous with the quartz-monzonite porphyry.

Several granitic plutons were intruded into the rocks of the Nilsen Plateau during the Ross Orogeny. The South Quartz Monzonite is found to have an age of 452 ± 14 m.y. During this time the Lonely Ridge Granodiorite was severely deformed cataclastically and the meta-volcanic rocks were reset isotopically to a date of 486 ± 10 m.y.

The same orogenic period was recorded in the Wisconsin Range by crystallization of a quartz-monzonite pluton at 479 ± 10 m.y. and by rhyolites dated at 498 ± 45 m.y. and 472 ± 11 m.y. (Faure and others, 1968). Metasedimentary rocks in the Wisconsin Range were found to have a reset date of 460 ± 16 m.y. by Montigny and Faure (1969). Gunner and Faure (1970) likewise found that an internal isochron on mineral separates from the Nimrod Group showed isotopic rehomog-

enization at 456 ± 14 m.y. Orogenic activity in the Wisconsin Range and the Queen Maud Mountains appears to have ceased about 50 m.y. sooner than in the Patuxent Range and the Thiel Mountains.

The cooling and period of erosion following the Ross Orogeny completes the known sequence of events in the formation of the basement complex of the Transantarctic Mountains. Lack of evidence of any post-Nimrod (or post-Bunger) orogenic activity in Coats Land suggested that, like Western Queen Maud Land, it is a part of the East Antarctic Shield and has not undergone the same history as the Transantarctic Mountains.

Appendix B: Sample Descriptions (Using Classification of Williams, Turner, and Gilbert, 1954)

Pensacola Mountains: Samples collected by D. L. Schmidt, U.S. Geological Survey, Federal Center, Denver, Colorado

O.S.U. No.

290 (Schmidt No. W21d.12.27.63)
Gambacorta Formation, Red-Brown Member, Bragg Valley, S. Neptune Range. Rhyolite, grayish red with prominent red-brown flow banding. Porphyritic, with highly embayed quartz, and pseudomorphs of sericite after feldspar. Inclusions of altered pumice.

291 (Schmidt No. N1.12.24.63)
Gambacorta Formation, Lower Member, Upper Jackson Valley, S. Neptune Range. Latite, aphanitic, greenish-gray, with dark greenish-gray streaks.

292 (N 2.1.12.64)
Gambacorta Formation, Hawkes Porphyry Member, west side of "Hawkes camp" valley, S. Neptune Range. Porphyritic quartz latite with phenocrysts of K-feldspar, plagioclase, and quartz in a dark red groundmass.

293 (S 25.12.29.64)
Gambacorta Formation, Hawkes Porphyry Member, middle "Bragg" valley, S. Neptune Range. Same as 292 except more phenocrysts (33%).

294 (S 2-11.12.63)
Pyroclastic rhyolite, autolithic breccia, from basal part of Elliott Sandstone, Pemberton section, one mile west of Wiens Peak, S. Neptune Range.

348 (45 Sa.13.12.65)
Gambacorta Fm., Hawkes Porphyry Mem., Hill Nunatak, Neptune Range. Rhyodacite, phenocrysts (20-25%) of quartz and altered K-feldspar in a greenish-gray aphanitic groundmass.

349 (73 S.17.12.65)
Gambacorta Fm., Hawkes Porphyry Mem., east face of Mount Hawkes, Neptune Range. Rhyodacite, similar to 348.

350 (46Sa.13.12.65)
Gambacorta Fm., Hawkes Porphyry Mem., Hill Nunatak area, Neptune Range. Rhyodacite, altered, olive-gray vitric-crystal tuff. Quartz (30%), alkali feldspar (10%), and plagioclase (15%) are identifiable.

351 (46 Sb.13.12.65)
Gambacorta Fm., Hawkes Porphyry Mem., Hill Nunatak area, Neptune Range. Vitric-crystal tuff similar to 350.

389 (23 S.28.12.63)
Gambacorta Fm., Red-Brown Mem., upper Bragg Valley, Neptune Range. Vitric-crystal tuff? Quartz and plagioclase in aphanitic groundmass.

390 (21 Wa.27.12.63)
Gambacorta Fm., Red-Brown Mem., Bragg Anticline, Neptune Range. Vitric-crystal tuff? Similar to 389, but with light and dark bands.

391 (5N.12.1.64)
Gambacorta Fm., Johnston Porphyry Mem., eastern Hood Ridge, Neptune Range. Black ash flow tuff, phenocrysts (33%) of quartz and plagioclase.

356 (47Wa.28.1.64)
Hypabyssal porphyry intrusive into Patuxent Fm. at Pope Nunatak, 120' diameter plug. Porphyritic felsite, phenocrysts of quartz, K-feldspar, and plagioclase. Black angular inclusions.

352 (12 Sa.11.1.66)
Rhyolite, east prong of Gorecki Peak, Schmidt Hills, Neptune Range. Light gray vitric-crystal tuff? Quartz and K-feldspar grains are abundant (60%). Black angular inclusions up to 1" long.

353 (32 Sa.7.2.64)
Rhyolite plug ($\sim$ 100' diameter) intrusive into Patuxent Formation, Williams Hills, Neptune Range, Phenocrysts of K-feldspar (15%) in a aphanitic groundmass.

354 (12.Sb.11.1.66)
Rhyolite, Gorecki Peak, Schmidt Hills, Neptune Range, Similar to 352.

355 (32 Sd.7.2.64)
Rhyolite, Williams Hills, Neptune Range, Different Outcrop, but similar to 353.

357 (18.SB.5.2.64)
Felsic tuff, east-central Williams Hills, Neptune Range. Numerous black angular inclusions (25%) in gray aphanitic rock.

358 (W44a.23.1.64)
Rhyolite, Gorecki Peak, Schmidt Hills, Neptune Range, Similar to 352, 354.

434 (1 Se.6.12.65)
Rhyolite, Williams Hills, Neptune Range. From area 1½ miles west of 353,355. Part of shear lense in folded Patuxent Fm. Quartz and plagioclase phenocrysts and minor K-feldspar. Sericite (?) abundant in groundmass.

435 (1 Si.6.12.65)
Rhyolite, Williams Hills, Neptune Range. From area 1½ miles west of #353,355. Similar to 434.

414 (Schmidt's No. S23-24B.2.7.64)
Basalt, Patuxent Fm., Williams Hills, Neptune Range. From interior of 30 m thick flow, Nunatak #6.

415 (S 5.2.4.64)
Basalt, Patuxent Fm., Nunatak #8, Williams Hills, Neptune Range. Moderately amygdaloidal, mostly chlorite, but some calcite.

416 (1 S.1.13.64)
Basalt, Patuxent Fm., Nunatak #2, Williams Hills, Neptune Range.

417 (B4.15.1.64)
Pillow basalt, Patuxent Fm., Nunatak #11, Williams Hills, Neptune Range. From interior of 30 cm. diameter pillow.

418 (10 Sa.11.1.66)
Diabase, Gorecki Peak, Schmidt Hills, Neptune Range, Medium-grained. From near base of 180' thick sill intrusive into Patuxent Fm. Sill is about 100' below rhyolite flows.

419 (10 Sb.11.1.66)
Diabase, 87' above sample 418.

420 (10 Sc.11.1.66)
Coarse grained diabase, 137" above sample 418.

421 (10 Sd.11.1.66)
Fine-grained diabase, 6 " below top of same sill as samples 418, 419, 420.

422 (B 30.1.64.BGP.11.D-3)
Medium-grained diabase, Nunatak #10, Schmidt Hills, Neptune Range. From interior of 300-400' thick sill.

423 (B 30.1.64.BGP.11.D-4)
Moderately coarse-grained diabase, same locality as 422.

424 (W 66a.11.2.64)
Granite gneiss, Serpan Peak, Neptune Range. Biotite (?) altered to chlorite.

425 (W 66 aa.11.2.64)
Granite gneiss, Serpan Peak, Neptune Range. Chlorite common.

426 (W 66 c.11.2.64)
Hornblende-biotite-sphene gneiss, Serpan Peak, Neptune Range. Biotite partly altered to chlorite.

427 (W 66 cc.11.2.64)
Hornblende-biotite-sphene gneiss, Serpan Peak, Neptune Range. Biotite altered to chlorite.

428 (W 66 d.11.2.64)
Granite gneiss, Serpan Peak, Neptune Range.

429 (W 66 e.11.2.64)
Hornblende-biotite-sphene gneiss, Serpan Peak, Neptune Range. Contains a dark alteration lenticule. Biotite is chloritized.

430 (W 66 f.11.2.64A)
Granite gneiss, Serpan Peak, Neptune Range.

431 (W 66 f.11.2.64B)
Granite gneiss, Serpan Peak, Neptune Range.

432 (18 S.2.12.64 R-1)
Coarse-grained granite, near Serpan Peak, Neptune Range. Red variety.

433 (18 S.2.12.64 W-3)
Coarse-grained granite, near Serpan Peak, Neptune Range, White variety.

436 (1 Sa.2.12.65)
Interbedded siltstone and slate, Patuxent Fm., Far West Peak, Patuxent Range. These samples of the Patuxent Fm. are numbered in geographic order, from North to South.

437 (5 S.12.4.62)
Laminated slate, Patuxent Fm., Seminole Nunatak, Patuxent Range.

438 (65 S.12.11.62)
Subgraywacke, Patuxent Fm., Winnebago Nunatak, Patuxent Range.

439 (9 S.2.12.65)
Slate, Patuxent Fm., Pueblo Nunataks area, Patuxent Range.

440 (1S.11.30.62)
(Subgraywacke, Patuxent Fm., Dash Nunatak, Patuxent Range.

441 (1 S.1.24.62a)
Interbedded siltstone and slate, Patuxent Fm., Mohawk, "A" Nunatak, Patuxent Range.

442 (2XS.11.13.62)
Slate, Patuxent Fm., Snowback Nunatak, Patuxent Range.

443 (95 Sb.22.12.65)
Subgraywacke, Patuxent Fm., Black Pyramid, Patuxent Range.

444 (3Sa.11.16.62)
Laminated siltstone and subgraywacke, Patuxent Fm., Corner Glacier area, Patuxent Range.

445 (S.1.2.63)
Laminated siltstone, Patuxent Fm., Bannock Ridge, Patuxent Range.

446 (65F-1.31.12.62)
Slate, Patuxent Fm., Ogalalla Ridge, Patuxent Range.

Thiel Mountains: Samples collected by A. B. Ford, U.S. Geological survey, Menlo Park, California

O.S.U. No.

493 (Ford's No. 5.12.61.15)
Cordierite-hypersthene quartz-monzonite porphyry, Thiel Mountains. See map of Thiel Mountains for location.

494 (7.12.61.1)
Cordierite-hypersthene quartz-monzonite porphyry, Thiel Mtns. Slightly recrystallized, biotite rims on hypersthene.

495 (31.1.61.9)
Cordierite-hypersthene quartz-monzonite porphyry, Thiel Mtns. Slightly recrystallized.

496 (10.1.62.20)
Cordierite-hypersthene quartz-monzonite porphyry, Thiel Mtns. Much recrystallized, adjacent to contact with biotite granite.

497 (10.1.62.10)
Biotite granite (quartz monzonite?), Thiel Mtns. Intrusive into C-H-Q porphyry. Sample is from contact zone, near #496.

498 (10.1.62.5)
Biotite granite, Thiel Mtns. Same as 497, but 100 m from contact.

499 (7.12.61.4)
Porphyritic quartz monzonite, Thiel Mtns. Intrusive into C-H-Q porphyry.

500 (27.12.61.8T)
Biotite quartz monzonite, Thiel Mtns. Intrusive into C-H-Q porphyry. Biotite partly chloritized, plagioclase sausseritized.

501 (28.12.61.3T)
Biotite quartz monzonite, Thiel Mtns. Similar to 500.

Nilsen Plateau: Samples collected by D. McLelland, made available to the author by M. J. Hibbard, University of Nevada, Reno.

O.S.U. No.

461 (McLelland's No. 77)
Metavolcanic, from spur SW into Cougar Canyon, 7000' ENE of base camp, Nilsen Plateau, Queen Maud Mtns. Phenocrysts of quartz, plagioclase, and biotite set in aphanitic light gray groundmass. Hematite staining around quartz phenocrysts.

462 (80)
Metavolcanic, same location as 461. Similar to 461, but less numerous phenocrysts (10%).

463 (87)
Metavolcanic, same location as 461. Brecciated and lacking hematite stain, but otherwise similar to 461.

464 (92)
Metavolcanic, same location as 461. Shows weak foliation.

465 (131)
Metavolcanic, Thermometer Ridge, east side of east branch of Cougar Canyon, Nilsen Plateau. Numerous phenocrysts (70%) of quartz, plagioclase, and biotite in gray aphanitic groundmass.

466 (132)
Metavolcanic, same location as 465.

467 (137)
Metavolcanic, same location as 465 and similar, but fewer phenocrysts (40%) and dark gray groundmass.

468 (143)
Cougar Canyon Quartz Monzonite, (?), near location of 465, but on opposite side of a fault. Quartz phenocrysts (15%) in medium to fine-grained groundmass of K-feldspar, plagioclase, and biotite.

469 (154)
Metavolcanic, South Ridge, Nilsen Plateau. Similar to 465.

470 (135)
Metavolcanic, same location and similar to 465.

471 (284)
Metasediment (phyllite), SW spur of Lonely Ridge. Inclusion in South Quartz Monzonite.

472 (260)
Metagraywacke, south side of mouth of Black Rock Glacier, Nilsen Plateau.

473 (267)
Metagraywacke, spur at head of Black Rock Glacier, Nilsen Plateau.

474 (271)
Metaquartzite, south side of head of Black Rock Glacier, Nilsen Plateau.

475 (324)
Metagraywacke, near location of 473.

476 (347)
Metaquartzite, spur just north of Black Rock Glacier, Nilsen Plateau.

477 (49)
Lonely Ridge Granodiorite, North side of Lonely Ridge, Nilsen Plateau. Medium-sized grains of plagioclase, quartz, and biotite. Shows a weak gneissic foliation.

478 (46)
Lonely Ridge Granodiorite, north side of Lonely Ridge. Similar to 477.

479 (44)
Lonely Ridge Granodiorite, north side of Lonely Ridge. Strong gneissic foliation, augen of plagioclase 1 cm wide.

480 (208)
Lonely Ridge Granodiorite, south side of Lonely Ridge. Similar to 477, not foliated.

481 (211)
Lonely Ridge Granodiorite, south side of Lonely Ridge. A "cataclastic gneiss," foliation more pronounced than 479.

482 (215)
Lonely Ridge Granodiorite, south side of Lonely Ridge. Thoroughly deformed cataclastic gneiss.

483 (216)
Lonely Ridge Granodiorite, south side of Lonely Ridge. Similar to 482, but more intense deformation.

506 (62)
South Quartz Monzonite, southwest wall of Cottonwood Canyon, Nilsen Plateau, Light gray, medium-grained, consisting mainly of quartz, K-feldspar, and plagioclase, some biotite.